Functional and Genomic Analyses of Klebsiella Pneumoniae Population Dynamics in the Gastrointestinal Tract

The Harvard community has made this article openly available. Please share how this access benefits you. Your story matters

Citation	Wardwell-Scott, Leslie Hansen. 2016. Functional and Genomic Analyses of Klebsiella Pneumoniae Population Dynamics in the Gastrointestinal Tract. Doctoral dissertation, Harvard University, Graduate School of Arts & Sciences.
Citable link	http://nrs.harvard.edu/urn-3:HUL.InstRepos:26718724
Terms of Use	This article was downloaded from Harvard University's DASH repository, and is made available under the terms and conditions applicable to Other Posted Material, as set forth at http://nrs.harvard.edu/urn-3:HUL.InstRepos:dash.current.terms-of-use#LAA

Functional and Genomic Analyses of *Klebsiella pneumoniae* Population Dynamics in the Gastrointestinal Tract

A dissertation presented

by

Leslie Hansen Wardwell-Scott

to

The Division of Medical Sciences

In partial fulfillment of the requirements
for the degree of

Doctor of Philosophy

in the subject of

Biological and Biomedical Sciences

Harvard University

Cambridge, Massachusetts

November 2015

Dissertation Advisor: Dr. Wendy Garrett Leslie Hansen Wardwell-Scott

Functional and Genomic Analyses of *Klebsiella pneumoniae* Population Dynamics in the Gastrointestinal Tract

ABSTRACT

The gastrointestinal tract is home to trillions of bacteria that interact with each other and with the host's mucosal immune system. Obligate and facultative anaerobes thrive in the small and large intestine. While many of these bacteria have beneficial relationships with their host, opportunistic pathogens can bloom in times of inflammation and prolong disease. *Klebsiella pneumoniae* is an opportunistic pathogen that is part of the gut microbiota in many healthy individuals. Here we explore the population dynamics of *K. pneumoniae* in the gastrointestinal tract in mouse models of health and disease.

To assess the role of intra-species genomic diversity in interactions with the host, a mouse *K. pneumoniae* isolate and three human clinical isolates from human stool, sputum, and urine were studied in the *T-bet*$^{-/-}$ *Rag2*$^{-/-}$ and dextran sodium sulfate models of ulcerative colitis and in a mouse model of systemic neonatal infection. Regardless of host origin, isolate site source, or genomic differences, all four *K. pneumoniae* isolates were able to stimulate colonic inflammation. However, only exposure to the murine *K. pneumoniae* isolate, and not human clinical isolates, led to neonatal death. In addition, this murine isolate correlated with differential shifts in levels of other *Enterobacteriaceae* species in the colon. Murine *K. pneumoniae* was found in higher amounts in host mesenteric lymph nodes compared to human isolates, suggesting subtle strain-based differences that affect response to *K. pneumoniae* in the gastrointestinal tract.

A defining feature of *K. pneumoniae* is its mucoid capsular polysaccharide coat. To begin investigating a role for *K. pneumoniae*'s capsule in the gastrointestinal tract, *K. pneumoniae* biogeography was assessed in gnotobiotic mice. Encapsulated *K. pneumoniae* were outcompeted by naturally arising variants with reduced capsule throughout the gastrointestinal tract of gnotobiotic mice, except in the distal small intestine. This portion of the small intestine was also the region with the highest host Paneth cell antimicrobial peptide expression. Micro-injection of *K. pneumoniae* into small intestinal organoids revealed increased growth of encapsulated *K. pneumoniae* in the presence of α-defensins and decreased survival of *K. pneumoniae* with reduced capsule production. Capsule also conferred an advantage when *K. pneumoniae* was part of a diverse microbiota. Competition assays between *K. pneumoniae* and *Escherichia coli* showed enhanced survival of encapsulated *K. pneumoniae* compared to isolates with reduced capsule production. These data suggest that host AMPs, in combination with bacterial-bacterial interactions, shape population dynamics of *K. pneumoniae* and select for encapsulated *K. pneumoniae* throughout the gastrointestinal tract. Overall, these studies provide a foundation for understanding interactions between *K. pneumoniae,* the host, and other bacteria in the gastrointestinal tract.

TABLE OF CONTENTS

ACKNOWLEDGEMENTS

There is a small village worth of people who I need to thank for their support, guidance, and contributions to my graduate school years. First and foremost, I would like to thank my PhD advisor, Wendy Garrett. I am extremely grateful for the numerous opportunities Wendy has presented me with, many of which fall well outside the realm of typical student experiences. I have learned so much from Wendy as a scientist and she has challenged me to think independently, continuously question results, and find alternative solutions to complex problems. Her office door is always open and she has supported me on a winding path that has included two internships and numerous life discussions as I transition towards a career in the commercialization of science.

I would also like to thank members of my dissertation advisory committee John Mekalanos, Jerry Pier, and Colleen Cavanaugh for their guidance over the years. Their thoughtful discussions and feedback have helped my project progress and develop. Thank you also to my defense committee members John Mekalanos, John Leong, Cammie Lesser, and Laurie Comstock for taking the time to read and discuss my work.

While in the Garrett lab, I have been surrounded by a fabulous group of scientists and I would like to thank them all. Their support has been immeasurable and their humor has carried me through many failed experiments. Special thank you to the original members with whom I've shared these 5 ½ years. I would like to thank Carey Ann Gallini for keeping the lab running, the music pumping, and for her friendship; Michael Howitt for being a phenomenal baymate, but more importantly, for being an unofficial PhD mentor. His future trainees will be lucky to have his support. Monia Michaud's experienced bench hands and knowledge have helped me though many protocols. I have

been fortunate to share my time in the lab with fellow student, Michelle Rooks- thank you for being a friend and for teaching us all balance. Thank you to Sonia Ballal for her deep discussions, genuine care, and for showing us how to combine the titles of physician, scientist, and mother into a single sentence every day. To Eunyoung Chun for her unwavering smile and for sharing her immense knowledge of immunology. To Sydney Lavoie, who makes me laugh on a constant basis. And finally, thank you to the more recent additions, Caitlin Brennan, Kathrin Fenn, and Nora Ou for helping make lab feel less like work and more like family.

Thank you to my mother Kristina, father Stephen, and sister Annie. This thesis would not be possible without their constant support over the past 29 years. I am grateful that they bought me my first microscope and forced me to look at magnified bug wings after I told them I wanted to grow up to be an artist. I have learned invaluable lessons about persistence, hard work, and thoughtful decision making from all three of them.

Finally, I would like to thank my husband Jonathan who has been the center of my support system since before I even declared biology as a major in college. His constant belief in me has pushed me academically and professionally to heights that I never thought possible (and also to ski faster than what is generally considered safe). Thank you for pretending to understand the devastation of contaminated germ-free mice and for distracting me from it with home cooked meals.

LIST OF FIGURES

LIST OF TABLES

LIST OF ABBREVIATIONS

AAD	antibiotic-associated diarrhea
AIEC	adherent and invasive *Escherichia coli*
AMP	antimicrobial peptide
ASF	altered Schaedler flora
CPS	capsular polysaccharides
DC	dendritic cell
DSS	dextran sodium sulfate
GF	germ-free
GI	gastrointestinal tract
HGT	horizontal gene transfer
KPC	*Klebsiella pneumoniae* carbapenemase
LCB	local collinear block
LDA	linear discriminant analysis
LPS	lipopolysaccharide
MUC	mucoid
NDM-1	New Delhi metallo-β-lactamase 1
NEC	necrotizing enterocolitis
NOD	nucleotide-binding oligomerization domain
NMV	non-mucoid variant
OTU	operational taxonomic unit
SFB	segmented filamentous bacteria
SPF	specified pathogen-free
T6SS	type VI secretion system
TLR	toll-like receptor
TNFα	tumor necrosis factor α
TRUC	*Tbet*$^{-/-}$ *Rag2*$^{-/-}$ ulcerative colitis mouse model
WGS	whole genome sequence
WT	wild-type

CHAPTER 1

INTRODUCTION

I. COPYRIGHT DISCLOSURE

Adapted in part from Wardwell L, Huttenhower C, Garrett W. Current concepts of the intestinal microbiota and the pathogenesis of infection. *Current Infectious Disease Reports* 13(1), 28-34 (2011).

II. OVERVIEW

The intestinal microbiome is the collection of bacteria, viruses, archaea, fungi, and parasites that reside in the gastrointestinal tract. Microbiome composition plays an important role in gut immune homeostasis and disruption of the microbiome can lead to dysbiosis and disease. Depending on host genetics and environmental factors, individual bacteria can be both beneficial and antagonistic to their host. For example, *Klebsiella pneumoniae* is an opportunistic pathogen found in the microbiome of healthy humans that can also cause pneumonia, urinary tract infections, diabetic liver abscesses, and bacteremia in susceptible individuals. Adding to *K. pneumoniae's* clinical burden is the global spread of highly antibiotic-resistant strains. While several metabolic genes are known to be necessary for *K. pneumoniae* colonization of the gastrointestinal tract, an awareness of colonization factors and behavior in the gut is incomplete. Since *K. pneumoniae* colonization of the gastrointestinal tract predisposes patients for *K. pneumoniae* infection, understanding this bacterium in its disease reservoir is of the utmost importance.

III. GASTROINTESTINAL MICROBIOTA AND THE INTESTINAL EPITHELIUM

Bacterial cells outnumber eukaryotic cells in the human body by greater than ten-fold. In the gastrointestinal tract alone, there are up to 10^{12} microbes per gram of stool, corresponding to up to 100 trillion bacteria in the human gut and representing several

hundred distinct bacterial species. These bacteria, known collectively as the intestinal microbiota, play an important role in a multitude of host functions including energy extractions from food, production of microbial metabolites, development of the host's immune system, and protection from and response to systemic and gastrointestinal infectious diseases (1, 2). These communities are in turn shaped by host genetics, diet, and the environment and thus exhibit substantial inter-individual variation (3). Advances in sequencing technology and the computational methodology to interpret these data have resulted in an increased appreciation for the role of gut microbiomes in the pathogenesis of obesity (4), inflammatory bowel disease (5), type 1 diabetes (6), and metabolic syndrome (7).

Intestinal epithelium

The gastrointestinal tract is divided into the small intestine (duodenum, jejunum and ileum), and the large intestine (colon). The intestinal epithelium is a single layer of cells separated from the microbial-rich lumen by a layer of mucus. Stem cells residing in the crypts of Lieberkuhn give rise to a variety of intestinal epithelial cells that are renewed every 4-5 days (8). Intestinal epithelial cells include enterocytes, mucus producing Goblet cells, enteroendocrine cells, antimicrobial producing Paneth cells, and Tuft cells. Intestinal epithelial cells are connected by tight junctions and form a barrier between the mucosal immune system and microbes within the lumen (9).

Paneth cells are specialized secretory epithelial cells. Primarily found within the small intestine, Paneth cell concentrations increase in a descending manner and reach their height in the distal ileum (10). Paneth cells produce and granocytose antimicrobial peptides (AMPs) into the lumen to aide in pathogen defense and in shaping composition

of the microbiome (11, 12). In humans these antimicrobial peptides include two small, cationic α-defensins (α-defensin 5 and α-defensin 6), lysozyme, phospholipase A_2, and RegIII α (13). In addition to these AMPs, murine Paneth cells produce many a-defensins, termed cryptdins, and angiogenin, an antimicrobial Rnase. Paneth cells constitutively produce AMPs with the exception of RegIIIγ (the mouse isoform of RegIIIα) and angiogenin, which are induced in the presence of symbiotic bacteria (13). Defects in Paneth cell function are associated with ileal Crohn's disease, highlighting the importance of this cell in gastrointestinal immune homeostasis (14).

Biogeography of gastrointestinal bacteria

Many bacteria of the upper digestive tract are killed by the harsh acidic pH of the stomach (pH<4) (15). Consequently, the duodenum, or proximal small intestine, is the area of the small and large bowel with the lowest concentration of luminal and mucosal bacteria. In addition to reducing numbers, selective pressures encountered in the stomach also affect diversity of bacterial communities. Large decreases in both phylogenetic and Shannon alpha diversity have been seen in the stomach and lower gastrointestinal bacterial communities as compared to those of the mouth (16). As bacteria move along the small intestine, total numbers and Shannon alpha diversity recover and reach a maximum in the cecum and throughout the colon.

Early studies on the microbiome have revealed phylum level differences in community composition according to gastrointestinal biogeography. The mouth microbiome is marked by a high relative abundance of *Fusobacteria*; *Proteobacteria* predominate in the stomach and retain a high representation in the proximal small intestine for some individuals (16). In contrast, the colon microbiome is dominated by

Gram-negative *Bacteroidetes* and Gram-positive *Firmicutes*, followed by less abundant gram-negative *Proteobacteria* (17). Rounding out the highly represented phyla of the colon microbiome are the *Actinobacteria* and *Deferribacteres*. In healthy individuals, the resident intestinal microbiota exists in dynamic balance with the host immune system; the intestinal epithelium provides an essential barrier that ensures a separate peace between host and microbe. However, there is constant crosstalk across this barrier between the immune system and microbiota that is equally important for homeostasis in the gut. The epithelium, innate and adaptive immune systems, and the intestinal mucus are all active participants in host defense from infectious diseases that target the gastrointestinal mucosa as their portal to invading their human hosts. Gut bacteria also provide an important line of defense for their hosts against invading pathogens, a process known as colonization resistance.

Colonization resistance

Colonization resistance is the process by which the indigenous gut microbiota protects a host from infectious microbes. Several mechanisms underpin colonization resistance, the foremost of which is competition for space and nutrients along the mucus layer and within the lumen (18). In addition, bacteria employ a number of mechanisms for direct competition with their microbial neighbors. Short-chain fatty acids, which are products of commensal bacterial metabolism, are also bactericidal for some enteric pathogens (19). Certain *Lactobacilli*, in particular members of the *acidophilus* subgroup, generate reactive oxygen species that are inhibitory to other bacteria in the gastrointestinal tract (20). Numerous commensals produce antimicrobial peptides, called bacteriocins, as defensive strategies. Bacteriocins fall into three general categories (I,

IIa/b/c, and III) and have distinct activities: nucleases, DNAses, cell wall component (eg, peptidoglycan) production inhibitors, and pore formers (21). Studies using mouse models suggest that the composition of a host's microbiota may influence susceptibility to enteropathogens (22). Furthermore, particular members of gut microbial communities impact the ability of pathogens to invade and beneficial microbes to colonize. Hosts with high *Escherichia coli* densities are more susceptible to *Salmonella enterica* infection, whereas hosts with high *Lactobacilli* counts are more easily colonized with other probiotic strains of *Lactobacilli* (22).

As a third mechanism of colonization resistance, bacteria can influence the host's immune system in a way that precludes invasion by pathogens. Presence of bacteria in the gastrointestinal tract induces Paneth cells in the small intestine to produce REGIIIγ, an antimicrobial peptide that limits invasion of Gram-positive bacteria across the epithelial mucus layer (23). Additionally, engagement of host toll like receptors (TLRs) by bacterial ligands ultimately leads to IgA production by B cells for defense at the mucosal barrier (24).

Symbiotic bacteria and the immune response

Symbiotic enteric bacteria are required for immune cell development and function within the gastrointestinal tract and systemically. Studies from germ-free (GF) and gnotobiotic mice (mice lacking endogenous microbes) demonstrate abnormal Peyer's patches, lymph nodes, and spleen; decreased numbers of mucosal and systemic innate and adaptive immune cells; and markedly reduced levels of immunoglobulins and other host defense molecules (25). Susceptibility to numerous bacterial, viral, and parasitic

infections is also increased in GF mice, resulting from loss of colonization resistance and impaired immune system responses.

Several studies have identified that select species or specific bacterial products play a critical role in the proper functioning of the immune system. Although *Bacteroides fragilis* is well known for its opportunistic role in intraperitoneal abscesses, it also bestows benefits to the host regarding the development of adaptive immunity in the gut and system-wide. A zwitterionic polysaccharide, polysaccharide A, expressed by *B. fragilis* is responsible for these beneficial effects on host immune cell development and homeostasis (26). In addition, polysaccharide A also appears to protect mice from experimentally induced inflammatory bowel disease and central nervous system inflammation (27, 28). T helper 17 cells (Th17), a subset of $CD4^+$ T cells named for its production of the proinflammatory cytokine IL-17, function in host defense against fungi and extracellular bacteria and have been implicated in the pathogenesis of numerous autoimmune diseases (29). In mice, the induction of intestinal Th17 cells requires that the small intestine is colonized with segmented filamentous bacteria (SFB), a group of anaerobic, spore-forming, gram-positive bacteria (30). SFB stimulate the expression of several genes involved in antimicrobial defenses and inflammation. The bacterial molecules, host sensors, and signaling pathways involved in this SFB-mediated Th17 development remain to be defined.

Both immune and non-immune system cells express a diverse repertoire of pattern recognition receptors that bind molecular patterns shared among microbes. The TLRs are one family of pattern recognition receptors. Flagellin, the TLR5 ligand, recently was shown to restore innate immune defenses against and decrease colonization levels of

vancomycin-resistant *Enterococcus* (31). The nucleotide-binding domain, leucine rich repeat containing proteins, are another family of microbial recognition receptors. Nucleotide-binding oligomerization domain protein (NOD) 2 has a broad specificity for peptidoglycan and NOD1 senses diaminopimelic acid-type peptidoglycan. Intestinal commensal bacterial-derived diaminopimelic acid-type peptidoglycan plays an important role in priming systemic innate immunity. Specifically, studies of NOD1-deficient and wild-type (WT) mice demonstrated that importance of NOD1 signaling for neutrophil killing of *Streptococcus pneumoniae* and *Staphylococcus aureus* (32). Thus, humans and our ancestors evolved a dual-purpose system for sensing microbes—a system that not only senses endogenous microbes for the proper development and functioning of the immune system, but also senses pathogenic invaders to initiate host defense programs.

Antibiotics and the Commensal Microbiota

Antibiotics can have several disruptive effects on the endogenous flora, the most familiar of which are the antibiotic-associated diarrheas. Recent genomic studies of the intestinal microbiota, both in human populations and mouse models, have revealed that antibiotics have unexpectedly widespread and enduring effects on endogenous gut microbes. Duration of treatment, type of antibiotic, and individual differences all influence antibiotic-induced changes in the composition of the gut bacterial community and the resiliency of gut community members to antibiotic treatment. 16S rDNA enumerations from human stool before and 4 weeks after ciprofloxacin treatment revealed that although the majority of gut microbes eventually returned to their pre-treatment relative abundance levels, taxa belonging to the *Clostridiales* order did not recover during the observation period (33). A common theme illuminated by studies of

the antibiotic effects on gut microbial composition is a reduction in relative abundance of members of the *Firmicutes* phylum and specifically several *Lactobacillus* species, many of which are considered beneficial microbes (34, 35). Broad-spectrum antibiotic treatment of mice revealed large proportional increases in the *Bacteroidales* order. After only 1 day of antibiotics, representation of this order increased to 95%, from basal levels of 60% to 70% of the total bacterial population (34). These perturbations have the potential to be significant in light of recent studies demonstrating a link between diabetes (36) and obesity (4) and decreased gut microbial diversity and altered *Bacteroidetes* to *Firmicutes* ratios.

Antibiotic-induced alterations of the composition or function of gut microbial communities are key effectors in susceptibility to several gastrointestinal bacterial diseases. Antibiotic-associated diarrhea (AAD) is a common complication of antibiotic use, and *Clostridium difficile* is the most frequent cause of AAD, colitis, and pseudomembranous colitis (37). *Klebsiella oxytoca, Clostridium perfringens, Salmonella* spp, *Candida* spp, and *Staphylococcus aureus* are far less common causes of AAD. Both the incidence and death rates of *C. difficile*–associated colitis have increased at an alarming rate over the past decade (117% increase in incidence between 2000 and 2006 and a 35% increase in mortality rates) (37). Estimates of asymptomatic carriage of *C. difficile* range between 1% and 55.4%, based on the population observed (38). A few studies have begun to delve into how the composition of the fecal microbiota affects susceptibility and risk of recurrence of *C. difficile*–associated diarrhea. A correlation between *C. difficile*–associated diarrhea and the extent and duration of decreased diversity in response to antibiotics is emerging (38). A recent study by Giel et

al. (39) provides mechanistic insight into how antibiotic treatment may result in *C. difficile* sporulation and subsequent AAD. Bile salt metabolism by the commensal microbiota appears to be a key effector. A cholestyramine-sensitive factor in cecal or intestinal extracts of antibiotic-treated mice stimulated *C. difficile* colony formation from spores much more efficiently than samples from untreated mice (39).

Antibiotics also increase susceptibility to invading microbes of the gastrointestinal tract. Treatment of mice with streptomycin or vancomycin lowered the inoculum dose required to cause morbidity with *Salmonella enterica* Serovar Typhimurium (40). The doses of antibiotics used in this study did not reduce total bacteria numbers in the gut, a finding emphasizing that composition and function of the community are important factors in mediating host resistance to invading pathogens. Beyond shifting relative abundances of gut bacteria, antibiotics also have the ability to influence the genomic potential and expression of the gut microbial community. Treatment with high doses of antibiotics selects for bacteria with antibiotic resistance genes on mobile genetic elements. Even though the typical members of the gut microbial community may re-colonize the gut over time, horizontal gene transfer of antibiotic resistance may irrevocably alter the intestinal microbiota.

Gut microbiota as reservoirs of resistance

The existence of lag times between when widespread clinical use of an antibiotic begins and when resistance becomes a problem—a few years for penicillin and more than 30 years for vancomycin (41)—suggests that gut bacteria living without exposure to antibiotics do not typically harbor resistance genes. However, bacteria in the soil, an ancient antibiotic resistance reservoir, have spent millions of years evolving in the

presence of natural antimicrobials, resulting in the expression and spread of many resistance genes via horizontal gene transfer (HGT) (42). The gut represents an environment that, like soil, is highly conducive for HGT—a dense population of bacterial cells, often found organized similar to a biofilm (41). Once in the gut, antibiotic resistance genes can disseminate throughout the bacterial population, especially under selection pressure from clinically administered antibiotics, and these effects of HGT can endure after selection is removed. After combined antibiotic treatment for *Helicobacter pylori* gastritis (with a clarithromycin and metronidazole regimen), gut enterococci exhibited high macrolide resistance for 1 year after treatment; for one patient, resistance remained even after 3 years (43). A study of the gut microbiotas of two healthy individuals with no antibiotic exposure in the preceding year found antibiotic resistance genes in both commensal and opportunistic fecal bacteria (44). Almost half of the antibiotic resistance genes identified from the sub-cultured fecal isolates were genetically identical to antibiotic resistance genes found in known human pathogens (44). Thus, the commensal gut microbiome represents a reservoir of antibiotic-resistance genes. Through HGT, otherwise harmless commensals have the potential to transfer antibiotic resistance determinants to pathogens, which may lead to the emergence of clinically problematic strains.

Viruses and gut bacterial communities

Viral gastroenteritis

Viruses are frequently the causative agent of gastroenteritis, one of the most common infectious diseases worldwide (45). Specifically, noroviruses were found to be responsible for 93% of viral gastroenteritis outbreaks in the United States during a 3-year

study period between 1997 and 2000 (46). Although viral gastroenteritis in adults is most commonly linked to noroviruses, gastroenteritis in children is caused by a broader group of viruses that, along with noroviruses, includes rotaviruses, astroviruses, and sapoviruses (47). Both astroviruses and rotaviruses have been shown to directly increase gut mucosal permeability (48). Loss of gut barrier integrity alters the delicate balance between the immune system and commensal microbiota, and thus compromises defenses against a broad range of gastrointestinal pathogens.

The variable attack rates of enteric viruses bring into question the role of the gut microbiota in shaping susceptibility. Undertaking prospective studies of the gut microbiota that follow populations over time may illuminate characteristics of microbial communities associated with resistance to viral gastroenteritis. Although it is not well understood if or how gut microbial populations affect infection with enteric viruses, rehydration therapy in conjunction with supplementation with multiple *Lactobacilli spp. (reuteri, acidophilus, delbrueckii bulgaricus*, and *casei*) and *Saccharomyces boulardii* reduced the duration of rotavirus-associated diarrhea and significantly reduced viral shedding (49, 50). Further research into how certain bacteria are able to aid the host in clearance of viral infections could be beneficial not only in understanding viral pathogenesis, but also in understanding relationships between viruses and bacteria in the gut.

Noroviruses and inflammatory bowel disease susceptibility

Commensal gut bacteria are important contributors to the pathophysiology of inflammatory bowel disease, and evidence suggests that the gastrointestinal microbiota of inflammatory bowel disease patients differ from healthy controls (5), with reduced

relative abundances of members of the *Bacteroidaceae* and *Lachnospiraceae* families (51). Recent evidence suggests that the contribution of microbes to inflammatory bowel disease extends beyond commensal bacteria to include enteric viruses. About 50% of individuals of European descent carry a mutant allele of the autophagy gene *Atg16L1*, which is a Crohn's disease susceptibility allele (52). A recent study using a mouse model with reduced *Atg16L1* function begins to explain the contributions of both viruses and bacteria to Crohn's disease susceptibility. Infection with a specific norovirus along with a full complement of gut bacteria was required for eliciting Crohn's disease-like pathology after intestinal injury was triggered in mice with reduced *Atg16L1* (53). In the absence of viral exposure or if the commensal bacteria were depleted with antibiotics, Crohn's disease-like inflammation did not develop, thus demonstrating that a complex web of microbial (viral and bacterial) and host factors underlie Crohn's disease. Although enteric viruses may not cause inflammatory bowel disease single-handedly, they have the potential to shape the host immune response and intestinal environment in a manner that promotes dysfunctional host-commensal interactions.

Gut bacterial viruses

Studies of human gut microbiota have revealed that coliphages (enteric bacterial viruses) infect many *Enterobacteriaceae* (*E. coli*, *Salmonella* spp, *Klebsiella* spp) and other *Bacteroidetes* and *Firmicutes* (54). Despite overwhelming evidence of viral-bacterial interactions in the human gut, the consequences of such interactions in the context of gastrointestinal disease have not been fully explored. Classical phage-bacterial host interactions are characterized by an evolutionary struggle for and against viral invasion. However, in the fecal microbial community of healthy humans, viral life cycles

tend to be temperate (non-lytic) with low variation over time, and with little genomic evidence of bacteria evolving mechanisms to prevent phage attachment and invasion (55). Enteric phages that are in constant contact with commensal bacteria in the gut have the potential to act in a commensal manner of their own and may confer growth advantages to their hosts (54). Several viral-like particles found in healthy human feces encode proteins involved in peptidoglycan synthesis, pyruvate and folate metabolism, and oxidative stress response (55). By introducing new genes and associated functions, viruses have the ability to change the microbiome of the gut. In light of recent findings that recognize associations between bacteria and human diseases, and between bacteria and viruses in the gut, future attention should be focused on the ways in which coliphages are able to shape the composition and function of commensal bacterial communities in the gastrointestinal tract.

Inflammatory bowel disease

Ulcerative colitis and Crohn's disease are the two main forms of inflammatory bowel disease and both are attributed to a combination of an individual's genetic susceptibilities, microbiota, and environment (56, 57). Ulcerative colitis and Crohn's disease are seen at higher rates in westernized countries and have been linked to factors such as stress, diet, medication and socioeconomic status (58). Despite some similarities, ulcerative colitis and Crohn's disease differ in several significant characteristics. In ulcerative colitis, inflammation occurs exclusively in the colon, while Crohn's disease can present throughout the gastrointestinal tract. Furthermore, ulcerative colitis and Crohn's disease differ in tissue pathology, genetic susceptibilities and therapeutic

treatment approaches (59). Ulcerative colitis has a greater incidence rate than Crohn's disease in the United States (60), with an estimated 15,000 new cases per year (61).

Currently there are 47 known risk loci associated with ulcerative colitis (62). Several mouse models have been used to recapitulate disease (56), including the acute dextran sulfate sodium (DSS) model, a sulfated polysaccharide that chemically induces barrier damage (63), and *IL-10*$^{-/-}$ or *IL-10R*$^{-/-}$ mice (64) that are missing gene products necessary for CD4^{+} T-regulatory cell maintenance of gut homeostasis (65). In the TRUC (*T-bet*$^{-/-}$ *Rag2*$^{-/-}$ ulcerative colitis) mouse model (66), *Rag2* (recombination activating 2) gene deletion leads to the loss of an adaptive immune response through disruption of VDJ recombination (67), which is necessary for the generation of B and T lymphocytes. Absence of *T-bet*, a transcription factor important for regulation of innate and adaptive proinflammatory responses (68), results in innate immune defects. In dendritic cells (DCs), *T-bet* binds the promoter of mouse TNFα (tumor-necrosis factor α) to repress TNFα transcription (66), and a consequence of *T-bet* loss is un-regulated production of TNFα by bone-marrow derived DCs.

IV. MOUSE MODELS AND MOLECULAR TOOLS USED TO STUDY MICROBIAL COMMUNITIES

Gnotobiotic mice and defined microbial communities

Understanding the role that individual bacteria play in the gastrointestinal tract, both in terms of host interactions and microbial community relationships, is difficult due to the complexity of the microbiota and redundancy in members and function. Tool advancements in the form of GF mice have revolutionized the way researchers can study

interactions between defined microbial communities and their hosts (69). GF mice are bred and maintained inside microisolators in a sterile environment. Modern GF facilities use a combination of techniques to ensure sterility of all equipment, food, and supplies including chlorine dioxide dunks, autoclaving, and ethylene oxide gas. Absence of microbes is confirmed with regular conventional culture and molecular tests on equipment swabs and mouse stool. Mouse lines can be derived GF via C-section of SPF females, dunking of the uterus into chlorine dioxide, and rearing of pups by a GF foster female.

While GF mice represent an ideal animal model for understanding interactions between single microbes and their host, animal development in a sterile environment leads to physiological deficiencies. GF mice gain weight more slowly than mice reared in the presence of microbes (specified pathogen-free, SPF) and increased calorie intake is required to maintain normal weight (70). These mice have abnormal Peyer's patches, lymph nodes, and spleens and their ceca are markedly larger in size. Development of the immune system is also impaired in GF mice with decreased numbers of mucosal and systemic immune cells and markedly reduced immunoglobulin-A levels in the colon (25).

In order to correct some of the defects observed in GF mice while maintaining an experimentally tractable microbiome, research groups have turned to the use of gnotobiotic mice with specific and defined bacterial inputs. In the 1960's, Russell Schaedler was the first to report colonizing gnotobiotic mice with a defined and reduced gut microbiota (71). A variation of the original flora, known commonly as the Altered Schaedler Flora (ASF), is used by many investigators to standardize gnotobiotic studies, allowing for environmental continuity between facilities and a reduction in community

complexity (72). ASF members are representative of abundant and functionally important gut bacteria in the healthy mouse microbiome, and are able to stimulate normal immune responses (73). Specifically, ASF mice show normal IgA secretion into the gut lumen and restoration of colonic T-regulatory cell populations. A practical advantage of an ASF microbiota is that all strains are culturable under anaerobic conditions. The ASF include the following bacterial species: *Clostridium* spp. (ASF356), *Lactobacillus* spp. (ASF360), *Lactobacillus murinus* (ASF361), *Mucispirillum schaedleri* (ASF457), *Eubacterium plexicaudatum* (ASF492), Firmicutes bacterium (ASF500), *Clostridium* spp. (ASF502), and *Parabacteroides* spp. (ASF519).

While the ASF has been used for many years, this community has a noted deficiency in *Bacteroidetes* and *Proteobacteria* in comparison to the human gut microbiota. Recently, groups have begun to refine defined consortia of bacteria for gnotobiotic colonization. Jeffrey Gordon and Andrew Goodman developed a defined gnotobiotic community composed of 14-bacteria to model the human colon; 6 *Bacteroidetes* spp., 7 *Firmicutes*, and an *Actinobacteria* (74) (**Table 1.1**). Koji Atarashi and Kenya Honda focused on the *Firmicutes*, and specifically the class *Clostridia*, in devising a human-derived microbial consortia (75).

16S rRNA gene survey for microbial community assessment

One of the biggest challenges of studying mixed microbial communities is defining which bacterial species are present. Before the advent of molecular techniques, standard culturing methods were needed to ask questions about microbial community composition. Despite hundreds of years of optimization of culturing methods, it is widely estimated that 99% of bacteria in a given environment remain unculturable. For the gut

Table 1.1. Defined microbial communities used in gnotobiotic mouse studies.

	ASF	**Goodman/Cordon Consortium**	**Clostridia cocktail**
Representing	Mouse gut microbiome	Human gut microbiome	Human Clostridia compartment
Firmicutes	*Clostridium* spp *Lactobacillus* spp *Lactobacillus murinus* *Eubacterium plexicaudatum* Firmicutes bacterium *Clostridium* spp	*Ruminococcus obeum* *Eubacterium rectale* *Dorea longicatena* *Clostridium symbiosum* *Clostridium spiroforme* *Clostridium scindens* *Ruminococcus torques*	*Clostridium asparagiforme* *Anaerotruncus colihominis* *Clostridiaceae* JC13 *Clostridium bolteae* *Clostridiales* 1_7_47FAA Lachnospiraceae 7 1 58FAA *Clostridium scindens* *Clostridium* 7 3 54FAA *Ruminococcus* sp. ID8 *Clostridium indolis* *Eubacterium fissicatena* *Clostridium ramosum* *Lachnospiraceae* 3_1_57FAA (2 isolates) *Clostridium* sp. 14774 *Blautia producta* *Clostridium hathewayi*
Bacteroidetes	*Parabacteroides* spp	*Parabacteroides distasonis* *Bacteroides WH2* *Bacteroides vulgatus* *Bacteroides uniformis* *Bacteroides thetaiotamicron* *Bacteroides ovatus* *Bacteroides caccae*	None
Proteobacteria	None	None	None
Actinobacteria	None	*Collinsella aerofaciens*	None
Deferribacteres	*Mucispirillum schaedleri*	None	None

microbiome, this number greatly decreases to 10% unculturability when anaerobic culturing techniques are combined with passage of human fecal communities through gnotobiotic mice (76), but the cost and time required for this dual approach can be prohibitive. *In vitro* culturing alone leaves 55% of species uncluturable.

In 1991 work from Norman Pace and colleagues demonstrated that PCR cloning and sequencing of the bacterial 16S ribosomal RNA (16S rRNA) gene from DNA extracted from bulk environmental samples could reveal phylogenetic diversity of mixed bacterial communities (77). The discriminative power of this approach is two-fold. First, ribosomal building blocks differ between Prokaryotes and Eukaryotes, allowing for selective amplification of conserved bacterial sequences in samples with Eukaryotic contamination, a principle pioneered by Carl Woese in 1977 (78). Second, the 16S rRNA component of the Prokaryotic 30S ribosomal subunit contains regions of discriminately significant variability between bacterial species (79). For analysis of bacterial community membership, PCR primers are designed to recognize a conserved region of the 16S rRNA gene and amplify across one or more of the nine hypervariable and discriminative regions. Depending on the hypervariable regions amplified, this approach can reveal genus level identification for all sequence reads within certain populations, and identification to the species level for a subset of sequences (79).

The sequencing technologies and platforms that have been used for 16S rRNA surveys are summarized in **Table 1.2**. Illumina, Life Technologies, and Roche all manufacture high throughput and benchtop machines that differ in read length, run capacity, and molecular technologies. While most early 16S surveys were performed using Roche's 454 Pyrosequencing platform, Illumina machines have captured the

majority market share in recent years due to their lower run costs, high accuracy, and large amount of data generated (80). Moving forward, Illumina machines will continue to gain market usage as Roche phases their 454 platform out of production.

Table 1.2. Sequencing technologies and platforms used for 16S rRNA amplicon surveys.

Company	Sequencing Platform	Technology Details	Notes
Illumina	HiSeq (high throughput)	—	Has generated 90% of the world's high throughput sequenced genetic material
	MiSeq (benchtop)	Read length: 300bp GB per run: 15 Reads per run: 30M	>50% market share in bench top sequencers; first FDA approved sequencing machine
Life Technologies	Ion Torrent PGM (benchtop)	Read length: 400bp GB per run: 2 Reads per run: 5M	FDA approved sequencing machine
	Ion Proton (benchtop)	Semiconductor chips to detect protons given off during nucleotide addition	—
	SOLiD (high throughput)	Sequencing by ligation	Overtaken by Illumina HiSeq
Roche	454 Pyrosequencing	Long read	Being phased out- production will stop by the end of 2015
	GS FLX (benchtop)	Read length: 700bp GB per run: 0.07 Reads per run: 0.1M	—

Computation tools for analysis of 16S rRNA amplicons

Depending on sequencing depth, 16S rRNA surveys can generate tens of thousands of reads per sample. Many computational analysis tools have been developed for processing and analyzing these large sequence datasets including QIIME (Quantitative Insights Into Microbial Ecology) to process sequences (81), PICRUSt (Phylogenetic Investigation of Communities by Reconstruction of Unobserved States) to predict metagenome and function from 16S sequences (82), and LefSe (Linear discriminant analysis Effect Size) to identify operational taxonomic units that are most likely to explain differences between classes (83). These tools have aided in a greater

understanding of microbial community membership and function across a diverse range of environments.

V. *KLEBSIELLA PNEUMONIAE* EPIDEMIOLOGY, TAXONOMY, AND ENVIRONMENTS

Klebsiella pneumoniae is a rod-shaped, Gram-negative species of *Proteobacteria* from the family *Enterobacteriaceae*. *K. pneumoniae* is a facultative anaerobe that was first observed by Edwin Klebs in 1875, and officially described in 1882 by Carl Friedlander as a bacterial cause of pneumonia (84). Since then, *K. pneumoniae* has been isolated from a diverse array of environments including water, soil, plants, and mucosal surfaces of mammals such as the skin, nasopharynx, lungs, mouth, urinary tract, and gastrointestinal (GI) tract (85). In the soil and in association with plants, *K. pneumoniae* is considered a plant growth promoting bacteria due to it's ability to fix nitrogen for uptake by plant roots (86). Conversely, *K. pneumoniae* is considered an opportunistic pathogen when associated with human hosts and is a common cause of pneumonia, urinary tract infections, bacteremia, liver abscesses and nosocomial infections (87).

K. pneumoniae virulence factors

K. pneumoniae has classically been studied from the context of virulence given this bacterium's role in disease. Several factors have been identified as virulence factors that aide in *K. pneumoniae*'s colonization of the host and evasion of immune defenses. These virulence factors include lipopolysaccharides (LPS), capsular polysaccharides (CPS), fimbriae, and siderophores (85).

LPS

LPS is common feature of Gram-negative bacteria and is the layer of extracellular polysaccharides anchored in the bacterial outer membrane by lipid A. A core oligosaccharide is covalently bound to lipid A on one side and the O-antigen on the other (88). Also known as endotoxin, LPS is a microbe-associated molecular pattern (MAMP) that is bound by toll-like receptor 4 (TLR4) on host immune cells including monocytes, dendritic cells, and macrophages. LPS can initiate a pro-inflammatory cascade and fever in mammalian hosts (89).

CPS

In addition to LPS, *K. pneumoniae* has another layer of extracellular polysaccharides known as CPS, or capsule. Over 80 capsule serotypes have been identified from *K. pneumoniae* isolates with several displaying increased virulence. Capsule serotypes K1 and K2 are especially virulent and cause severe liver abscesses in diabetic and immune compromised patients (90, 91). *K. pneumoniae* capsule consists of glucose, glucuronic acid, and 1 to 4 variable sugars (92). Variable sugars found within *K. pneumoniae* capsule include, mannose, rhamnose, and fucose (93). The presence of a capsule has been shown to protect *K. pneumoniae* from phagocytosis and complement opsonization, allowing evasion of the host's immune system (94). Non-mucoid variants (NMVs) of *K. pneumoniae*, which have reduced production of CPS, have been observed at low frequency *in vitro* (95) and at least once *in vivo* from a patient with a urinary tract infection (96). However, a role for these *K. pneumoniae* NMVs has not been defined *in vivo*. Since the majority of *K. pneumoniae* isolates recovered from both infected and

healthy humans are mucoid, there are likely advantages to capsule production outside of a virulence context.

K. pneumoniae capsule is encoded on single copy loci within the bacterial chromosome that ranges from 16-25 ORFs (93). The *K. pneumoniae* CPS locus is divided into three regions. Starting at the 5' end are a group of conserved genes, including *galF, orf2, wzi*- an outer membrane protein*, wza*- which forms a multimeric translocation channel*,* and *wzc*- a tyrosine autokinase*.* Protein products of these genes are involved in capsule polymer translocation from the inner membrane to the outer membrane. 6-10 isolate specific glycosyltransferases lie in the middle of the loci, along with the conserved glycosyltransferases *wbaP* and *wcaJ*. *WbaP* and *wcaJ* are responsible for transfer of sugar nucleotides to lipid receptors (97). Serotype specific glycosyltransferases are thought to connect repeating nucleotide sugar subunits to each other (97) and are a major source of variation between the many *K. pneumoniae* serotypes (93), although the exact role that each glycosyltransferase plays in capsule synthesis is undefined for *K. pneumoniae*. On the 3' end of the capsule loci are a set of genes whose protein products participate in modification of the nucleotide linked sugars. Conserved genes in this region include *ugd* and *uge,* which are involved in the synthesis of UDP-glucuronic acid from UDP-glucose (98). Variable genes in this region could include *manC/B* for synthesis of GDP-D-mannose, or *rmlA/C/D* for synthesis of dTDP-L-rhamnose (99).

Regulation of capsule production is complex and incompletely defined. Several master transcriptional regulators have been shown to influence CPS production in *K. pneumoniae*, including Fur. Fur activates CPS synthesis in environments with ample iron and represses synthesis in times of iron stress (100). In addition to Fur, *K. pneumoniae*

CPS production is also regulated by RcsBCD, a two-component phosphorylation cascade that leads to transcriptional activation at the CPS promoter in response to environmental stimuli. The RcsBCD two-component system can also be activated by RmpA, the protein product of *rmpA*, which is carried on the 180-kb virulence plasmid, pKP100 (101). Plasmid pKP100 is typically found in isolates of the virulent K1 and K2 serotypes. A second virulence plasmid, pLVPK contains both *rmpA* and *rmpA2*. RmpA2 is a transcriptional activator of the LuxR family and can bind with RcsB or directly to the CPS promoter to stimulate capsule production (101). While diverse capsule regulation mechanisms have been detailed, it is not clear how these multiple inputs are integrated by *K. pneumoniae*.

Fimbriae

K. pneumoniae are non-motile and lack flagella. However, they do have fimbriae, projections composed of curlin protein, extending from their outer membrane. These projections measure approximately 4.2 nanometers in diameter and 1.5um in length (102). Fimbriae contain adhesins that aide in the attachment of bacteria to each other and to host cells. Two fimbriae types have been observed in the *K. pneumoniae* genus, type 1 and type 3 (103). Type 1 fimbriae have been identified in many species of *Enterobacteriaceae* and are used by bacteria to adhere to the urogenital epithelium in a mannose dependent manner (104). Type 3 fimbriae have been found to agglutinate erythrocytes, are thought to play an important role in biofilm formation, and are mannose insensitive (105).

The presence of a capsule impedes the ability of fimbriae to adhere to neighboring cells. Several reports suggest that fimbriae and capsule may be opositionally regulated

and coordinated to both the anatomical location and stage of infection (106). Fimbriae are especially important in establishing urinary tract infections, but do not influence *K. pneumoniae*'s ability to colonize the gastrointestinal tract or nasopharynx (107).

Siderophores

While essential for bacterial growth, iron is limited under normal conditions in mammalian hosts and sequestered by host proteins including hemoglobin, transferrin, lactoferrin, and ferritin. For this reason, many bacteria produce siderophores- compounds with a strong affinity for iron that are released by bacteria and taken back up after they have acquired ferric iron and formed soluble Fe^{3+} compounds (108). *K. pneumoniae* produces several known siderophores, the most common being enterobactin (109). Hypervirulent isolates have been found to produce additional siderophores including yersiniabactin, salmochelin, and aerobactein. Aerobactin is particulary important in supporting both *ex vivo* growth and virulence of hypervirulent *K. pneumoniae* (110).

Klebsiella genome and plasmids

The advent of whole genome sequencing and analysis tools has significantly contributed to an understanding of genome structure and diversity with the *K. pneumoniae* species. On average, the *K. pneumoniae* genome is 5.3 mega base pairs. Of the 5,705 genes per genome (median), 1,743 are conserved across 328 isolates and are considered part of the core *K. pneumoniae* genome (111). Much of the large accessory genome shows evidence of acquisition through horizontal gene transfer due to altered G+C content relative to the core genome. These transfer events likely occurred with other bacterial species such as *Vibrio* and *Acinetobacter* (111).

Comparative genomics pipelines have been used to identify strain based virulence determinants in *K. pneumoniae* strains (112). A popular tool for comparative genomics is OrthoMCL(113), a graph-based Markov-clustering algorithm that allows parsing of proteomes into protein groups representing orthologs, paralogs and co-orthologs. A comparative genomics analysis of *K. pneumoniae* plasmids revealed similarities across isolate types that suggest a strong role for horizontal gene transfer in the genomic evolution of the species (114). Many of *K. pneumoiae*'s plasmids carry important virulence determinants, including the previously mentioned plasmids pkP100 and pLVPK, which are involved in regulation of capsule production.

Antibiotic resistance of *K. pneumoniae*

Antibiotic resistant *K. pneumoniae* represents a large and recent threat to human health. The first *K. pneumoniae* isolate with resistance to a broad range of antibiotics was discovered in 1996 in a patient from North Carolina (115). This isolate produced *Klebsiella pneumoniae* carbapenemase (KPC), conferring weak resistance to carbapenems, which are beta lactam antibiotics widely used to treat bacterial infections. *Enterobacteriaceae* carrying plasmid-encoded New Delhi metallo-β-lactamase 1 (NDM-1) were later observed in 2010 in Taiwan (116). Unlike KPC, NDM-1 producing *K. pneumoniae* are strongly resistant to carbapenems. While Asian countries remain the hotbed of NDM-1 producing isolates (top three: Indonesia, Vietnam, and Philippines), resistance has spread rapidly world-wide and infections are now reported throughout North America, South America, and Europe.

While carbapenem resistance can be transferred between and among many species of *Enterobacteriaceae*, *K. pneumoniae* represents the largest reservoir and accounts for

39% of carbapenem-resistant *Enterobacteriaceae* in Asia, followed by *E. coli* with 22% (117). In 2013, the US Centers for Disease Control classified carbapenem-resistant *K. pneumoniae* as an urgent threat, giving it the highest threat level amongst drug-resistant bacteria (115). Recent epidemiology studies suggest an incidence rate of carbapenem-resistant *K. pneumoniae* infections in 2.93 out of 100,000 people in the US (118) and clusters of infections are beginning to manifest in clinical settings. In the most well documented outbreak in the US, 18 infections and 6 deaths were attributed to carbapenem-resistant *K. pneumoniae* at the US National Institutes of Health Clinical Center (119). Genomic comparisons from infected patients suggested a single patient origin with 3 independent transmission events between patients. Complicating transmission of antibiotic resistant *K. pneumoniae* further is the fact that this bacteria is carried by healthy humans in the gastrointestinal tract. Recently it was found that gut colonization by KPC producing *K. pneumoniae* is a risk factor with an odds ratio of 13.33 for mortality in diabetic patients with foot infections (120).

K. pneumoniae in the gastrointestinal tract

An estimated 5-38% of the general population carries *K. pneumoniae* in their gastrointestinal tract and these numbers increase in hospital settings where up to 77% of caregivers and patients are *K. pneumoniae* positive (85). Regions of East Asia, such as Taiwan, also report these higher GI carriage rates in healthy populations (121). Epidemiological work following diabetic patients with liver abscesses and foot infections suggest that GI carriage predisposes people to infection and serves as a general reservoir for *K. pneumoniae* disease (122, 120). Similarly, gut colonization by *K. pneumoniae* has been shown to precede bloodstream infections in patients undergoing stem cell

transplantation (123). While *K. pneumoniae* has not been implicated in driving inflammatory bowel disease or other infections in the gastrointestinal tract, patients with Crohn's disease have high antibody responses against *K pneumoniae* (124).

Signature tagged mutagenesis identified several genes that are necessary for colonization of the gastrointestinal tract by *K. pneumoniae* (125). Of particular importance are genes involved in metabolism, including glucose and nitrogen metabolism and urea utilization. Mutation of an uncharacterized adhesion attenuates both colonization and attachment to human epithelial cells *in vitro* (125). In mice, *K. pneumoniae* can be found in increasing numbers descending the small intestine and into the colon (126). Regardless of intestinal geography, *K. pneumoniae* is most abundant in the luminal content adjacent to the intestinal epithelium (126).

Gaps in understanding and rationale for this work

A murine isolate of *K. pneumoniae* is able to drive colonic inflammation in mice (127), but a role for this bacterium in driving inflammatory bowel disease in humans is undefined. **Chapter 2** details our aim to further investigate the inflammatory potential of *K. pneumoniae* in the gastrointestinal tract with a diverse panel of murine and human clinical isolates.

In addition, while several studies have attempted to define *K. pneumoniae* colonization factors in the gastrointestinal tract, screens have not been saturating and the role of bacterial competition with other members of the microbiome have been overlooked. For example, there have been contradictory data on the role of capsule when *K. pneumoniae* colonizes the gastrointestinal tract (128-130). Most recently, encapsulated *K. pneumoniae* and mutants with decreased capsule production were found to have

equivalent gastrointestinal colonization levels as measured by fecal bacterial counts in streptomycin treated mice (129). Streptomycin treated mice harbor a microbiota reduced in complexity and diversity, presenting less colonization resistance than a healthy microbiota. This suggests that capsule may play a role in successful and competitive interactions with other bacteria in the gut. **Chapter 3** investigates the role of both host factors and bacterial competition on capsule population dynamics of *K. pneumoniae* throughout the gastrointestinal tract.

CHAPTER 2

KLEBSIELLA PNEUMONIAE AND DISEASE: ASSESSING STRAIN-DEPENDENT VIRULENCE AND DEFINING THE MINIMAL MICROBIAL COMMUNITY NECESSARY FOR DISEASE INDUCTION

I. ATTRIBUTIONS

Leslie Wardwell-Scott performed all experiments and analyses, except as follows: the *Klebseilla* sequencing group at the Broad Institute performed whole genome sequencing of *K. pneumoniae* strains. Qiandong Zeng of the Broad Institute annotated whole genomes. Comparative genomic analyses (**Figure 2.5, 2.5**) were performed in collaboration with Ashlee Earl and Abigail McGuire of the Broad Institute. 16S rRNA amplicon sequencing was undertaken by Research and Testing in Lubbock, Texas (**Figures 2.7, 2.8**). Tissue samples were sectioned and stained by the Histopathology Core at Harvard Medical School and sections were analyzed for inflammation by pathologists Jonathan Glickman and Roderick Bronson (**Figure 2.2**).

II. ABSTRACT

Klebsiella pneumoniae is an opportunistic pathogen that causes several human diseases including pneumonia, urinary tract infections, bacteremia, and liver abscesses. There is a high degree of genetic diversity within the *K. pneumoniae* species, and many of these differences relate to an isolate's virulence potential in certain infection models. In this chapter, we characterized four isolates of *K. pneumoniae* taken from both mouse and human host environments. Whole genome sequencing and comparative genomics revealed genome level differences in *K. pneumoniae* depending on host organism (human or mouse) and host anatomical location (stool, sputum, or urine).

To assess the role of intra-species genomic diversity on interactions with the host, these *K. pneumoniae* isolates were studied in the *T-bet*$^{-/-}$ *Rag2*$^{-/-}$ and dextran sodium sulfate models of ulcerative colitis and in a mouse model of systemic neonatal infection.

Despite genome diversity, *K. pneumoniae* isolates did not differ in their ability to stimulate colonic inflammation. Additionally, *K. pneumoniae* was unable to drive ulcerative colitis in germ-free mice or in gnotobiotic mice stably colonized with 8 bacterial species, suggesting importance of a full microbiota for *K. pneumoniae* driven virulence in the gastrointestinal tract.

While there was no differential virulence of *K. pneumoniae* isolates in the adult mouse colon, exposure to murine *K. pneumoniae,* but not human clinical isolates, led to neonatal death. In addition, this isolate induced differential shifts in levels of other *Enterobacteriaceae* species in the colon. More murine *K. pneumoniae* was found in host mesenteric lymph nodes compared to human isolates, suggesting subtle strain-based differences that affect response to *K. pneumoniae* in the gastrointestinal tract.

III. INTRODUCTION

The recovery of *K. pneumoniae* from many environmental and host sites suggests a significant degree of diversity within the species. For example, the genomic content necessary for successful colonization of the gastrointestinal tract is likely to be distinct from functions necessary for bacterial interactions and nitrogen fixing abilities in the plant rhizosphere. Many studies have attempted to reveal genome level *K. pneumoniae* strain-based differences with the use of unbiased comparative genomic approaches (111, 112, 131). Hybridization techniques comparing 15 clinical *K. pneumoniae* strains identified genomic signatures of putative virulence factors that correlated with severity of infection *in vivo* (112). In the largest *K. pneumoniae* comparative genomics endeavor to

date, analysis of 288 strains revealed such a high level of diversity that the species could be divided into three distinct phylotypes (111).

While comparative genomics has revealed strain based virulence determinants in liver abscess and meningitis causing *K. pneumoniae* strains (112), comparative virulence potential has not been assessed in models of ulcerative colitis or neonatal infection. In this work we interrogate the role of *K. pneumoniae* isolated from inflamed *T-bet*$^{-/-}$ *Rag2*$^{-/-}$ mice in the context of ulcerative colitis and neonatal infection with comparative genomics of 4 *K. pneumoniae* isolates taken from diverse host environments. *In vivo* differential virulence studies were conducted using *T-bet*$^{-/-}$ *Rag2*$^{-/-}$ and *Rag2*$^{-/-}$ mouse models of ulcerative colitis and neonatal infection.

Necrotizing enterocolitis (NEC) is a gastrointestinal disorder affecting preterm infants and causing death in 16-42% of those afflicted (132). Inflammation is thought to result following translocation of intestinal bacteria across the epithelium in preterm infants with an underdeveloped gastrointestinal tract and compromised mucosal immunity (133, 134). *K. pneumoniae* has been associated with NEC in human infants (135) and is also known to drive NEC-like intestinal inflammation in neonatal mouse models (136). In this work we devise a model of neonatal infection mimicking the underdeveloped immune system of preterm infants by inoculating *Rag2*$^{-/-}$ pups at birth.

To study gastrointestinal inflammation in adult mice, we employed the *T-bet*$^{-/-}$ *Rag2*$^{-/-}$ mouse model, which is an applicable tool for studying ulcerative colitis due to its high disease penetrance and features resembling human ulcerative colitis, such as mono- and polymophonuclear cell infiltrates of the lamina propria, neutrophil infiltration of crypts, and epithelial injury restricted to the colon (66). Furthermore, increased colonic

tumor necrosis factor α (TNFα) levels are typical of human and *T-bet*$^{-/-}$ *Rag2*$^{-/-}$ colitis and both forms of the disease can be ameliorated by anti-TNFα therapy. In *T-bet*$^{-/-}$ *Rag2*$^{-/-}$ mice, increased TNFα is driven by the absence of *T-bet*, which normally acts as a transcriptional activator of cytokine expression.

Another similarity between *T-bet*$^{-/-}$ *Rag2*$^{-/-}$ and human ulcerative colitis is the importance of bacteria in perpetuating aberrant immune responses. Conventional culture from stool identified 7 bacterial strains unique to *T-bet*$^{-/-}$ *Rag2*$^{-/-}$ compared to *Rag2*$^{-/-}$ and wild-type (WT) mice (127). Of these seven, *K. pneumoniae* and *Proteus mirabilis* showed identical sensitivity profiles to antibiotics able to ameliorate colitis *in vivo*. *K. pneumoniae* and *P. mirabilis,* individually and in combination, were able to induce colitis in *Rag2*$^{-/-}$ and WT mice (127). Although to date no published studies link *K. pneumoniae* to human ulcerative colitis, subsets of patients with Crohn's disease show increased antibody responses against *K. pneumoniae* compared to healthy controls (124), and 16S profiling from biopsies of Crohn's disease patients indicate the presence of *K. pneumoniae* (137). While not specifically focused on ulcerative colitis, these studies justify examining *K. pneumoniae* in the setting of inflammatory bowel disease.

Although able to colonize the colon, a combination of *K. pneumoniae* and *P. mirabilis* is unable to cause colitis in gnotobiotic *T-bet*$^{-/-}$ *Rag2*$^{-/-}$ mice (127), highlighting the importance of interactions between these *Enterobacteriaceae,* other resident members of the microbiota, and the host immune system. Based on reports suggesting that gnotobiotic mice associated with the Altered Schaedler Flora (ASF) display active immune responses (73), we hypothesized that a combination of ASF strains plus *K. pneumoniae* and *P. mirabilis* would cause colitis in gnotobiotic *T-bet*$^{-/-}$ *Rag2*$^{-/-}$ mice.

Alternatively, the ASF may represent too minimalistic a gut microbiota, and other features not represented in this consortium may be needed for *K. pneumoniae* and *P. mirabilis* to induce inflammation.

IV. RESULTS

K. pneumoniae isolates do not vary in their ability to incite inflammation in the colons of specified pathogen-free *Rag2*$^{-/-}$ mice.

K. pneumoniae is enriched in the gastrointestinal tract of TRUC mice compared to *Rag2*$^{-/-}$ and WT mice (127). However, when *K. pneumoniae* WGLW5, isolated from *T-bet*$^{-/-}$ *Rag2*$^{-/-}$ mice, is fed regularly to specified pathogen-free (SPF) *Rag2*$^{-/-}$ and WT mice, colitis develops (127). In order to assess the contribution of *K. pneumoniae* to colonic inflammation, we obtained three human clinical isolates of *K. pneumoniae* taken from patient urine, sputum, and stool (three independent patients). All patients were sick at time of culture. Culture of *K. pneumoniae* WGLW5 and these three human clinical isolates on MacConkey agar revealed a shared mucoid phenotype with varying degrees of mucoviscosity as assessed by the sting test (138) (**Figure 2.1**). Hypermucoviscosity is defined by the formation of a viscous capsule string, at least 10mm in length, when a bacteriological loop is lifted away from a colony on agar (139). While all four isolates produced a thick, visible capsule, WGLW2 was the only isolate that did not display a hypermucoviscosity capsule phenotype. WGLW5 consistently produced the longest string throughout all experiments and manipulations.

K. pneumoniae isolates resuspended in PBS were fed from pipette tips to 4-week old SPF *Rag2*$^{-/-}$ mice every third day for 8 weeks (**Figure 2.2A**). Upon sacrifice, colons were fixed in paraformaldehyde, paraffin embedded, sectioned, and stained with

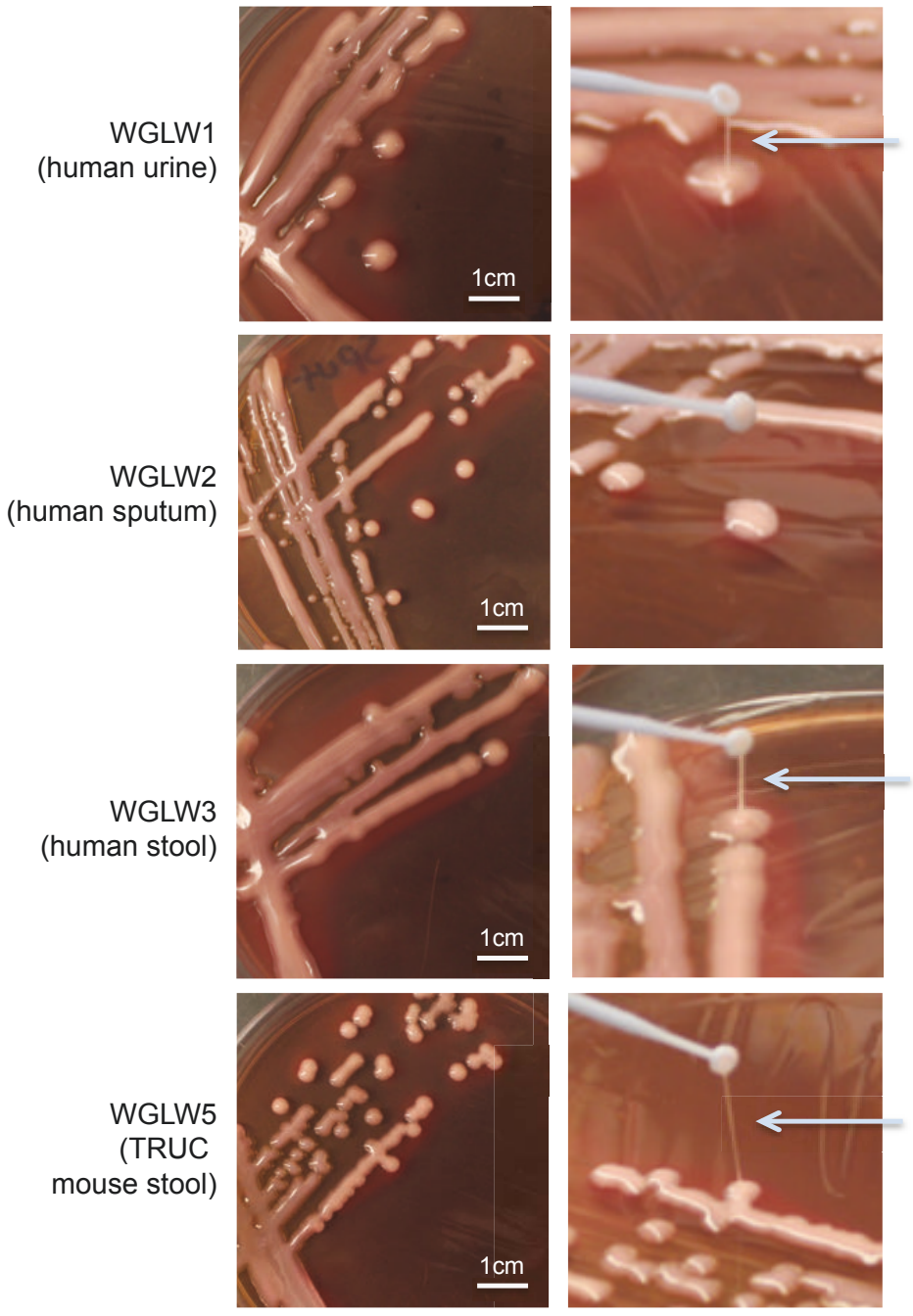

Figure 2.1. Mouse and human clinical *K. pneumoniae* isolates on MacConkey agar. Overnight growth at 37°C. Right panel, string test showing hypermucoviscosity phenotype (arrows).

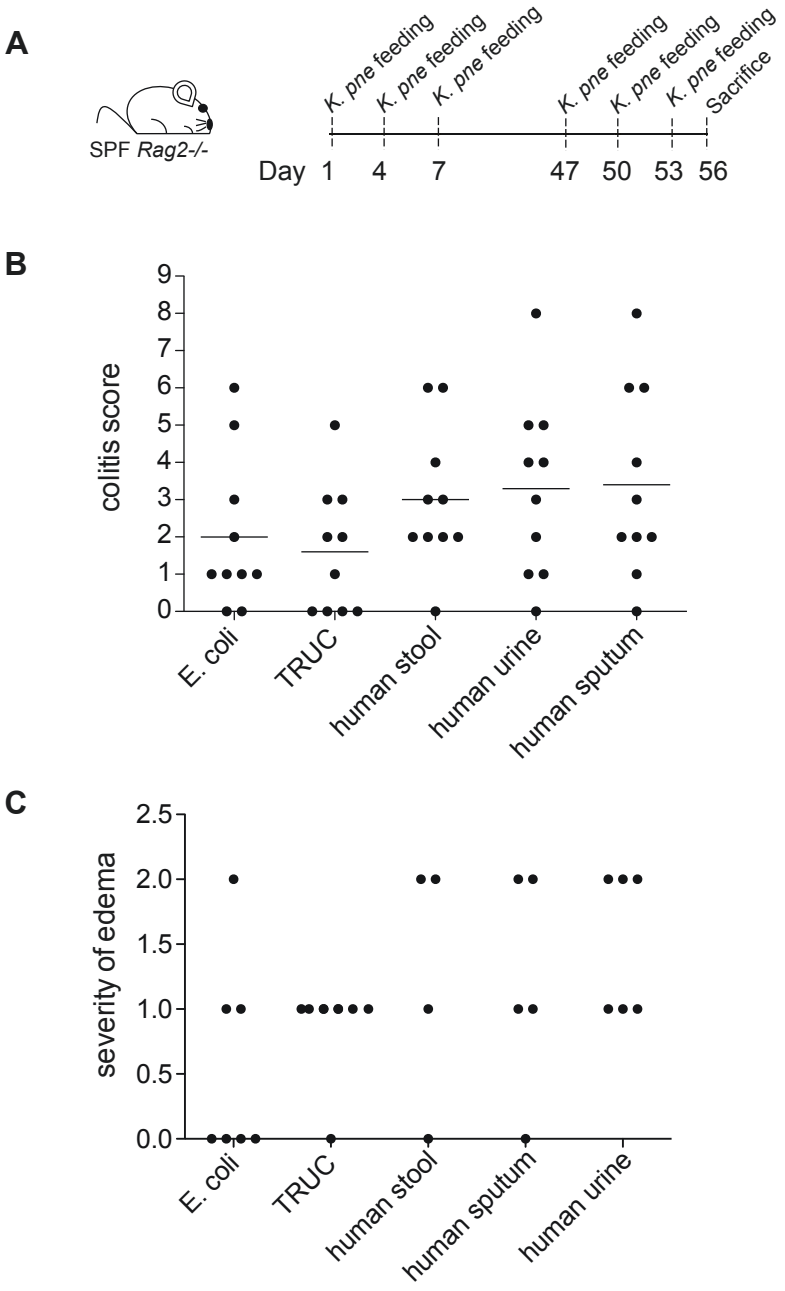

Figure 2.2. *K. pneumoniae* isolates do not significantly differ in their ability to initiate colonic inflammation. (A) Experimental schema for *K. pneumoniae* feeding of SPF *Rag2*$^{-/-}$ mice. Beginning at 4-weeks of age, mice were fed 1.5x10^{8} CFU *K. pneumoniae* isolate in 25 μl PBS every third day for 8 weeks. Mice were sacrificed and colons were processed for histology on day 56. **(B)** Cumulative colitis score for mice fed *K. pneumoniae* isolates. 0-3 score each for crypt hyperplasia, mononuclear cell infiltrates, polymorphonuclear cell infiltrates, and epithelial injury. Each group n=10. No significant difference between groups, Mann-Whitney test. **(C)** Edema score for a random subset of mice in (B). No significant difference between groups, Mann-Whitney test. TRUC is *K. pneumoniae* WGLW5.

hematoxylin and eosin. Two independent pathology score systems revealed no significant differences in colitis metrics between mice fed any of the 4 *K. pneumoniae* isolates or an *E. coli* control (**Figure 2.2B and C**).

Differential virulence of *K. pneumoniae* in a mouse model of neonatal infection.

In order to assess the virulence of *K. pneumoniae* isolates outside of the gastrointestinal tract, we devised a systemic neonatal infection model. *Rag2*$^{-/-}$ pups were cutaneously inoculated close to the mouth (termed "sprinkled") with $1.3x10^8$ CFU *K. pneumoniae* isolates in 20 µl PBS daily for 8 days beginning on the day of birth. Pups sprinkled with human stool, sputum, or urine *K. pneumoniae* isolates displayed 100% survival over the course of the experiment. In contrast, pups sprinkled with *K. pneumoniae* WGLW5 had a 30% mortality rate (**Figure 2.3A**). To confirm spread of *K. pneumoniae* beyond the gastrointestinal and genitourinary tracts, spleens and livers were aseptically removed from three pups undergoing *K. pneumoniae* WGLW5 sprinkling. One of the pups had been dead for less than 4 hours. The other two pups were littermates- one appeared sickly in movement, color, and growth while the other appeared healthy. As expected, the healthy pup had 100-fold lower *K. pneumoniae* counts in the spleen and 20-fold lower counts in the liver as compared to sickly and dead pups, confirming the presence of systemic *K. pneumoniae* infection driven by neonatal sprinkling of bacteria (**Figure 2.3B**).

Pups surviving early life *K. pneumoniae* inoculation (**Figure 2.3A**) were assessed for stable *K. pneumoniae* gastrointestinal colonization 7-weeks after their final *K. pneumoniae* exposure. While all *K. pneumoniae* isolates stably colonized the gastrointestinal tract of these mice, only *K. pneumoniae* WGLW5 sprinkling led to a

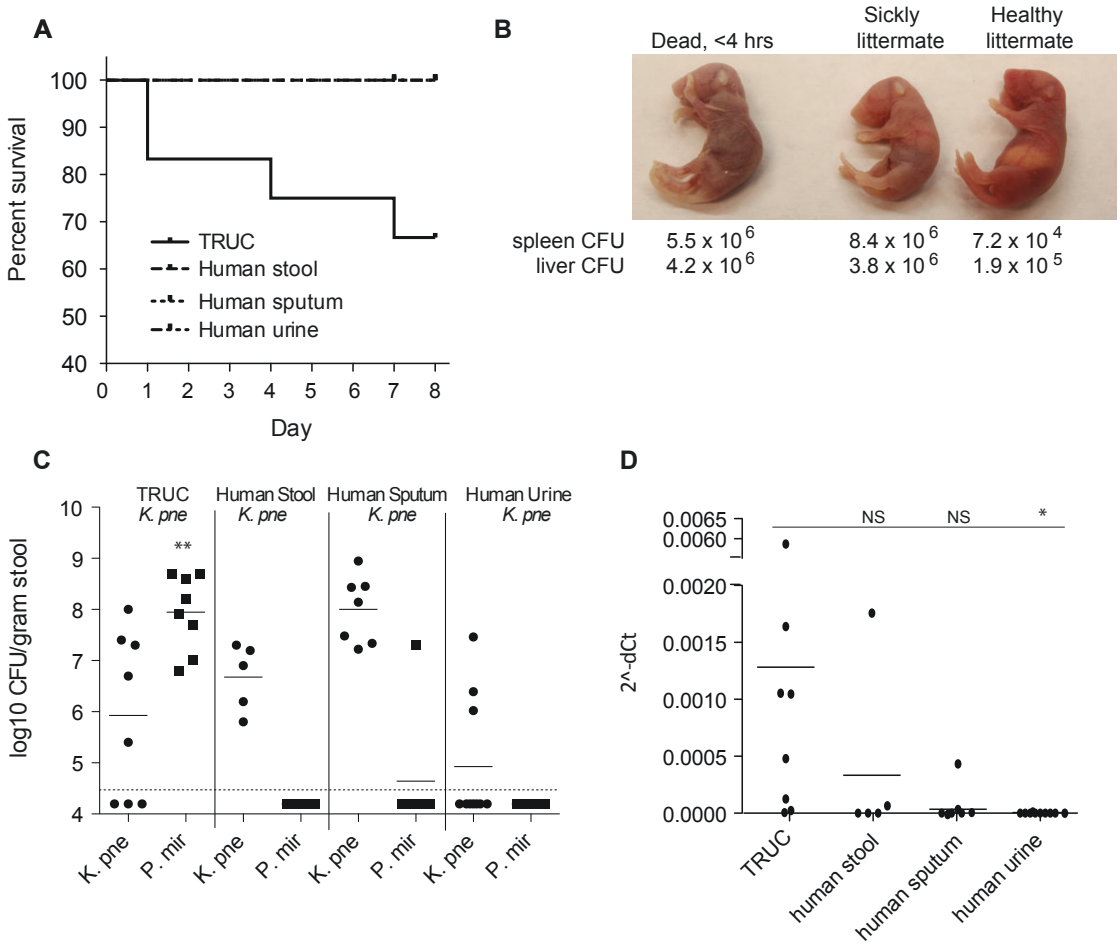

Figure 2.3. TRUC *K. pneumoniae* WGLW5 induces systemic neonatal infection and stably colonizes survivors. (A) Survival curve of *Rag2*$^{-/-}$ pups sprinkled daily with 1.3x10^{8} CFU *K. pneumoniae* isolate in 20 µl PBS. *K. pneumoniae* WGLW5 n=12, human sputum *K. pneumoniae* n=7, human stool *K. pneumoniae* n=5, human urine *K. pneumoniae* n=10. **(B)** *K. pneumoniae* CFU counts were assessed from the spleen and liver of *K. pneumoniae* WGLW5 sprinkled pups. Left- pup dead for less than 4 hours, middle- a sickly pup, and right- its healthy littermate. **(C)** CFU counts of *K. pneumoniae* and *P. mirabilis* from stool of 2-month old pups that survived the *K. pneumoniae* sprinkling in (A). **(D)** *K. pneumoniae* load in the mesenteric lymph nodes of 2-month old pups in (C) as assessed by *K. pneumoniae* 23S expression relative to total 16S (QPCR). Mann-Whitney statistical test, * $P \leq 0.05$. ** $P \leq 0.01$. TRUC is *K. pneumoniae* WGLW5.

concurrent colonic bloom of *P. mirabilis* as measured by CFU counts on MacConkey agar (**Figure 2.3C**), suggesting strain based differences between mouse and human derived isolates of the same bacterial species, with the caveat of small samples sizes of *K. pneumoniae* isolates in these experiments. In addition, only *K. pneumoniae* WGLW5 sprinkled mice had detectable levels of *K. pneumoniae* in their mesenteric lymph nodes by real-time quantitative PCR (**Figure 2.3D**).

Comparative genomics of *K. pneumoniae* isolates reveals genome level differences.

Based on the differential virulence capacity of *K. pneumoniae* WGLW5 in the neonatal infection model and long-term gastrointestinal colonization dynamics compared to human clinical isolates (**Figure 2.3**), we sought to assess the genomic diversity amongst *K. pneumoniae* strains. Whole genome sequences were generated for our 4 *K. pneumoniae* isolates on an Illumina MiSeq by the Broad Institute through the *Klebsiella* group Sequencing Project. Genomes were annotated with Prodigal (140). For comparison to a broad range of *K. pneumoniae* isolates, 5 published genomes were re-annotated with Prodigal. The final group of *K. pneumoniae* genomes consisted of 7 human isolates, an environmental isolate, and a mouse isolate (**Table 2.1**). Genome size fell between 5.33 and 5.92 Mb, corresponding to 5,069 - 5,448 predicted genes (**Table 2.1**).

Following annotation, genomes were translated to proteomes and matched to protein databases using BLASTP (http://blast.ncbi.nlm.nih.gov). OrthoMCL, a graph-based Markov-clustering algorithm (113), was then used to parse proteomes into protein groups representing orthologs, paralogs, and co-orthologs (141). By default, proteins that did not fall into clusters of orthologs represented the auxiliary genome of each *K. pneumoniae* isolate. Based upon the presence and absence of predicted proteins called by

Table 2.1. *K. pneumoniae* genome details for comparative genomics study.

***K. pneumoniae* Genome**	**Source Site**	**Location**	**Size (Mb)**	**GC%**	**Predicted Genes (#)**
WGLW1	human urine	Boston, MA	5.55	57.3	5,170
WGLW2	human sputum	Boston, MA	5.75	56.9	5,292
WGLW3	human stool	Boston, MA	5.55	57.3	5,159
WGLW5	TRUC stool	Boston, MA	5.82	56.8	5,448
342	*Zea mays* root	UK	5.92	56.9	5,936
HS11286	human sputum	China	5.33	57.5	5,404
NTUH-K2044	human liver abscess	Taiwan	5.47	57.4	5,386
1084	human liver abscess	Taiwan	5.39	57.4	5.069
MGH78578	human sputum	Boston, MA	5.69	57.2	5,305

orthoMCL, a heatmap was constructed to visualize relationships between isolates (**Figure 2.4A**). Unexpectedly, *K. pneumoniae* WGLW5 was most closely related to human sputum isolates, and more distantly related to those from stool or urine. An independent maximum likelihood phylogeny tool, RAxML (Randomized Axelerated Maximum Likelihood (142)), confirmed the relationship between WGLW5 and human sputum *K. pneumoniae* (**Figure 2.4B**).

OrthoMCL revealed that the majority of predicted proteins were shared by *K.pneumoniae* isolates from diverse environments (core proteome in blue, **Figure 2.5**). *K. pneumoniae* WGLW5 had the largest auxiliary proteome with 886 non-core proteins and 445 unique predicted proteins. Venny (http://omictools.com/venny-s6319.html) was used to compare orthoMCL clusters between *K. pneumoniae* WGLW5 and the 3 human clinical isolates from **Figure 2.2** and **2.3**. This analysis revealed 74 proteins with annotated KEGG gene pathways or Pfam protein domains that were unique to *K. pneumoniae* WGLW5 and 44 unique to the human clinical isolates (**Table 2.2**). Included among the cluster unique to WGLW5 were proteins involved in conjugation, toxin anti-toxin systems, phage, heavy metal resistance, secretion systems, and metabolism. The presence of genes encoding these predicted proteins may contribute to the differential

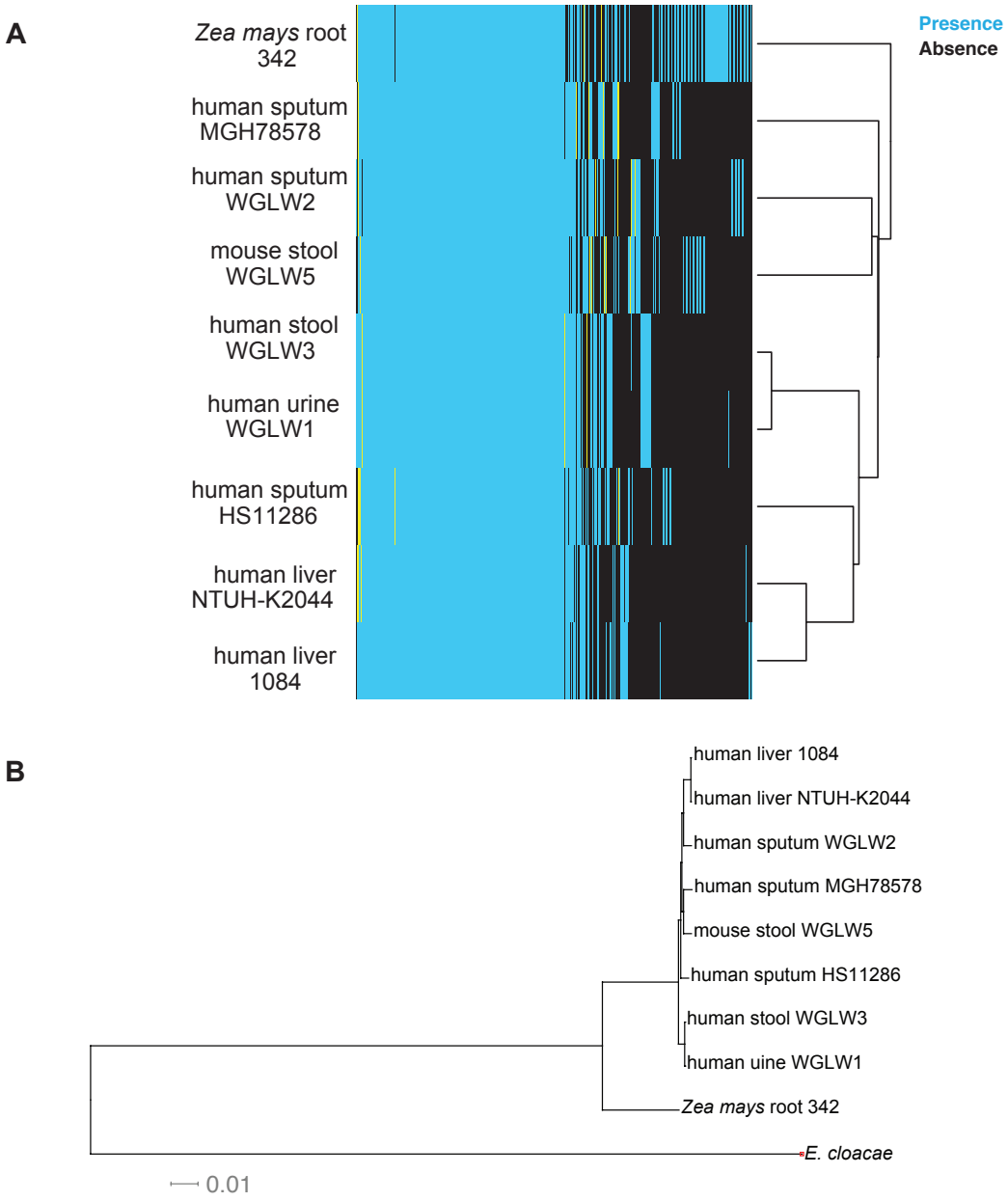

Figure 2.4. Relationships between 9 *K. pneumoniae* isolates based on comparative genomics from whole genome sequence. (A) Heatmap and relatedness tree based on predicted protein presence and absence parsed via orthoMCL. Blue lines denote protein presence; black lines represent protein absence. **(B)** RAxML phylogenetic tree of 9 *K. pneumoniae* isolates anchored by an *E. cloacae* genome.

virulence and gastrointestinal colonization potential observed for *K. pneumoniae* WGLW5 in comparison to human clinical isolates in specified pathogen-free (SPF) mouse models. It is also likely that the 494 predicted hypothetical proteins unique to TRUC contribute to these behaviors. Further analysis of these uncharacterized proteins is necessary to fully understand the unique activity of *K. pneumoniae* WGLW5 in mouse models.

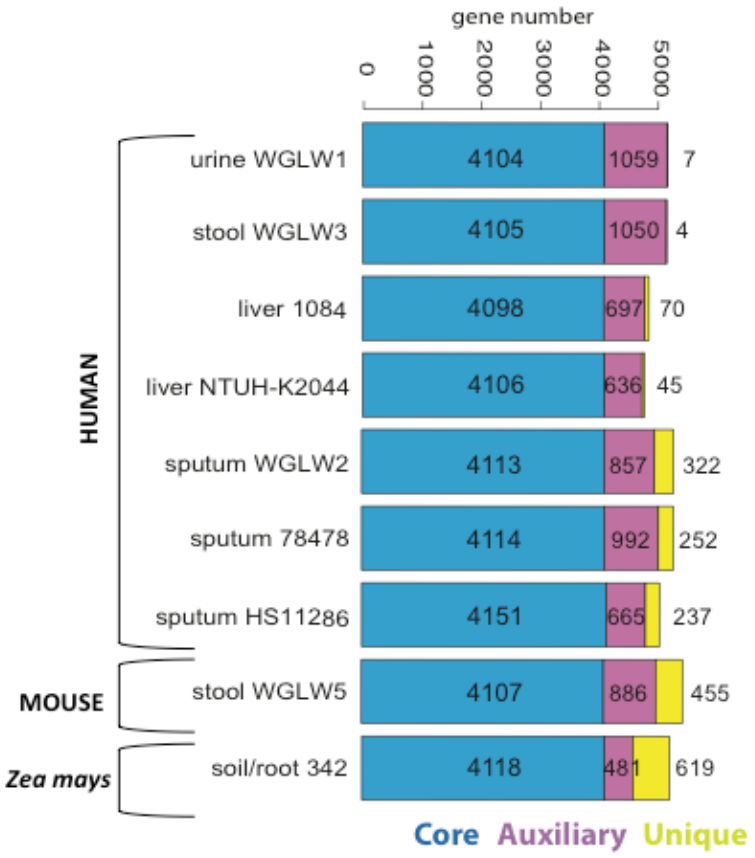

Figure 2.5. OrthoMCL gene clusters of 9 *K. pneumoniae* isolates. Core genome in blue, auxiliary genome in purple, and unique genome in yellow.

Table 2.2. Differential predicted proteins identified by OrthoMCL between *K. pneumoniae* isolates.

Predicted proteins present in WGLW5 and absent from WGLW1, 2, 3		Predicted proteins present in WGLW1, 2, 3 and absent from WGLW5
acetaldehyde_dehydrogenase__acetylating_	major_tail_sheath_protein	aromatic_amino_acid_aminotransferase
acetate_CoA_transferase_subunit_alpha	major_tail_tube_protein	aromatic_amino_acid_transporter_AroP
acetate_CoA_transferase_subunit_beta	membrane_fusion_protein_RaxA	betaine_carnitine_choline_transporter__BCCT__family_transporter
acetoacetate_metabolism_regulatory_protein_AtoC	mercuric_resistence_transcriptional_repressor_protein_MerD	D_3_phosphoglycerate_dehydrogenase
altronate_oxidoreductase	molybdenum_pterin_binding_domain_containing_protein	diguanylate_cyclase__GGDEF__domain_containing_protein
aminoglycoside_3__phosphotransferase	mRNA_interferase_PemK	dihydrolipoyl_dehydrogenase
antitoxin_PemI	NodT_family_efflux_transporter__outer_membrane_factor__OMF	fructose_bisphosphate_aldolase__class_I
arsenate_reductase	P_type_conjugative_transfer_ATPase_TrbB	glutathione_S_transferase
chlorophyll_synthesis_pathway_protein_BchC	P_type_conjugative_transfer_protein_TrbG	glycerol_uptake_operon_antiterminator
chromate_ion_transporter__CHR__family_chromate_transporter	P_type_conjugative_transfer_protein_TrbJ	IS605_OrfB_family_transposase
conjugative_transfer_signal_peptidase_TraF	P_type_conjugative_transfer_protein_TrbL	L_xylulokinase
DGQHR_domain_containing_protein	PBSX_family_phage_portal_protein	LacI_family_transcriptional_regulator
diguanylate_cyclase__GGDEF__domain_containing_protein	PFL2_glycerol_dehydratase_family_glycyl_radical_enzyme	low_calcium_response_locus_protein_S
dihydrofolate_reductase_type_A13	phage_baseplate_assembly_protein_V	LuxR_family_transcriptional_regulator__maltose_regulon_positive_regulatory_protein
dihydropteroate_synthase_type_1	phage_tail_tape_measure_protein__TP901_family__core_region	lysozyme
DNA__cytosine_5___methyltransferase	phage_virion_morphogenesis_protein	MFS_transporter__ACS_family__glucarate_transporter
DNA_adenine_methylase	plasmid_transfer_ATPase_TraJ	O_antigen_export_system_ATP_binding_protein_RfbB
DNA_adenine_methylase	portal_protein	O_antigen_export_system_permease_rfbA
DNA_repair_protein_RadC	quaternary_ammonium_compound_resistance_protein_qacE	outer_membrane_usher_protein
DNA_repair_protein_RadC	RelB_DinJ_family_addiction_module_antitoxin	ParB_like_partition_protein
efflux_transporter__RND_family__MFP_subunit	RelB_DinJ_family_addiction_module_antitoxin	phosphoglycerate_dehydrogenase
general_secretion_pathway_protein_S	replication_A_protein	protein_samA
glycyl_radical_enzyme_activating_protein_family	short_chain_fatty_acids_transporter	protein_TolA
His_Glu_Gln_Arg_opine_family_amino_ABC_transporter	signal_transduction_histidine_protein_kinase_AtoS	PTS_system__galactitol_specific_IIC_component
His_Xaa_Ser_repeat_protein_HxsA	single_stranded_DNA_binding_protein	pyruvate_dehydrogenase_complex_dihydrolipoamide_acetyltransferase
His_Xaa_Ser_system_radical_SAM_maturase_HxsB	small_GTP_binding_protein_domain	pyruvate_dehydrogenase_E1_component_subunit_alpha
His_Xaa_Ser_system_radical_SAM_maturase_HxsC	sugar_porter__SP__family_MFS_transporter	pyruvate_dehydrogenase_E1_component_subunit_beta
HK97_family_phage_major_capsid_protein	toxin_YkfI	ribokinase
HK97_family_phage_prohead_protease	transposase	ribose_transport_system_substrate_binding_protein
HK97_gp10_family_phage_protein	transposase_insC_for_insertion_element_IS2H	simple_sugar_transport_system_ATP_binding_protein
inner_membrane_protein_yagU	transposase_insD_for_insertion_element_IS2A_D_F_H_I_K	simple_sugar_transport_system_ATP_binding_protein
insertion_element_IS1_8_protein_insB	transposase_insF_for_insertion_sequence_IS3C	simple_sugar_transport_system_permease

Table 2.2. Continued.

integrase_recombinase	transposase_insH_for_insertion_sequence_element_IS5Y	simple_sugar_transport_system_permease
L_galactonate_transporter	transposon_Tn3_resolvase	simple_sugar_transport_system_permease
lambda_family_phage_tail_tape_measure_protein	type_I_restriction_enzyme_EcoprrI	simple_sugar_transport_system_substrate_binding_protein
lambda_family_phage_tail_tape_measure_protein	type_I_restriction_enzyme_EcoprrI_M_protein	single_stranded_DNA_binding_protein
major_capsid_protein	VirB4_family_type_IV_secretion_conjugal_transfer_ATPase	stable_plasmid_inheritance_protein
		succinyl_diaminopimelate_desuccinylase
		thiaminase__transcriptional_activator_TenA_
		transposase_insC_for_insertion_element
		TraR_family_phage_conjugal_plasmid_C_4_type_zinc_finger_protein
		UDP_galactopyranose_mutase
		UPF0380_protein_yubP
		UPF0401_protein_yubL
		X_polypeptide

Defining the minimal microbial community necessary for *K. pneumoniae* induced colitis in gnotobiotic *Tbet*$^{-/-}$ *Rag2*$^{-/-}$ mice.

K. pneumoniae and *P. mirabilis* were sufficient to induce colitis in SPF-WT and SPF-*Rag2*$^{-/-}$ mice. However, neither bacterium alone or in combination was sufficient to induce inflammation in gnotobiotic *Tbet*$^{-/-}$ *Rag2*$^{-/-}$ mice despite successful colonization of the colon (127). This points to the necessity of an endogenous microbiota for *K. pneumoniae* and *P. mirabilis* to cause inflammation. To confirm that GF-*Tbet*$^{-/-}$ *Rag2*$^{-/-}$ mice are able to develop colitis, GF-*Tbet*$^{-/-}$ *Rag2*$^{-/-}$ mice were associated with stool from a prolapsed *Tbet*$^{-/-}$ *Rag2*$^{-/-}$ female with a SPF microbiota. Mice were sacrificed after a 4-week (n=4) or 8-week (n=17) incubation, colons were processed for histology, and stool was processed for 16S rRNA amplicon sequencing. Colonic inflammation developed in the presence of a complex microbial community in these gnotobiotic mice (**Figure 2.6A**). The large distribution of colitis scores in gnotobiotic *Tbet*$^{-/-}$ *Rag2*$^{-/-}$ mice receiving fecal transplants prompted a further analysis of the associated metadata. While colitis score spread was not explained by caging effects, age, or length of fecal association, sex was a

significant contributing factor with male mice developing more severe disease than female littermates (**Figure 2.6**).

There are several well-researched examples of sexual dimorphisms in bacterially mediated disease, often in the direction of increased male susceptibility. Studies have demonstrated increased LPS sepsis susceptibility in male mice and patients when compared to females (143). Men display higher tuberculosis infection rates worldwide (144), and vaccination against *Helicobacter pylori* is less effective in male mice (145). Sexual dimorphisms in relation to human ulcerative colitis are controversial with some studies finding no differences in prevalence between the sexes (146-148) and other studies identifying a higher disease incidence in men (149, 150). While a sex bias was never observed in our SPF-*Tbet*$^{-/-}$ *Rag2*$^{-/-}$ colony, increased colitis severity in male gnotobiotic *Tbet*$^{-/-}$ *Rag2*$^{-/-}$ mice prompted us to examine the gut microbiota for colitis-associated bacterial signatures.

DNA was extracted from frozen stool collected on the day of mouse sacrifice. Library construction, amplification of the 16S V5-V6 region, and 454 pyrosequencing was performed by Research and Testing in Lubbock Texas. Sequences were processed with QIIME (Quantitative Insights Into Microbial Ecology) (81), revealing phylum level differences in bacterial abundance between individual mice and across mice grouped according to sex (**Figure 2.7A**). Next, LEfSe (Linear Discriminant Analysis with Effect Size) (83) was used to identify microbial clade differences between the sexes. LEfSe

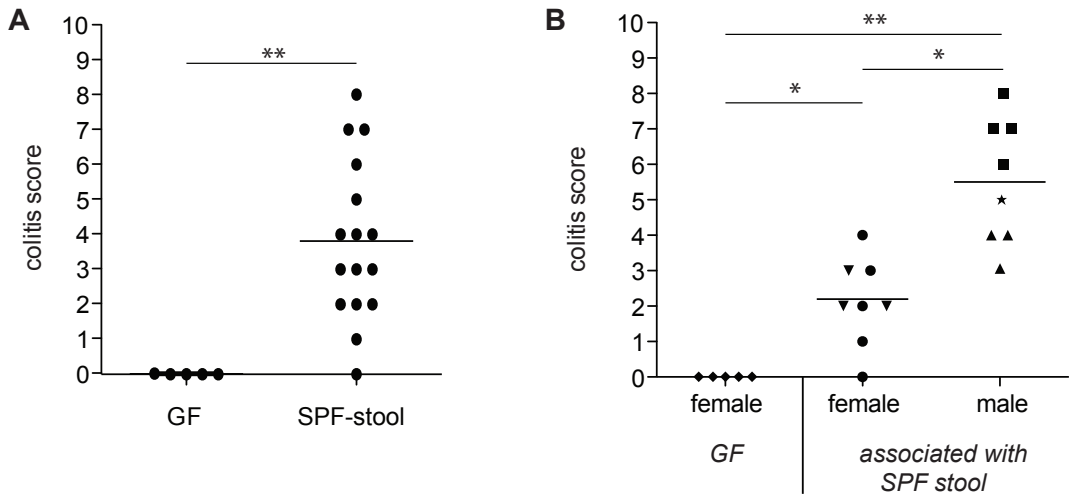

Figure 2.6. **Sexual dimorphism of colitis severity in gnotobiotic *Tbet*$^{-/-}$ *Rag2*$^{-/-}$ mice associated with stool from sick SPF-*Tbet*$^{-/-}$ *Rag2*$^{-/-}$ mice. (A)** Histologic colitis scores from GF *Tbet*$^{-/-}$ *Rag2*$^{-/-}$ mice associated with SPF-*Tbet*$^{-/-}$ *Rag2*$^{-/-}$ stool for 8 or 4 weeks. **(B)** Histologic colitis scores for the same mice as in (A), separated by sex. Symbols represent cages. The 4 males with the lowest colitis scores were associated for 4 weeks, all other mice were associated for 8 weeks. Mann-Whitney statistical test, * $P \leq 0.05$. ** $P \leq 0.01$.

revealed an enrichment of *Bacteroidetes* in stool from sick male mice and an enrichment of *Firmicutes* in their healthier female littermates (**Figure 2.7B**). Specifically, OTUs from the families *Rikenellaceae* and *Porphyromonadaceae* were discriminate for male mice, and *Bacilli* and *Clostridia* for female mice. When comparing mice with low histologic score (0-4) to mice with severe colitis (5-8) regardless of sex, the *Bacteroidetes* and *Firmicutes* difference held (**Figure 2.7C**). Interestingly, *Bacteroidetes* species have been shown to induce colitis in mouse models, however, their abundance in diseased mice was not increased compared to healthy controls (151). In human 16S surveys, *Rikenellaceae* and *Porphyromonadaceae* are more abundant in control groups compared to IBD subjects (152), however mouse studies have identified enrichment of these families in disease groups of colitis induced by IL-22 deficiency (153), in dextran sodium sulfate-induced colitis(154), and for Type I diabetes (6).

Comparing females to male mice housed in cage4 revealed a greater number of differential OTUs (**Figure 2.8**). In addition to the associations presented in **Figure 2.7**, male mice from cage4 had enrichments in the *Actinobacteria* and *Proteobacteria* (both beta and delta) phyla. Specifically, *Desulfovibriaceae* was associated with sick male mice in cage4. *Desulfovibrio* spp. have been identified at higher abundance in human patients with both acute and chronic ulcerative colitis (155).

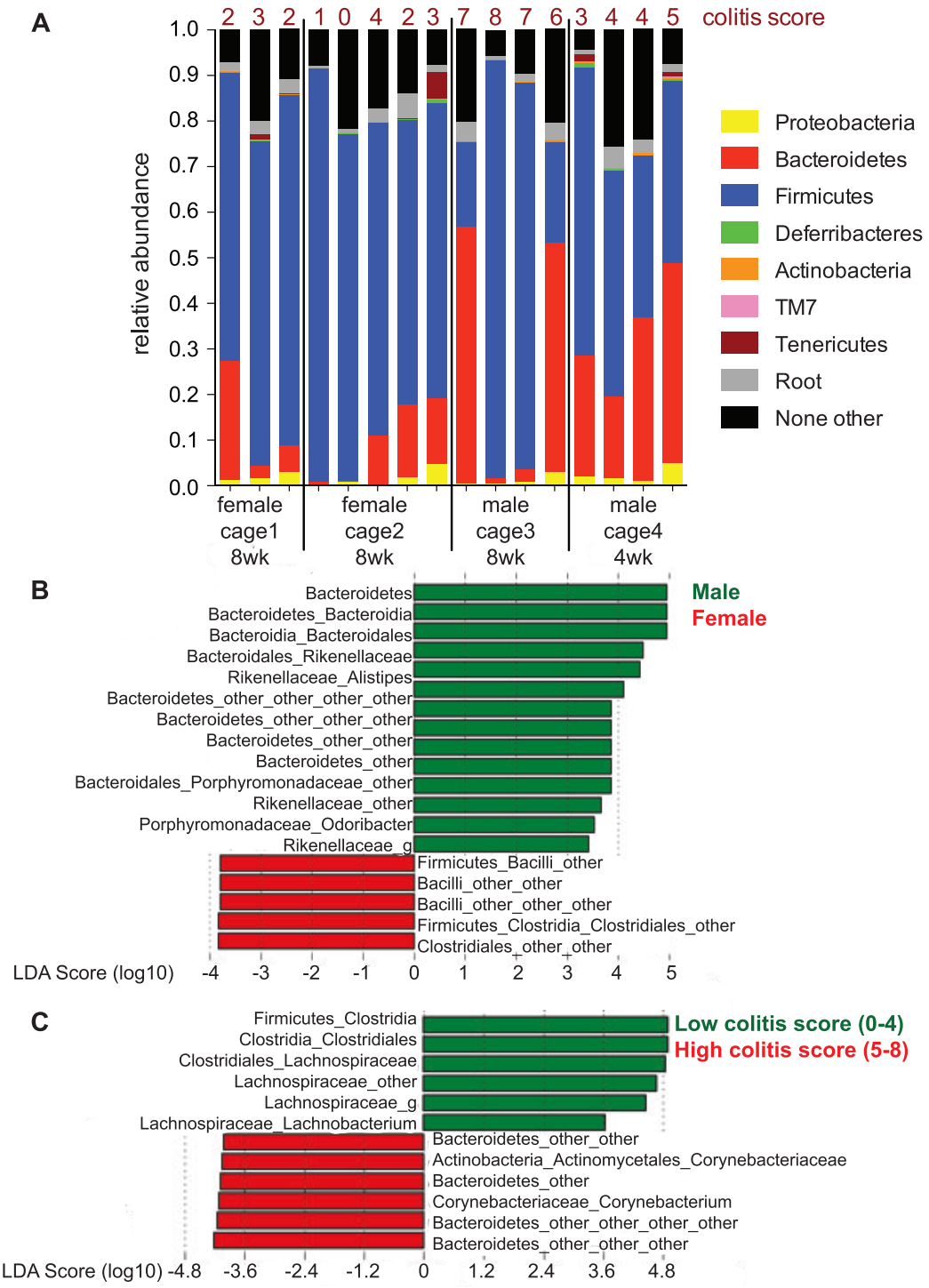

Figure 2.7. **Microbial signatures in the gut correlate with severity of intestinal inflammation and mouse sex. (A)** Relative abundance of bacterial phyla in stool from GF-*Tbet*$^{-/-}$ *Rag2*$^{-/-}$ mice associated with stool from an SPF-*Tbet*$^{-/-}$ *Rag2*$^{-/-}$ mouse. Histologic colitis scores on top. **(B)** LEfSe plots showing significant differences in bacterial taxa between male and female mice and in **(C)** between mice with low and high colitis scores. LDA effect size on the bottom.

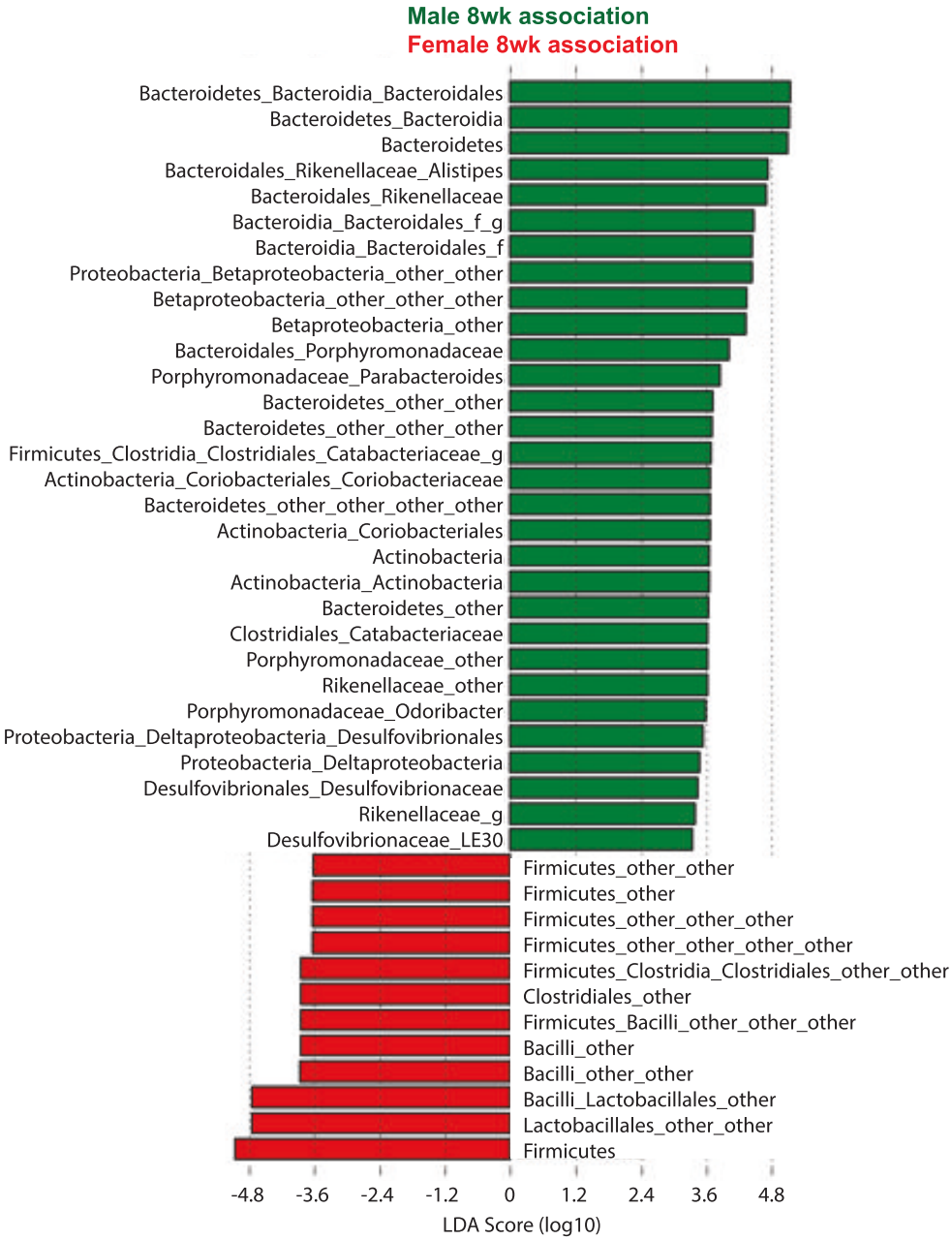

Figure 2.8. **Discriminate bacterial taxa between female mice and a subset of male mice.** Significant differences in bacterial phyla in stool from GF-*Tbet*$^{-/-}$ *Rag2*$^{-/-}$ mice associated with stool from an SPF-*Tbet*$^{-/-}$ *Rag2*$^{-/-}$ mouse LEfSe plot with LDA effect size along the bottom.

Establishing a gnotobiotic ASF-*Tbet*$^{-/-}$ *Rag2*$^{-/-}$ and ASF-WT mouse colony.

Having established that colonic inflammation can be recapitulated by a consortium of colonic bacteria in GF-*Tbet*$^{-/-}$ *Rag2*$^{-/-}$ mice, we sought to identify the minimal microbial community necessary to incite colitis. For these experiments, we established breeding colonies of gnotobiotic mice with a defined microbiota consisting of the 8 bacterial strains of the Altered Schaedler Flora (ASF) and housed in sterile isolators. GF-*Tbet*$^{-/-}$ *Rag2*$^{-/-}$ and GF-WT mice were orally inoculated with cecal contents of C3H/HeN:Tac gnotobiotic ASF mice obtained from Dr. Michael Wannemuehler of Iowa State University (156). Following a second inoculation one week later, ASF mice were bred. PCR confirmed that all pups of ASF associated breeders were positive for the 8 ASF bacterial strains (**Figure 2.9A**). Presence of 7 of the ASF strains can be confirmed from DNA extracted from stool. Presence of ASF 361, an esophageal colonizer, was confirmed with a PCR on DNA extracted from cecal contents. Colonization with the ASF partially reversed the enlarged cecum phenotype observed in GF animals (**Figure 2.9B**), although ceca were still large in comparison to Balb/C SPF mice.

In order to assess whether the ASF is a sufficient microbial community for *K. pneumoniae* driven colonic inflammation, F1 ASF-*Tbet*$^{-/-}$ *Rag2*$^{-/-}$ and ASF-WT mice were orally inoculated with *K. pneumoniae* WGLW5. While this isolate induces colitis in SPF mice (127), there were no signs of histologic colitis in ASF gnotobiotic mice after an 8-week association with *K. pneumoniae* WGLW5 alone or in combination with *P. mirabilis* (**Figure 2.10**). Given the significantly reduced diversity of the ASF compared to SPF microbial communities, perhaps the ASF is too minimal of a community for *K. pneumoniae* induced colitis. Specifically, the absence of *Bacteroidetes* from the ASF is

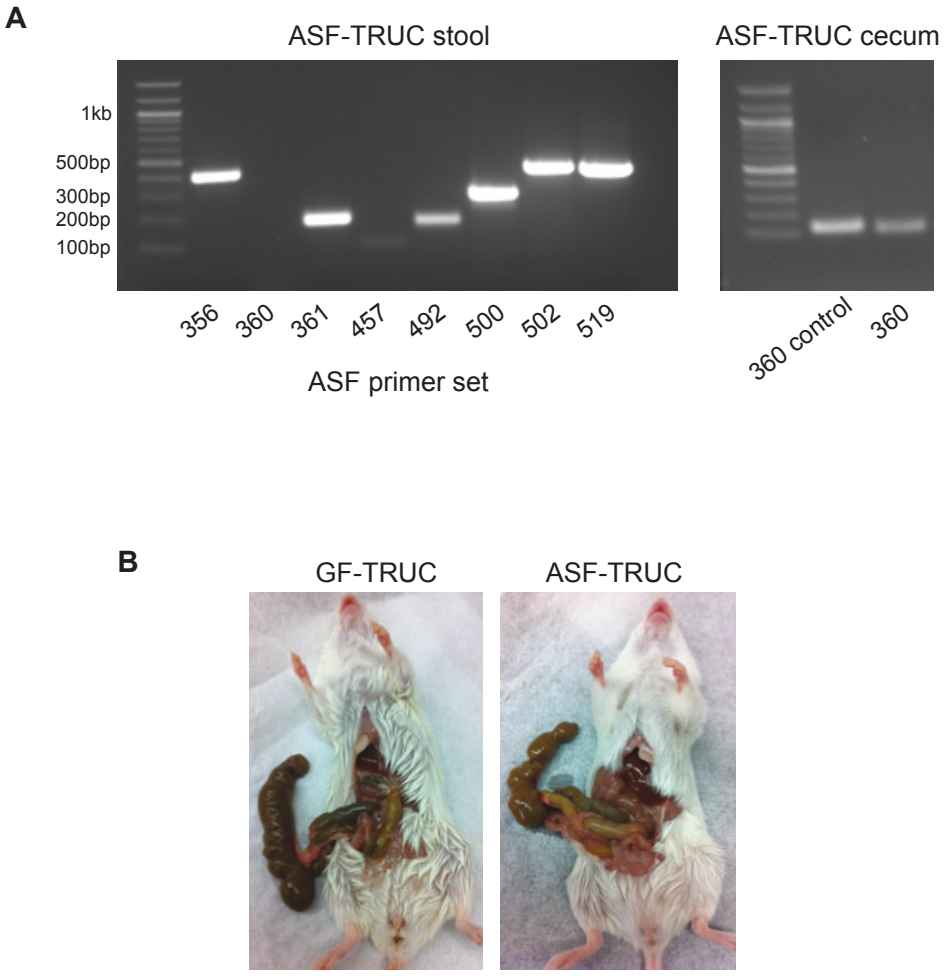

Figure 2.9. **Generation of gnotobiotic ASF colonies. (A)** PCR confirmation of 8 ASF species in the F1 generation of ASF-*Tbet*$^{-/-}$ *Rag2*$^{-/-}$ breeders. DNA extracted from ceca upon sacrifice. **(B)** Enlarged cecum from an ASF-*Tbet*$^{-/-}$ *Rag2*$^{-/-}$ breeder associated in adulthood (left) and smaller cecum in her pup colonized with the ASF via parental transfer at birth (right).

troubling given the enrichment of this phylum in our 16S assessment of inflamed gnotobiotic mice (**Figure 2.7 and 2.8**). Additional strains can be associated in conjunction with the ASF for future fine-tune resolution of a colitogenic minimal microbial community.

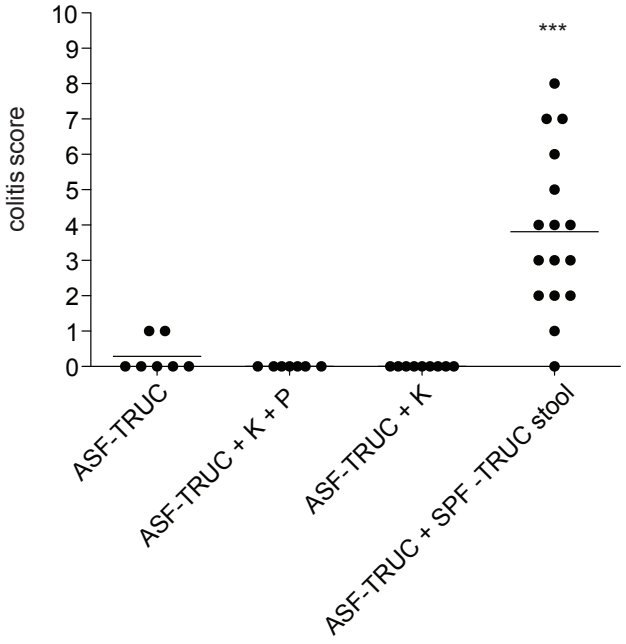

Figure 2.10. ***K. pneumoniae*** **and** ***P. mirabilis*** **do not induce colitis in ASF-*Tbet*$^{-/-}$ *Rag2*$^{-/-}$ mice**. 8 week associations in gnotobiotic isolators. Data points represent individual mice. Mann-Whitney statistical test, *** $P \leq 0.001$. *Tbet*$^{-/-}$ *Rag2*$^{-/-}$, TRUC.

V. DISCUSSION

As an opportunistic pathogen, *K. pneumoniae* thrives in an inflamed host environment and may participate in the initiation of an inflammatory state. While *K. pneumoniae*'s role in driving pneumonia and urinary tract infections is well defined, it is not widely accepted as a driver of inflammatory bowel disease. Several studies have identified an association between Crohn's disease and *Klebsiella* in stool (157), but *Klebsiella* has not been implicated as a causative agent of disease.

Previous studies in mouse models of inflammatory bowel disease, specifically ulcerative colitis, revealed that a strain of *K. pneumoniae* isolated from mouse stool was able to induce colonic inflammation (127). The work of this thesis aimed to discover whether this effect was strain specific or a shared ability of human clinical *K. pneumoniae* isolates. Despite genomic diversity, 4 strains of *K. pneumoniae*, including 3 isolates from humans, were able to drive ulcerative colitis in mice (**Figure 2.2**). These finding have implications for human health since *K. pneumoniae* is carried as part of the normal gut microbiota in 5-38% of the general population (85). Given the complex, multi-factorial nature of inflammatory bowel disease, it is attractive to speculate that carriage of *K. pneumoniae* in the gastrointestinal tract predisposes people to inflammatory bowel disease or puts inflammatory bowel disease patients at increased risk for flares. Even if not the initial cause of inflammation, native *K. pneumoniae* populations could presumably bloom and potentiate colitis in carriers.

Interestingly, we found that not all *K. pneumoniae* isolates are equally virulent in mouse models of systemic neonatal infection. The most important factor for the ability to incite severe infection was found to be the original host species and not anatomical

location since human stool *K. pneumoniae* did not lead to neonatal death but a murine stool isolate did (**Figure 2.3**). The differential ability of WGLW5 to cross epithelial barriers was confirmed by the finding of higher WGLW5 levels in mesenteric lymph nodes than any of the other *K. pneumoniae* isolates. Not only does the host seem to respond differently to *K. pneumoniae* WGLW5, but so does the gut microbiota. Fecal blooms of closely related *P. mirabilis* only in the presence of WGLW5 suggests that, 1) *K. pneumoniae* WGLW5 may indirectly change a colonic niche to make it more favorable to *P. mirabilis* growth, or that, 2) presence of *K. pneumoniae* WGLW5 may provide *P. mirabilis* with clues about the colonic environment. Further investigation of the genomic differences between *K. pneumoniae* WGLW2, 3, and 5 may reveal gene signatures associated with these observations.

A surprising finding of the studies presented in this chapter was evidence of sexual dimorphism in colitis severity when an SPF microbiota was transferred to genetically susceptible GF mice (**Figure 2.6**). As mentioned in the results section, while males are more susceptible to several bacterial-driven diseases, we had not previously observed increased male colitis severity in our SPF-*Tbet*$^{-/-}$ *Rag2*$^{-/-}$ colony. This suggests complexity in sexual dimorphism that may be mirrored in susceptibility of mice to diabetes. Non-obese diabetic (NOD) mice develop type I diabetes, with increased female susceptibility compared to males. However, when maintained under GF conditions, diabetes incidence is equivalent in male and female mice (158). Importantly, both host hormone and glycerophospholipid metabolite levels were different between SPF-NOD and GF-NOD mice. Perhaps the altered sex hormone milieu of male GF mice compared

to SPF controls could contribute to increased susceptibility to colitis in our GF-*Tbet*$^{-/-}$ *Rag2*$^{-/-}$ model.

Interestingly, the microbial abundance profile of the colitis-associated sexual dimorphism (**Figure 2.7**) was atypical in comparison to other microbiota-associated disease states. In both obese mouse models (159) and human populations (160), obesity is associated with an increased relative abundance of *Firmicutes*. The same pattern holds true for children with type I diabetes (161). In inflammatory bowel disease, a larger emphasis has been placed on an expanded *Proteobacteria* population in driving disease, however relative abundances of entire gut communities do show a decrease in *Bacteroidetes* in sick patients compared to controls (162). Our 16S rRNA amplicon survey showed the opposite, with an enrichment of *Bacteroidetes* and depletion of *Firmicutes* in male mice with more severe colitis. These conflicting results may be due to microbiota composition changes driven by the altered development state of GF mice. Alternatively, studies have shown that almost every step in the 16S rRNA sequencing pipeline, from DNA prep, 16S amplification, and sequencing protocol, can significantly affect study output (163-165). Based on these findings, caution should taken when comparing results from 16S surveys across different methodologies, and with current knowledge, we may not be able to speculate on the biological relevance of the increased *Bacteroidetes* to *Firmicutes* ratio observed in our study.

VI. MATERIALS AND METHODS

Bacterial strains and conventional culture

K. pneumoniae WGLW5 (BEI HM-749) was previously cultured from the stool of BALB/c *T-bet*$^{-/-}$ *Rag2*$^{-/-}$ mice (127). *K. pneumoniae* WGLW1 (BEI HM-750), WGLW2 (BEI HM-751) and WGLW3 (BEI HM-748) are clinical isolates cultured from human urine, sputum, and stool respectively. Bacteria were cultured in Luria-Bertani (LB) broth shaking aerobically at 37°C overnight or on MacConkey agar. For culturable *K. pneumoniae* CFU counts from stool, stool was collected from individual mice and serially diluted 10-fold using sterile PBS onto MacConkey agar and incubated for 24 h at 37° C. Colonies were counted on plates with bacterial densities of 30-300 CFU. Log_{10} CFU/ g stool bacteria were calculated after accounting for dry and wet fecal weights.

ASF strains- *Clostridium* sp. (ASF356), *Lactobacillus* sp. (ASF360), *Lactobacillus murinus* (ASF361), *Mucispirillum schaedleri* (ASF457), *Eubacterium plexicaudatum* (ASF492), *Firmicutes* bacterium (ASF500), *Clostridium* sp. (ASF502), and *Parabacteroides* sp. (ASF519) were received from Iowa State University (156).

SPF *K. pneumoniae* colonic inflammation model

4-week old SPF BALB/c *Rag2*$^{-/-}$ mice (Charles River, strain 028) were fed $1.5x10^8$ CFU *K. pneumoniae* isolate in 25 μl PBS from P200 pipette tips every third day for 8 weeks. Mice were sacrificed and colons were processed for histology on day 56.

Histology

At the time of sacrifice, colons were harvested, removed of colonic contents, and fixed in a solution of PBS with 4% paraformaldehyde. Tissue was paraffin embedded, cut into 0.5 um thick sections and stained with hematoxylin and eosin. Slides were scored by

pathologists in a blinded manner. Dr. Jonathan Glickman assigned colitis scores based on the cumulative sum of four criteria with a severity ranking between 0-4: mononuclear cell infiltration, polymorphonuclear cell infiltration, epithelial crypt hyperplasia, and epithelial injury. 0-absent, 1-mild, 2-moderate, 3-severe as described previously (166). Dr. Roderick Bronson assessed a subset of slides for edema and ranked samples according to severity. 1-low, 2-medium, 3-high.

SPF *K. pneumoniae* neonatal infection model

Beginning on the day of birth, SPF BALB/c *Rag2*$^{-/-}$ pups were sprinkled (cutaneous inoculation around the mouth) with 1.3 x 10^8 CFU *K. pneumoniae* in 20 μl PBS daily for 7 days. To confirm systemic *K. pneumoniae* infection in pups dying in this 7-day window, *K. pneumoniae* CFU counts were assessed from the spleen and liver of a *K. pneumoniae* WGLW5 sprinkled pup dead for less than 4 hours, a sickly sprinkled pup, and its healthy sprinkled littermate. Tissue was treated similar to stool and assessed for *K. pneumoniae* CFU as explained previously. 7-weeks after the final *K. pneumonia*e inoculation, stool was assessed from surviving pups for culturable counts of *K. pneumoniae* and *P. mirabilis* as above.

Real-time (RT)-qPCR

Mesenteric lymph nodes were harvested at the time of mouse sacrifice and stored in RNAlater (Ambion) at -80° C. Tissue was washed with PBS prior to physical homogenization in QIAzol lysis reagent (Qiagen). RNA was extracted (Qiagan RNeasy Mini Kit), DNase treated, and reverse transcribed into cDNA (Bio-Rad iScript cDNA Synthesis Kit). RT-qPCR was performed using the SYBR FAST Universal qPCR Kit

(KAPA Biosystems). *K. pneumoniae* 23S expression was normalized to total bacterial 16S expression. Primer sequences are shown in **Table 2.3**.

Table 2.3. *K. pneumoniae* 28S RT-qPCR primers.

Primer	**Sequence 5'-3'**
K. pneumo-OFF2551	GGTAGCACAGAGAGCTTG
K. pneumo- OFF2552	ACTTTGGTCTTGCGAC

K. pneumoniae comparative genomics

The *Klebsiella* group sequencing project at the Broad Institute generated Illumina MiSeq whole genome sequences for WGLW1, 2, 3, and 5. These 4 genomes and the genomes of 5 previously published *K. pneumoniae* genomes (**Table 2.1**) were annotated by Prodigal. Genomes were translated to proteomes and matched to protein databases using BLASTP (http://blast.ncbi.nlm.nih.gov). OrthoMCL(113) was run to parse proteomes into protein groups representing orthologs, paralogs, and co-orthologs (141). An independent maximum likelihood phylogeny tool, RAxML (Randomized Axelerated Maximum Likelihood (142)), was used to generate a phylogenetic tree relating the 9 *K. pneumoniae* genomes used in this study.

Gnotobiotic associations

Stool from a prolapsed SPF-*T-bet*$^{-/-}$ *Rag2*$^{-/-}$ female was frozen in PBS at -80° C. Aliquots were thawed and fed from pipette tips to GF-*T-bet*$^{-/-}$ *Rag2*$^{-/-}$ and GF-WT mice bred and housed under sterile conditions in semi-rigid gnotobiotic isolators at Children's Hospital Boston. After either 4 or 8 weeks, mice were sacrificed, their colons were processed for histologic examination of colitis, and stool was homogenized and stored in PBS at -80° C.

16S microbial community assessment

DNA was extracted from stool that had previously been homogenized and stored at -80° C in PBS on the day of mouse sacrifice. DNA was extracted with phenol chloroform following mechanical bacterial lysis with 2 minutes of bead beating. Extracted DNA was sent to Research and Testing in Lubbock Texas for library construction and tag-encoded FLX amplicon bTEFAP 454 pyrosequencing with 8x coverage. Primers 784-1016 (167) (**Table 2.4**) were used to amplify the V5-V6 region of the 16S gene. Following sequencing, QIIME (81) was employed for sequence processing. Following the standard QIIME workflow, sequences were subjected to denoising, inflation, OTU picking, chimera removal, and taxonomy assignment with Green Genes 2011. Next, LEfSe (Linear Discriminant Analysis with Effect Size) (83) was used to identify bacterial OTUs that were depleted or enriched due to mouse sex.

Table 2.4. 16S primers used for microbial survey assessment.

Primer	**Sequence 5'-3'**
784F	AGGATTAGATACCCTGGTA
1061R_1	CRRCACGAGCTGACGAC

ASF gnotobiotic colony generation

For generation of ASF-*T-bet*$^{-/-}$ *Rag2*$^{-/-}$ and ASF-WT colonies, ceca from gnotobiotic C3H/HeN:Tac-ASF mice were thawed, and cecal contents were re-suspended under sterile conditions in PBS-0.5% cysteine. Aliquots were fed to GF-*T-bet*$^{-/-}$ *Rag2*$^{-/-}$ and GF-WT mice in gnotobiotic isolators. PCR on DNA isolated from stool with primer sets specific for each of the eight ASF strains (**Table 2.5**) was used to confirm colonization (168). Following the original association, all but ASF457 and ASF361 were confirmed in stool of associated gnotobiotic TRUC mice. One week later, a second association was performed to introduce ASF457, which requires the presence of other

microbes to reduce redox-potential of the host before successful colonization can occur. ASF361, an esophageal colonizer was confirmed vie PCR on DNA extracted from cecal contents upon sacrifice.

Table 2.5. Primers for PCR confirmation of the 8 ASF flora in stool from gnotobiotic mice.

ASF strain	Forward Primer 5'-3'	Reverse Primer 5'-3'
ASF356	CGGTGACTAATACCGCATACGG	CCTTGCCGCCTACTCTCCC
ASF360	CTTCGGTGATGACGCTGG	GCAATAGCCATGCAGCTATTGTTG
ASF361	GCAATGATGCGTAGCCGAAC	GCACTTTCTTCTCTAACAACAGGG
ASF457	CCGAAAGGTGAGCTAATGCCGG	GGGACGCGAGTCCATCTTTC
ASF492	CTGCGGAATTCCTTCGGGG	CCCATACCACCGGAGTTTTC
ASF500	GTCGCATGGCACTGGACATC	CCTCAGGTACCGTCACTTGCTTC
ASF502	CGGTACCGCATGGTACAGAGG	CAATGCAATTCCGGGGTTGG
ASF519	CACAGTAAGCGGCACAGCG	CCGCTCACACGGTAGCTG

Statistical analyses

Statistical calculations were performed using GraphPad Prism® software. Utilized tests include Mann-Whitney and one-way ANOVA with Dunnett's post-test.

CHAPTER 3

THE GUT MICROBIOTA AND HOST ANTIMICROBIAL PEPTIDES INFLUENCE *KLEBSIELLA PNEUMONIAE* CAPSULAR POLYSACCHARIDE POPULATION DYNAMICS

I. ATTRIBUTIONS

This chapter is adapted from a manuscript in preparation with the following authorship:

Leslie Wardwell-Scott[1], Sarah S. Wilson[2], Xochitl C. Morgan[3], Curtis Huttenhower[3], Jason G. Smith[2], Wendy S. Garrett[1,4,5]

[1] Departments of Immunology and Infectious Diseases and Genetics and Complex Diseases, Harvard T.H. Chan School of Public Health, Boston, MA, USA
[2] Department of Microbiology, University of Washington, Seattle, WA, USA
[3] Biostatistics Department, Harvard T. H. Chan School of Public Health, Boston, MA, USA
[4] The Broad Institute of MIT and Harvard, Cambridge, MA, USA
[5] Department of Medical Oncology, Dana-Farber Cancer Institute, Boston, MA, USA

Leslie Wardwell-Scott performed all experiments and analyses, except as follows: the *Klebseilla* sequencing group at the Broad Institute performed whole genome sequencing of *K. pneumoniae* WGLW2, 3, 5. The Biopolymers Core of Harvard Medical School sequenced variants of *K. pneumoniae* WGLW5. Xochitl Morgan of Harvard T.H. Chan School of Public Health assembled and annotated the *K. pneumoniae* CPS variant genomes. Sarah Wilson of the University of Washington performed organoid experiments.

II. ABSTRACT

Klebsiella pneumoniae is a member of the gut microbiota of healthy individuals. Whether *K. pneumoniae*'s mucoid capsular polysaccharide (CPS) coat helps or hinders gastrointestinal tract colonization is unclear. To define a role for CPS in gastrointestinal colonization dynamics, *K. pneumoniae* biogeography was assessed in gnotobiotic mice. Naturally-arising *K. pneumoniae* variants with reduced CPS, which displayed enhanced

survival in response to bile salts and low pH, outcompeted mucoid populations throughout the gastrointestinal tract, except in the distal small intestine. Mucoid population levels correlated with regions of high Paneth cell antimicrobial peptide (AMP) expression and use of small intestinal organoid cultures revealed increased mucoid *K. pneumoniae* growth in the presence of Paneth cell α-defensins and decreased survival of non-mucoid variants. CPS also conferred an advantage when *K. pneumoniae* was part of a diverse microbiota. Introduction of a diverse microbiota to gnotobiotic mice colonized with *K. pneumoniae* resulted in a decline of non-mucoid variants, while mucoid populations remained stable. Inoculation of conventionally-reared mice with CPS variants revealed selective maintenance of mucoid *K. pneumoniae* populations, supporting that a CPS coat provides a competitive advantage against other bacteria in the densely populated, polymicrobial environment of the gastrointestinal tract. Enhanced survival of mucoid compared to non-mucoid variants in competition assays between *K. pneumoniae* and *Escherichia coli in vitro* reinforced this concept. Collectively, these data suggest that host AMPs, in combination with bacterial-bacterial interactions, shape population dynamics of *K. pneumoniae* and select for mucoid *K. pneumoniae* throughout the gastrointestinal tract.

III. INTRODUCTION

Klebsiella pneumoniae are species of *Enterobacteriaceae* that are responsible for nosocomial and opportunistic infections of the lungs, urinary tract, liver, and blood (169). Despite the clinical challenges *K. pneumoniae* presents, it coexists with other bacterial members of the gut microbiota in healthy human hosts. An estimated 5-38% of the

general population carries *K. pneumoniae* in their gastrointestinal tract; however these carriage numbers increase in hospital settings where up to 77% of caregivers and patients are *K. pneumoniae* positive (85). Regions of East Asia, such as Taiwan, also report these higher gastrointestinal carriage rates in healthy populations (121). Patient populations with *K. pneumoniae* liver abscesses have shown 100% co-colonization of the gastrointestinal tract, prompting the hypothesis that gastrointestinal carriage represents a predisposition for liver abscesses and serves as a general reservoir for *K. pneumoniae* disease (122).

A defining feature of *K. pneumoniae* is its mucoid capsular polysaccharide (CPS) coat, which consists of glucuronic acid, glucose, variable additional sugars- typically mannose, rhamnose, or fucose (92). There are upwards of 80 *K. pneumoniae* CPS serotypes, which differ in composition of the CPS glycosyltransferase core and in incorporated sugars (93). Sequenced CPS gene clusters range in size from 21 to 30 kb with 16-25 open reading frames (93). *K. pneumoniae* capsule has been studied as a virulence factor (169), as CPS protects bacteria from phagocytosis (170, 171) and complement opsonization (172), facilitating evasion of host immune defenses (94). The majority of clinical isolates are mucoid, but variation resulting in loss of CPS production has been reported during *in vitro* culture (95, 173).

Since the gastrointestinal tract is *K. pneumoniae*'s reservoir for disease (174), understanding *K. pneumoniae* population dynamics in mammalian gastrointestinal tracts in homeostatic states may inform studies of transmission and pathogenicity. A few studies have attempted to address the importance of CPS for gastrointestinal colonization with conflicting results that may be explained by use of different colonization

environments including germ-free (GF) chicken intestine (128) and antibiotic treated mice (129, 175). Experiments to deconstruct *K. pneumoniae's* behavior in the gastrointestinal tract are challenging. In this environment *K. pneumoniae* must compete for space and nutrients with a multitude of bacterial species, while participating in a delicate balance with the host immune system. By mapping *K. pneumoniae'*s intestinal colonization biogeography, assessing colonization dynamics in GF and gnotobiotic mouse models, and using a small intestinal organoid culture system, we implicate CPS in inter-species bacterial interactions and protection against antimicrobial peptides produced by host Paneth cells in the small intestine. While CPS has been shown to be protective for *K. pneumoniae* during *in vitro* culture with antimicrobial peptides (176, 177), we elucidate factors shaping capsular variation *in vivo*. Herein, we define a role for *K. pneumoniae* CPS outside of the traditional virulence context and highlight the effect of bacterial interactions with other members of the microbiota on shaping populations of individual bacterial species.

IV. RESULTS

K. pneumoniae CPS loss following colonization of gnotobiotic mice.

To assess *K. pneumoniae* colonization in the gastrointestinal tract, GF BALB/c mice were orally inoculated with murine *K. pneumoniae* strain WGLW5 (**Figure 3.1A**). *K. pneumoniae* WGLW5 has a mucoid CPS coat that is maintained *in vitro*. Beginning 48h after inoculation, *K. pneumoniae* fecal isolates displayed diverse colony phenotypes distinguishable on MacConkey agar, a differential media for selective culture of

Enterobacteriaceae (**Figure 3.1B**, 4-wks post inoculation). 16S rRNA amplicon sequencing and a negative indole test confirmed that all isolates were *K. pneumoniae*.

These *K. pneumoniae* isolates appeared to have reduced CPS (**Figure 3.1B**). To confirm decreased CPS production, we performed glucuronic acid measurement of bacterial membranes from five colonies representative of the diverse colony phenotypes isolated from *K. pneumoniae* mono-colonized mice. Glucuronic acid measurement demonstrated that *K. pneumoniae* isolates lacking a parent mucoid phenotype had significantly reduced CPS production ($P \leq 0.001$) both on agar plates (**Figure 3.1C**) and in liquid culture (**Supplemental Figure 3.1**). We termed low CPS producing isolates non-mucoid variants (NMVs).

An 8-wk *K. pneumoniae* colonization time course in GF mice (**Figure 3.1A**) revealed that the majority of recovered fecal *K. pneumoniae* isolates were NMVs as assessed by colony phenotype on MacConkey agar (**Figure 3.1D**). Although GF mice represent a model system for evaluating the behavior of single microorganisms in a host, GF mice have significant immune alterations compared to conventionally colonized mice (26). To address this issue, *K. pneumoniae* associations were repeated in gnotobiotic mice colonized with the Altered Schaedler Flora (ASF), a microbial community comprised of 8 bacterial species found in the gut of healthy mice (168, 72). Although a simplified microbiota, the ASF in gnotobiotic mice promotes expansion of gut mucosal T-regulatory cell populations (73) and restores luminal IgA secretion (178). The absence of *Proteobacteria* and direct niche competition in the ASF led us to hypothesize that *K. pneumoniae* would readily colonize the gastrointestinal tract. While total *K. pneumoniae* fecal CFU were slightly reduced in ASF compared to GF mice (**Supplemental Table**

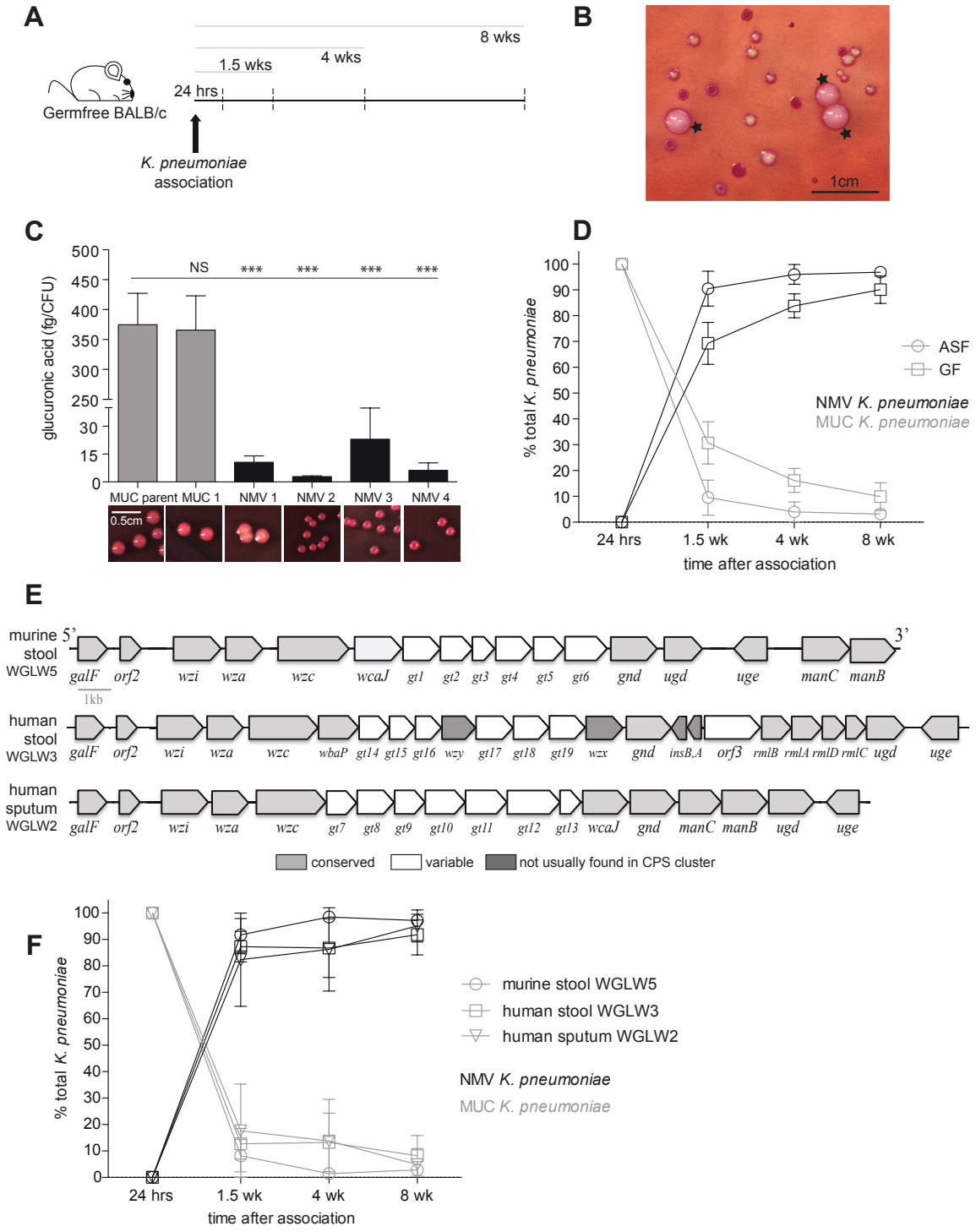

Figure 3.1. *K. pneumoniae* CPS population shift following GI colonization of gnotobiotic mice. (A) Gnotobiotic mouse *K. pneumoniae* association experimental chema. Dashed lines represent time points for stool sampling and CFU enumeration. **(B)** Fecal *K. pneumoniae* colonies on MacConkey agar after 4-week colonization of a germ-free (GF) mouse with WGLW5. Stars indicate mucoid (MUC) colonies, all others colonies are NMVs. **(C)** Glucuronic acid content of the membrane fraction of overnight *K. pneumoniae* variants grown on MacConkey agar. Data

(*Figure 3.1 Continued)* reflect mean ± SD of 3 experiments. **(D)** 8-wk association of GF (squares) and ASF (circles) mice with WGLW5. MUC population (gray); NMV population (black). **(E)** Scale representation of CPS gene clusters of isolates assembled from WGSs. **(F)** 8-wk association of ASF mice with the 3 isolates from (E). MUC population (gray); NMV population (black). For (D) and (F), data points represent mean population percentages ± SD for n=6 mice. ***, $P \leq 0.001$, one-way ANOVA with Dunnett's post-test.

3.1), loss of CPS and out-competition of parental mucoid *K. pneumoniae* by NMVs were similar (**Figure 3.1D**).

CPS gene clusters of murine *K. pneumoniae* (WGLW5) and two human clinical isolates (WGLW2- from human sputum, WGLW3- from human stool) were assembled from whole genome sequences (WGSs) (**Figure 3.1E**). Serotype identity was assigned using the *wzc* gene sequencing method, a recently described alternative to serum serotyping based on strain based differences in genomic sequences (179). *K. pneumoniae* WGLW5 was identified as serotype K25, WGLW3 was indeterminate, and WGLW2 was serotype K2. Despite diversity in CPS serotype, all three isolates displayed CPS variation when introduced into gnotobiotic ASF mice (**Figure 3.1F**), suggesting that reduction of *K. pneumoniae* CPS in a gnotobiotic host harboring a simplified gut microbial community is a shared feature of the species.

CPS reduction is not likely caused by genetic mutation or plasmid loss.

NMV *K. pneumoniae* does not revert to producing capsule under varied *in vitro* culture conditions or upon passage through mice (**Table 3.1**). To investigate if the NMV phenotype was driven by genetic mutation, WGSs were generated for 4 NMV and 2 mucoid variants. After alignment to *K. pneumoniae* WGLW5, single nucleotide polymorphisms (SNPs) were identified between each CPS variant and the reference (**Supplemental Table 3.2**). There were no SNPs shared among NMV *K. pneumoniae* in

any single gene or in any predicated pathway across the sequenced genome, including within the CPS gene cluster. Additionally, plasmid profiles of all variants looked similar (**Figure 3.2**) arguing against plasmid loss leading to reduced CPS.

Table 3.1. *In vitro* culture conditions and *in vivo* gnotobiotic associations with *K. pneumoniae* WGLW5 and corresponding shifts in CPS phenotype. Y indicates appearance of a different CPS phenotype from the starting population. N indicates no shift in CPS phenotype. MUC, mucoid; NA, non-applicable.

		Phenotype Switch	
		MUC → NMV	**NMV → MUC**
in vitro Culture Conditions (24 and 48hr)	MacConkey agar/broth	N	N
	LB agar/broth	N	N
	BHI agar/broth	N	N
	M9 minimal agar/broth	N	N
	Fecal extract broth	N	N
	30°C (all media)	N	N
	37°C (all media)	N	N
	39°C (all media)	N	N
	H_2O_2 (LB)	N	N
	pH 3.0 (LB)	N	N
	pH 6.8 (all media)	N	N
	Aerobic (all media)	N	N
	Anaerobic (all media)	N	N
	Microaerophilic (all media)	N	N
	Sub-inhibitory rifampicin (LB)	N	N
	Sub-inhibitory ampicillin (LB)	N	N
	Sub-inhibitory streptomycin (LB)	N	N
	1% bile salts (LB)	N	N
	Mucin coated wells (LB)	N	N
	10% SDS (LB)	**Y**	N
	Co-culture with *E. coli* (LB)	N	N
in vivo Associations	GF association	**Y**	NA
	ASF association	**Y**	NA
	E. coli co-association	**Y**	N
	P. mirabilis co-association	**Y**	NA
	Dextran sodium sulfate in drinking water	**Y**	N
	Mice fed NIH-31M diet	**Y**	NA
	Mice fed RMH3000 diet	**Y**	NA

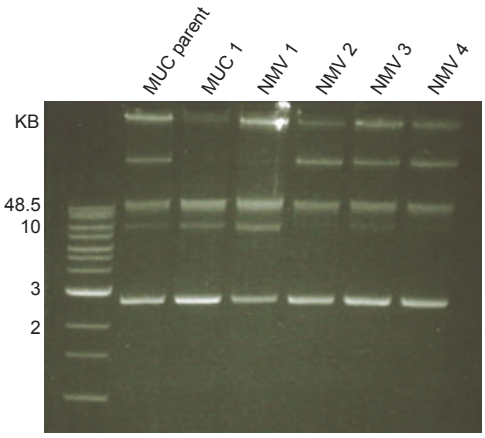

Figure 3.2. Plasmid profiles of mucoid (MUC) and NMV *K. pneumoniae*. Plasmids were isolated from overnight LB cultures using a Qiagen miniprep kit and visualized on a 1% agarose gel.

We investigated whether the mucoid phenotype was driven by major genomic rearrangements by assembling genomes, aligning contigs to the WGLW5 scaffold, and aligning variant genomes with Progressive Mauve (180). Only NMV4 showed a significant chromosomal rearrangement (**Supplemental Figure 3.2A**). In agreement with the Progressive Mauve alignment, when reads were aligned to the WGLW5 reference genome, there were no disagreements in gaps between mucoid variants (**Supplemental Figure 3.2B**). Differences in genomic content were assessed by aligning assembly reads to each annotated gene. After filtering proteins with poor sequencing coverage (median coverage > 2 IQR below 25th percentile), total divergence in genomic content was < 1.2% between variants, indicating low genomic loss (**Supplemental Table 3.3**). No genes were uniquely gained or lost between mucoid and NMV variants.

NMV *K. pneumoniae* display fitness advantages in response to environmental features of the gastrointestinal tract.

Given that mice are coprophagic, mice in our gnotobiotic model are constantly re-inoculating themselves with *K. pneumoniae*, sourced either from their littermates' or their own stool. In this model of self-inoculation, *K. pneumoniae* would need to survive in the dry, aerobic environment of a desiccating stool pellet for several hours in between hosts. To assess whether mucoid *K. pneumoniae* is less fit outside the gut, we compared culturable counts of NMV and mucoid *K. pneumoniae* in stool pellets over a 24-hr air-dry desiccation period. Populations of mucoid vs. NMV *K. pneumoniae* did not change in this desiccation time period (**Figure 3.3)**, suggesting that NMV population increases are driven by host factors and not by time spent *ex vivo.*

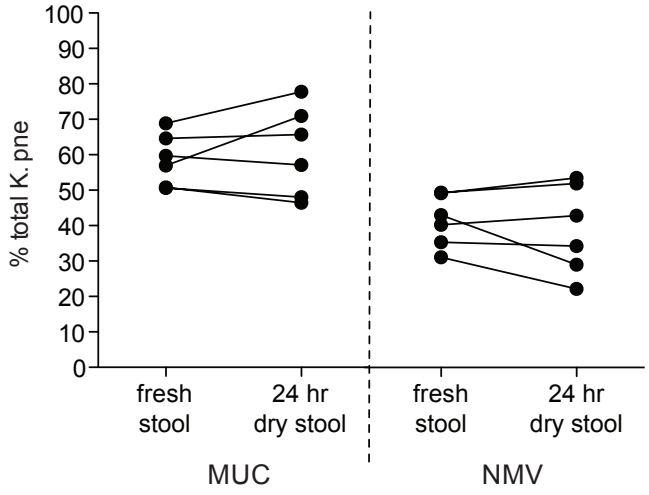

Figure 3.3. *K. pneumoniae* populations do not shift after 24 hours in desiccated stool. Stool from ASF-WT mice associated for 5 days with *K. pneumoniae* WGLW5 was assessed for culturable *K. pneumoniae* counts following collection and after 24 hours of desiccation at room temperature. Data points represent a stool pellet from individual mice (n=6). Lines connect stool from the same mouse.

To identify host selective pressures contributing to *K. pneumoniae* CPS loss, we investigated the response of CPS variants to gastrointestinal tract environmental conditions. A barrier to gastrointestinal colonization is the stomach's low pH. When challenged with low pH (pH 3.2; murine stomach pH is 3.0-4.0 (181)) more NMV *K. pneumoniae* survived than mucoid variants ($P \leq 0.05$ - $P \leq 0.001$) (**Figure 3.4A**). Also, NMVs population numbers recovered more quickly than mucoid *K. pneumoniae* following transfer from low pH to a neutral pH (**Figure 3.4B**). As an important control, in an absence of pH stress, NMV and MUC *K. pneumoniae* display similar growth dynamics, suggesting that MUC *K. pneumoniae* is able to grow as fast as NMVs *in vitro* (**Supplemental Figure 3.3**).

Bile salts are another host selective pressure in the gastrointestinal tract. Bile salts are present throughout the small intestine at concentrations between 0.2-2% (182, 183). In the presence of physiological bile salt concentrations (1%), NMV *K. pneumoniae* grew faster than mucoid variants (**Figure 3.4C**). More mucoid *K. pneumoniae* died during incubation in 2% bile acid than NMVs ($P \leq 0.05$ - $P \leq 0.001$) (**Figure 3.4D**). The superior survival and growth of NMV *K. pneumoniae* in environmental conditions encountered along the gastrointestinal tract help explain how NMVs may outcompete mucoid variants during gastrointestinal colonization over the course of several weeks.

CPS does not confer an advantage to *K. pneumoniae* in inflamed colons.

A CPS coat has been shown to protect *K. pneumoniae* from the host immune response, for example, from phagocytosis by macrophages (170, 171) and complement opsonization (172). For this reason, and given that our gnotobiotic mice were free from histologic signs of colonic inflammation, we hypothesized that NMV *K. pneumoniae*

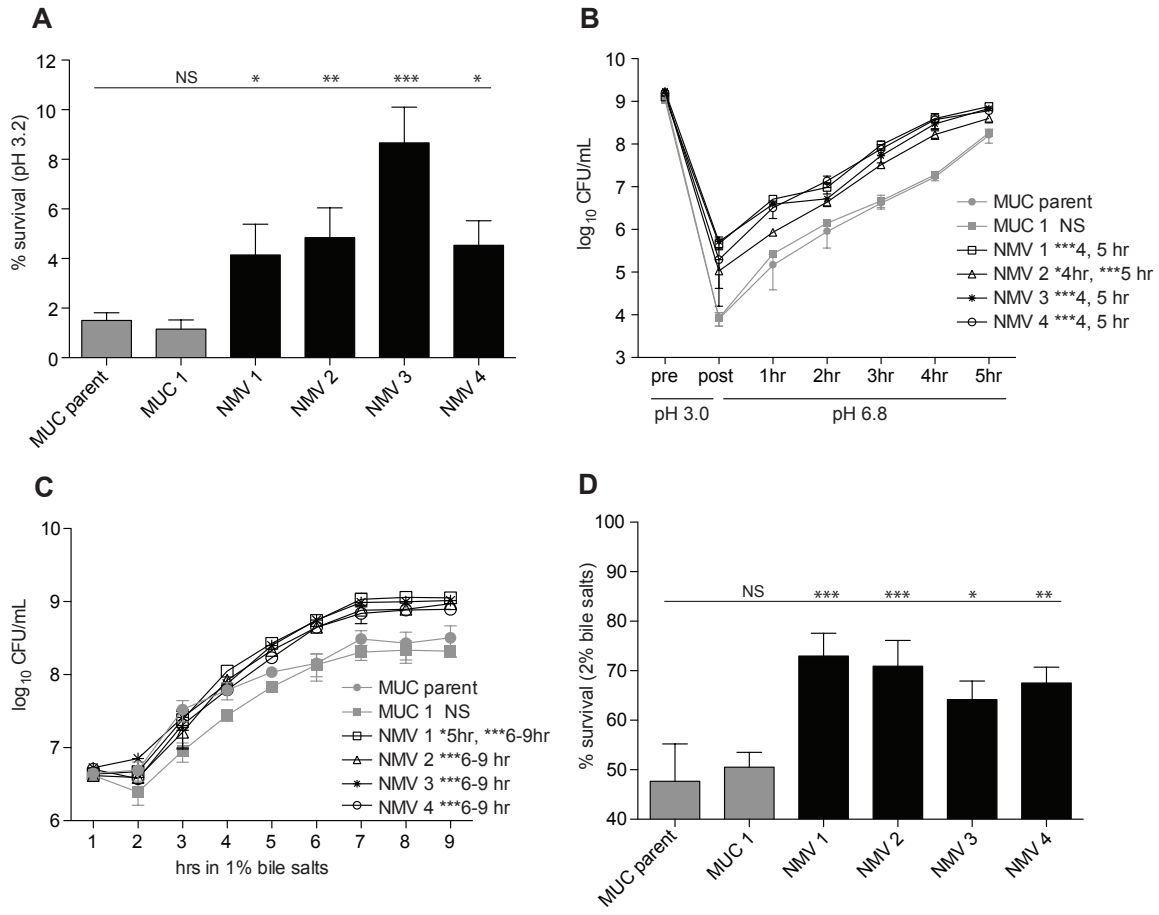

Figure 3.4. Fitness advantage of NMV *K. pneumoniae* in response to gastrointestinal tract environmental features. (A) Variant survival following incubation of overnight cultures in LB pH 3.2 for 2 h. Percentage survival compared to CFU counts prior to low pH. MUC- mucoid *K. pneumoniae*. **(B)** Recovery of variant CFU numbers following 2 h in LB pH 3.0 and resuspension in LB pH 6.8. **(C)** CFU growth curve of variants in the presence of 1% bile salts. **(D)** Variant survival following incubation of overnight cultures in 2% bile salts. Percentage survival compared to CFU counts prior to bile salt addition. Bars and data points represent mean ± SD of 3 biological replicates. *** $P \leq 0.001$, ** $P \leq 0.01$, * $P \leq 0.05$, one-way ANOVA with Dunnett's post-test in (A), (D), and two-way ANOVA with Bonferroni post-tests in comparison to MUC parent in (B) and (C).

would be less fit in an inflamed colon. To test this hypothesis, ASF-*Tbet*$^{-/-}$ *Rag2*$^{-/-}$ and GF-*Tbet*$^{-/-}$ *Rag2*$^{-/-}$ mice were colonized with *K. pneumoniae* WGLW5 for 4-weeks. At this time point, the fecal *K. pneumoniae* population is dominated by NMV variants (**Figure 3.1D**). Mice were then administered either 1.5% or 3% dextran sodium sulfate (DSS) in their drinking water for 9 days to induce epithelial injury and inflammation. Histology revealed that in the gnotobiotic ASF setting, 3% DSS induced colitis and 1.5% did not (**Figure 3.5A**). Fecal *K. pneumoniae* counts measured prior to and after DSS administration revealed an increase in fecal *K. pneumoniae* in the presence of DSS. Mucoid *K. pneumoniae* populations significantly increased in mice treated with both 1.5% and 3% DSS (**Figure 3.5B**), despite an absence of histologic colitis in mice receiving the lower dose. While mucoid *K. pneumoniae* increased in an inflamed colon, numbers of NMV *K. pneumoniae* did not significantly change.

Despite pre-established NMV *K. pneumoniae* populations being unaffected by the onset of inflammation in a pre-colonized colon, we asked whether inflammation prior to colonization would confer a competitive advantage to mucoid *K. pneumoniae* populations. ASF-WT mice were treated with 3% DSS for 5 days prior to inoculation with mucoid WGLW5. Counts of fecal *K. pneumoniae* over the course of 8 days on DSS revealed that inflammation did not stop the appearance of NMV *K. pneumoniae* (**Figure 3.5C**). Rather, the mucoid *K. pneumoniae* population slightly decreased by the end of the experiment compared to control mice. All mice had signs of histologic colitis (**Figure 3.5D**). Take together, these DSS experiments suggest that inflammation does not confer a competitive advantage to mucoid *K. pneumoniae* in the setting of the colon. These

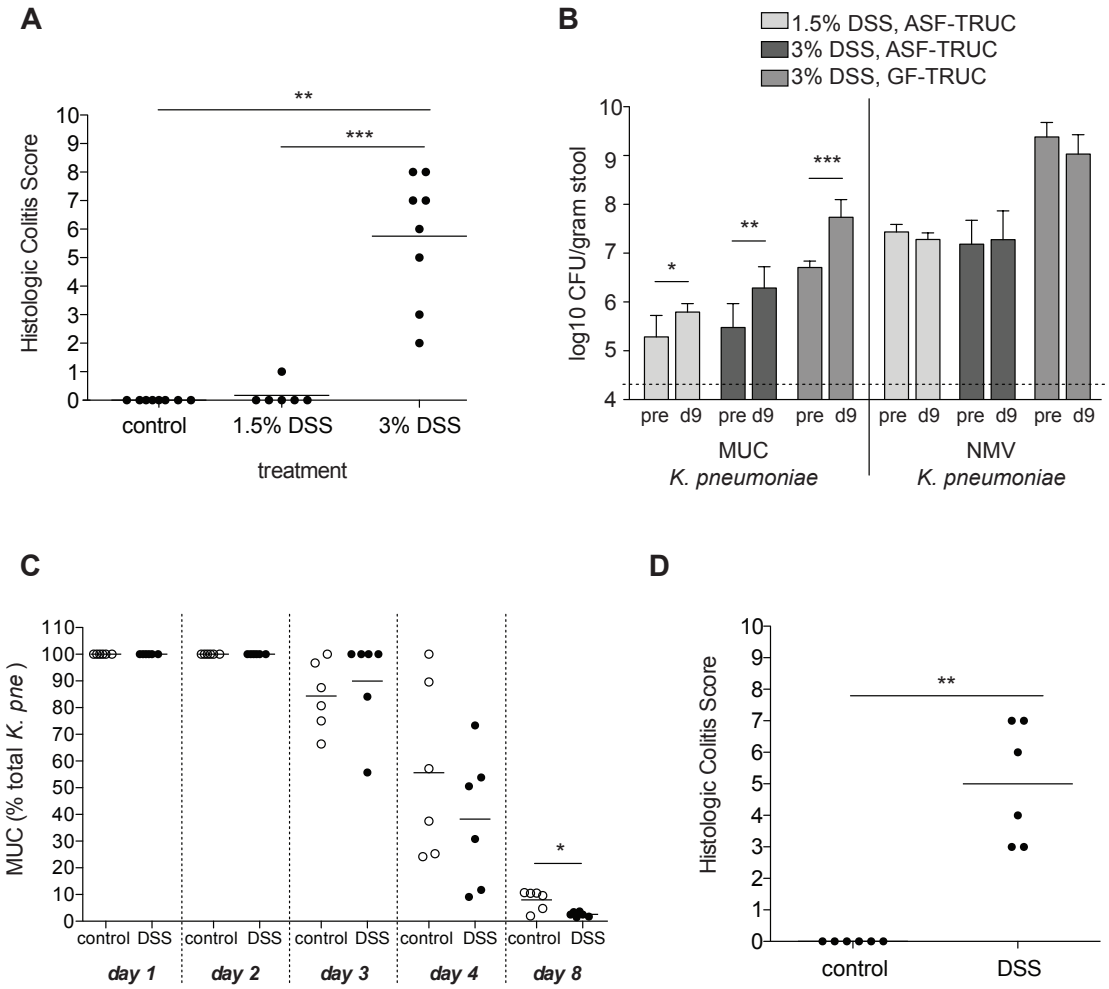

Figure 3.5. NMV *K. pneumoniae* colonization is not adversely affected by DSS-induced inflammation in the colon. **(A)** Histologic colitis score of colons from gnotobiotic ASF-TRUC mice associated with *K. pneumoniae* WGLW5 and administered 1.5% (n=6) or 3% DSS (n=8) in drinking water for 9 days. Control- DSS-free drinking water (n=8). **(B)** Log_{10} CFU/gram stool *K. pneumoniae* counts from stool before (pre) and after (d9) DSS administration in drinking water. Same mice as in (A), with the addition of WGLW5 colonized GF-TRUC receiving 3% DSS (n=8). **(C)** ASF-TRUC mice administered 3% DSS for 5 days, followed by colonization with mucoid (MUC) WGLW5. Counts of fecal *K. pneumoniae* were collected for 8 days following colonization and recorded as MUC colonies as a percentage of the whole *K. pneumoniae* population. 3% DSS continued for full length of experiment. n=6 for each group. **(D)** Histologic colitis score from mice from (C). Date points represent individual mice in (A), (C), (D). *** $P \leq 0.001$, ** $P \leq 0.01$, * $P \leq 0.05$, Mann-Whitney U test.

experiments also suggest that an absence of inflammation does not explain appearance of a large NMV population in our gnotobiotic mice.

CPS confers a competitive advantage to *K. pneumoniae* in the presence of a diverse microbiota.

Although we identified gastrointestinal tract selective pressures favoring NMV population expansion, emergence of spontaneous NMVs was not observed in our specified pathogen free (SPF) mice. To determine whether a more diverse microbiota could affect *K. pneumoniae* CPS shifts, ASF mice were colonized with *K. pneumoniae* for 4-wks and then inoculated with the colonic contents of SPF mice with no prior *K. pneumoniae* exposure. 8-wks after diverse microbiota inoculation, culturable counts of fecal *K. pneumoniae* decreased by several logs (**Figure 3.6A**). Fecal mucoid *K. pneumoniae* decreased by an average of 0.11 $\log_{10}$ CFU/g stool. In contrast, there was a large decline in NMV *K. pneumoniae* (average decrease of 2.3 $\log_{10}$ CFU/g stool; $P \leq 0.01$) (**Figure 3.6B**), suggesting that NMV *K. pneumoniae* is less fit when part of a diverse microbial community.

During host colonization and transmission, *K. pneumoniae* does not have the colonization advantage seen in our gnotobiotic model and must establish itself in the presence of many microbes. To address this, we developed a colonization model that introduced *K. pneumoniae* to mice concurrently with other symbionts. SPF pups were sprinkled with either mucoid or NMV *K. pneumoniae* daily for 7d beginning on their date of birth (**Figure 3.6C)**). 3-weeks after the final *K. pneumoniae* exposure, stool CFUs were quantified. Mucoid *K. pneumoniae* stably colonized SPF pups, whereas NMV *K. pneumoniae* were below the limit of fecal culture-based detection (3.7 $\log_{10}$ CFU/g stool, $P \leq 0.01$) (**Figure 3.6C**) and did not revert to producing CPS. Mucoid *K. pneumoniae* did

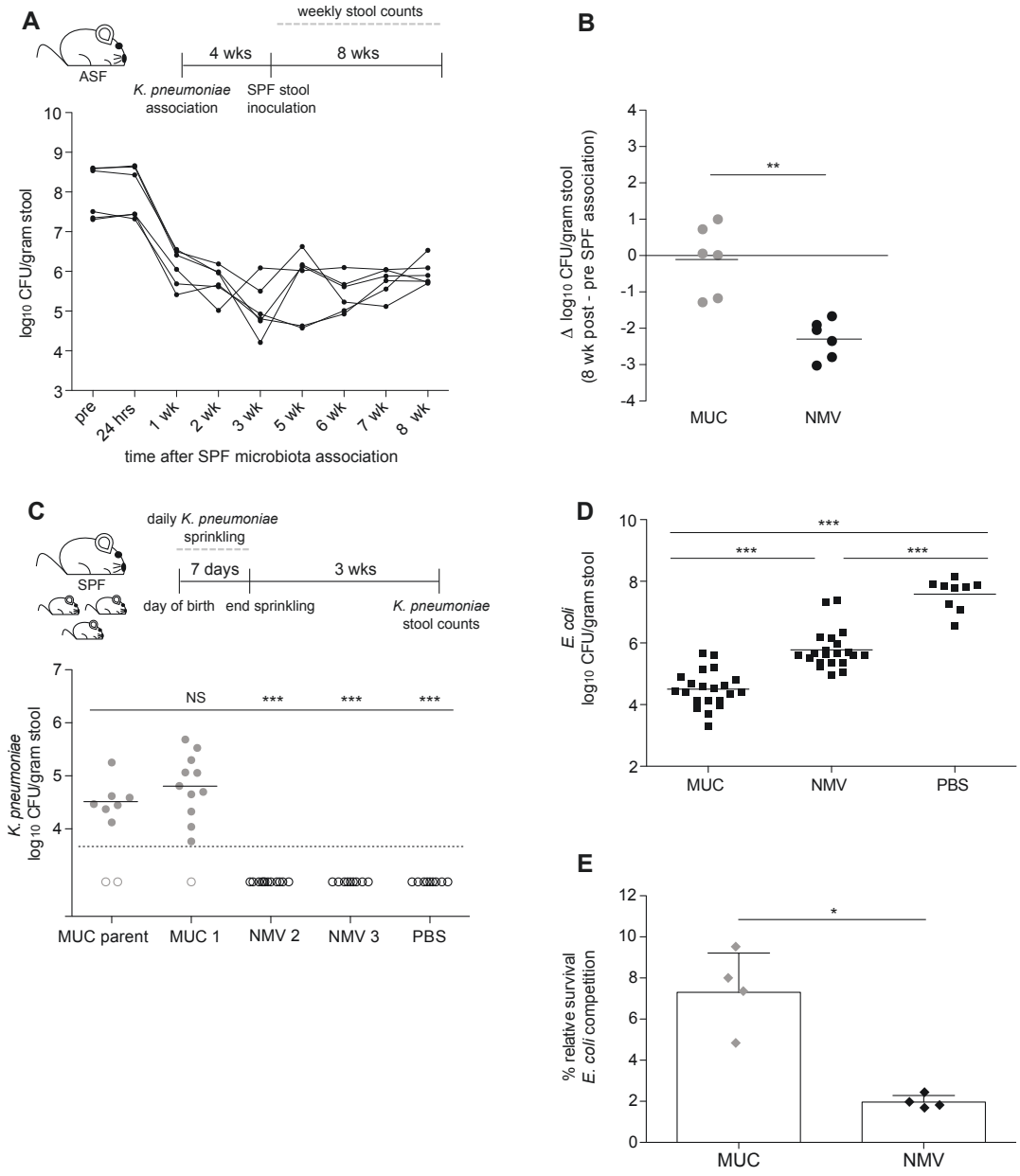

Figure 3.6. CPS affords *K. pneumoniae* a competitive advantage in the presence of a diverse microbiota. (A) ASF-WT mice (n=6) with a 4-wk established *K. pneumoniae* population were associated with stool from SPF mice. Total *K. pneumoniae* $\log_{10}$ CFU/g stool decline over 8-wks in the presence of SPF microbiota. Lines follow individual mice. **(B)** Change in mucoid (MUC) and NMV populations after 8-wks with a SPF-stool microbiota (from mice in A). **(C)** *K. pneumoniae* stool counts from 4-wk old SPF mice sprinkled with *K. pneumoniae* variants for 7d following birth (MUCparent, NMV3, and PBS n=9; MUC1 and NMV2 n=12). Counts were taken 3 wks after cessation of *K. pneumoniae* sprinkling. Limit of detection (LOD), 3.7 log10 CFU/g stool (dashed line). **(D)** *E. coli* stool counts from mice in (C). MUC group includes *E. coli* counts from pups sprinkled with MUCparent and MUC1; NMV group includes NMV2 and NMV3. Symbols in (C) and (D) represent individual mice. **(E)** *in vitro* competition between *K. pneumoniae* variants and *E. coli*. Each symbol represents survival of a *K. pneumoniae* isolate compared to growth in the absence of *E. coli*. *** $P \leq 0.001$, ** $P \leq 0.01$, Mann Whitney test. In (C), undetectable samples were given a value of the LOD for statistical analysis.

not give rise to NMVs in SPF mice, unlike the results of GF and gnotobiotic associations. These experiments also revealed that fecal *E. coli* levels differed between groups receiving a PBS control or CPS variants. Mucoid-sprinkled pups showed the lowest *E. coli* levels, whereas pups receiving PBS were colonized at much higher levels ($P \leq 0.001$) (**Figure 3.6D**).

While colonization resistance and niche fulfillment may play a role in balancing related bacteria in the gastrointestinal tract, direct inter-bacterial warfare is also possible (184, 185). To determine if *E. coli* and *K. pneumoniae* have an antagonistic relationship, competition assays were performed against an *E. coli* isolated from stool of a SPF-*Tbet*$^{-/-}$ *Rag2*$^{-/-}$ mouse (termed TRUC *E. coli* from here on). Since the *K. pneumoniae* variants described above had adapted to a GF environment in the absence of bacterial competition for 4-wks prior to isolation, competition experiments utilized 4 mucoid and 4 NMV *K. pneumoniae* isolates cultured from stool of GF mice colonized for only 1.5 wks with *K. pneumoniae*. Although all *K. pneumoniae* isolates were adversely affected by the presence of *E. coli*, mucoid *K. pneumoniae* displayed enhanced survival compared to NMVs (**Figure 3.6E**).

The TRUC *E. coli* genome contains multiple anti-bacterial systems that may contribute towards *K. pneumoniae* killing.

To investigate the antagonistic relationship observed between TRUC *E. coli* and *K. pneumoniae*, we performed a genomic analysis of our TRUC *E. coli* isolate. The TRUC *E. coli* genome was sequenced on an Illumina MiSeq by the Biopolymers Core of Harvard Medical School. After adapter trimming and removal of low quality reads, the Velvet assembler (186) was used for genome assembly, leading to a genome with 86 contigs. Genome annotation was performed with PROKKA (187).

Comparison of the TRUC *E. coli* genome to three additional gastrointestinal *E. coli* isolates with Progressive Mauve (180) revealed similar genome organization and overlap with *E. coli* LF82 (**Figure 3.7A**), an adherent and invasive (AIEC) strain originally isolated from the stool of a patient with Crohn's disease (188). TRUC *E. coli* displayed more breaks in homologous sequences, called local collinear blocks, or LCBs, with *E. coli* UM146, an AIEC strain from stool of a patient with Crohn's disease (189) (**Figure 3.7B**), SE11 from stool of a healthy human (190) (**Figure 3.7C**), and K12 MG1655, from the stool of a patient with gastroenteritis (191) **(Figure 3.7D**). This close genomic relationship between AIEC LF82 and TRUC *E. coli* was confirmed with the BLAST Ring Image Generator (BRIG) (192) (**Figure 3.8**).

Understanding that many differences observed between bacterial strains of the same species can be driven by genetic content contained on plasmids and within mobile genetic elements, the genomic island content of TRUC *E. coli* was assessed with Island Viewer (193). Island Viewer integrates the SIGI-HMM and IslandPath-DIMOB prediction methods. SIGI-HMM uses a hidden Markov Model to measure codon usage and IslandPath-DIMOB looks for genome regions with altered GC content relative to the whole genome, codon bias, transposases, and integrases. Island Viewer revealed that the majority of TRUC *E. coli*'s genomic island content is not shared with the LF82 genome and is unique to TRUC *E. coli* (**Figure 3.9**).

Island Viewer predicted 1327 genes contained within genomic islands for TRUC *E. coli*. 54% of this list mapped to hypothetical proteins according to PROKKA annotation. The 610 predicted proteins with annotation were binned into functional categories that include toxins and effector molecules, secretion and efflux systems, outer

membrane virulence factors, and phage (**Table 3.2**). This analysis revealed two loci for Type VI secretion systems (T6SS) within TRUC *E. coli*'s genome.

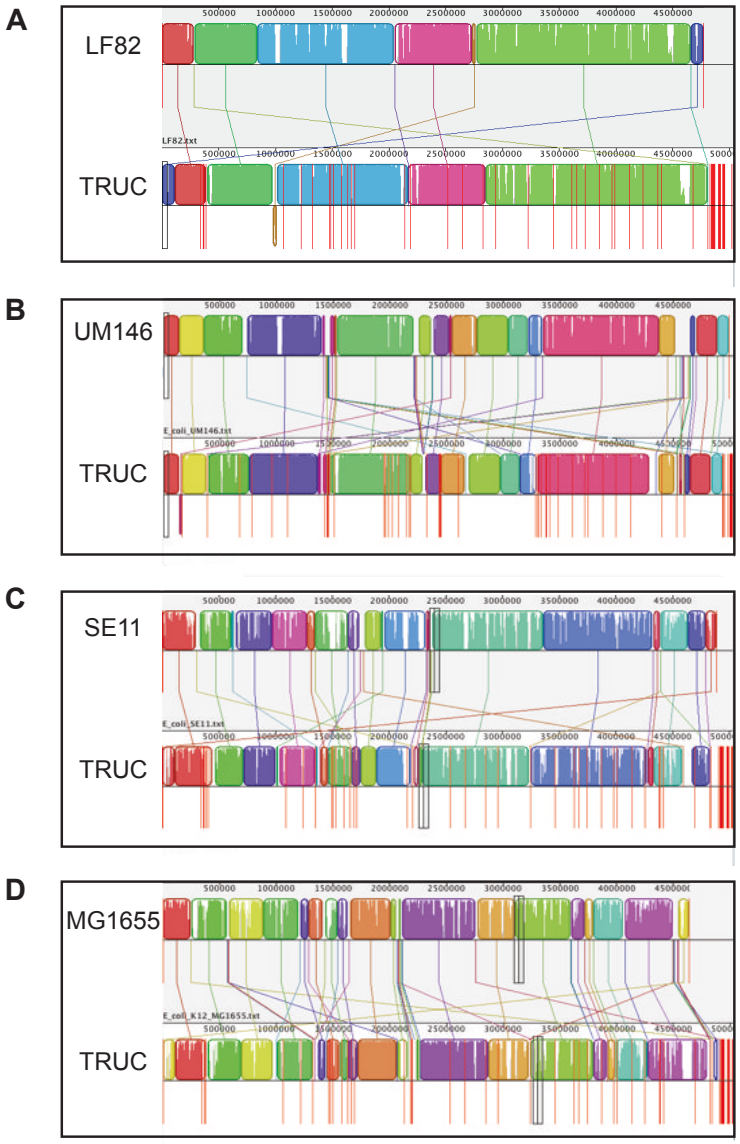

Figure 3.7. Mauve alignment of the TRUC *E. coli* genome to other gastrointestinal *E. coli* isolates. Rearrangement of the TRUC *E. coli* genome in comparison to the human *E. coli* isolates LF82 **(A)**, UM146 **(B)**, SE11 **(C)**, and MG1655 **(D)**. Vertical red lines mark contig boundaries of assembled genomes. Lines connecting genomes show rearrangements of local collinear blocks (LCBs). Homologous sequence without rearrangements are represented as rectangular LCBs.

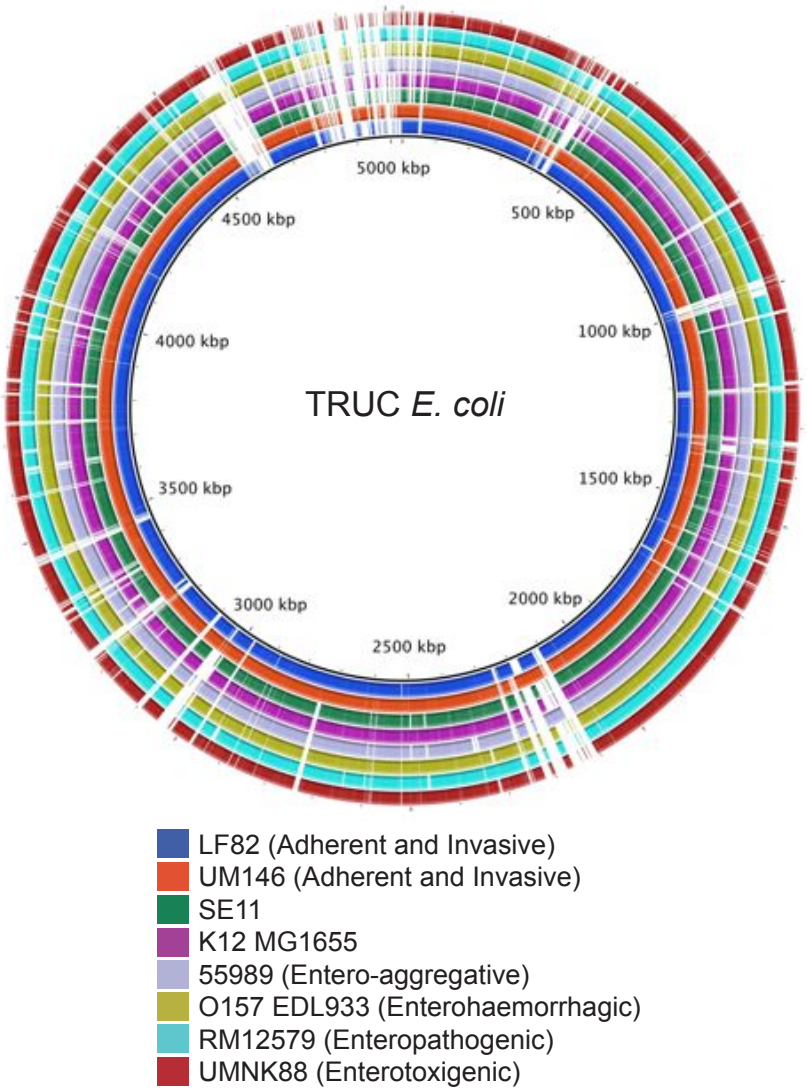

Figure 3.8. BLAST ring image of TRUC *E. coli* genome compared to 8 human gastrointestinal *E. coli* isolates. Image generated with BRIG. White spaces correspond to genomic content present in TRUC *E. coli* and absent from the associated human isolate.

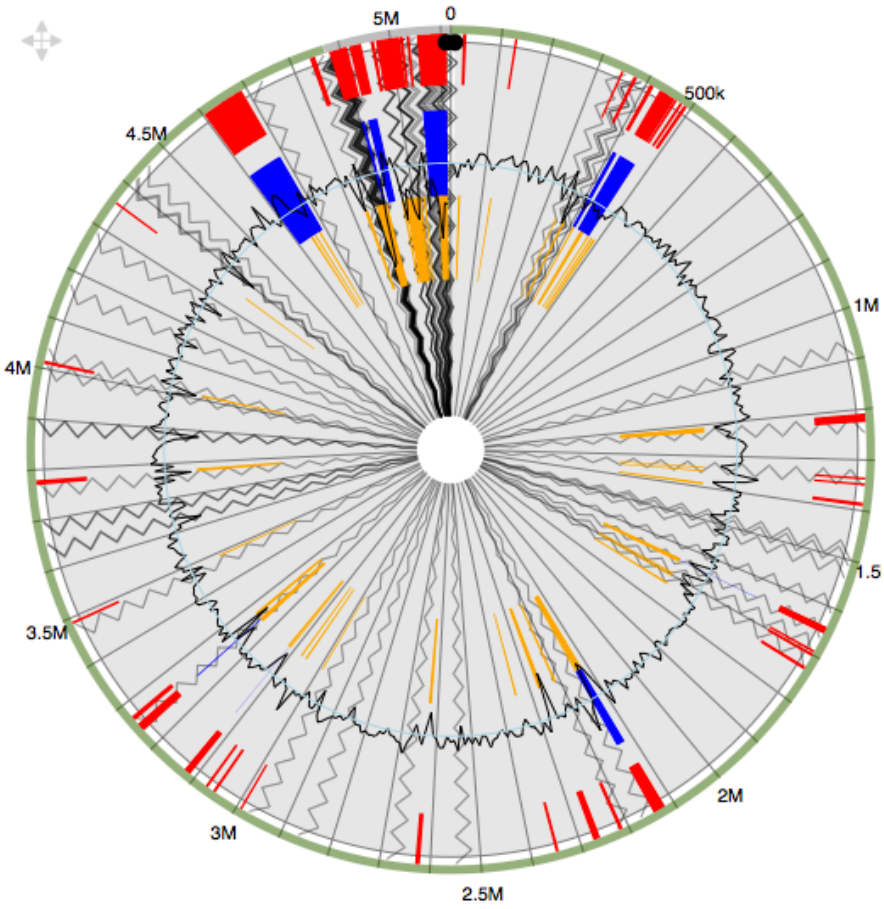

Figure 3.9. Genomic island content of TRUC *E. coli*. Island Viewer output showing genomic island content for TRUC *E. coli* aligned to *E. coli* LF82. Yellow- SIGI-HMM prediction method, blue- IslandPath-DIMOB prediction method, red- integrated results. Green circle rim represents shared genomic content between TRUC and LF82 *E. coli*. Gray circle rim shows the genomic content unique to TRUC *E. coli.*

Table 3.2. Predicted genomic island content of TRUC *E. coli.* Functional categories of genes predicted to lie within genomic islands using Island Viewer.

Functional Category	TRUC and LF82 Shared Accessory Proteins	Unique TRUC Accessory Proteins
DNA editing	Restriction enzymes Transcription factors Cas1/3/6 and CRISPR associated proteins	None
Toxins and effector molecules	Virulence activator VirF (TF) Toxic protein SymE Toxin-antitoxin (6 pairs) Small toxic polypeptide 121 Small toxic polypeptide LdrD Colicin E7 immunity, Colicin 1 receptor Lysozyme RrrD	Toxin RTX-1
Secretion and efflux	Type II secretion system T6SS(1 and 2) Conjugal transfer ABC transporter (multidrug resistance) Multidrug eflux pumps Mercury Resistance Ferric enterobactin transport system Siderophore transport system Sialic acid transport system Chemotaxis Quorum sensing	Type I secretion (RTX) Type II secretion Type IV secretion Siderophore transport system Plasmid conjugal transfer proteins Outer membrane efflux system
Outer membrane virulence factors	CPS biosynthesis LPS biosynthesis Fimbriae Flagella components Biofilm formation Curli (CdsgG/F/E)	Flagella Adhesin YadA
Phage	Bacteriophage proteins (lambda and others)	Prophage

Given the emerging role of T6SS in bacterial inter and intra species competition, we further defined the T6SS loci identified within the TRUC *E. coli* genome. While PROKKA labeled the majority of the genes in these regions as hypothetical proteins, manual BLAST comparisons revealed relationships to previously defined T6SS loci (**Figure 3.10**). Comparison of TRUC *E. coli*'s two T6SS loci to those studied in other *E. coli* isolates revealed a strong similarity in gene presence and organization to LF82,

uropathogenic, and avian pathogenic *E*. coli (194). Of the two loci identified, T6SS1 is thought to contribute to bacterial competition while T6SS2 has been implicated in the pathogenesis of meningitis (194). The strain specific regions of T6SS loci (light gray region in **Figure 3.10**) typically contain effector proteins. BLAST did not reveal annotated matches for TRUC-specific T6SS genes, however PGAP1-like protein domains have been found in effector proteins from other T6SS loci (195, 194) and it is possible that this protein in TRUC *E. coli*'s T6SS1 loci plays a role in bacterial killing. Experiments with *E. coli* T6SS1 mutants should be performed to confirm a role for T6SS in interactions with *K. pneumoniae.*

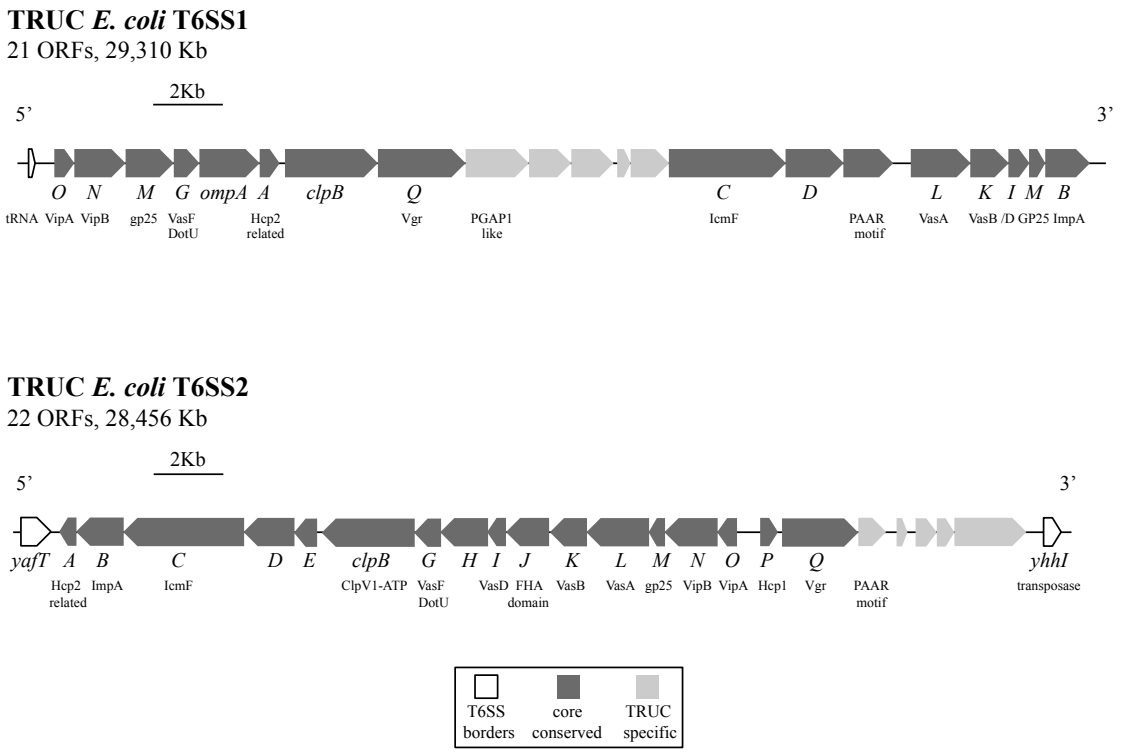

Figure 3.10. T6SS1 and T6SS2 of TRUC *E. coli.* T6SS were defined using a combination of PROKKA annotation and manual BLAST comparisons. Gene labeling according to the scheme used by Ma, et al. 2014. Predicted protein family, domain, or motif recorded below gene label. Loci shown to scale. Genes shaded light gray represent regions unique to TRUC *E. coli*'s T6SS loci as assessed by BLAST. All other genes are found in previously identified *E. coli* T6SS loci.

Biogeography of mucoid *K. pneumoniae* populations correlate with regions of high Paneth cell antimicrobial expression in the gastrointestinal tract.

Despite NMV *K. pneumoniae*'s fitness advantages over mucoid variants in the absence of bacterial competition, a small population of mucoid *K. pneumoniae* was maintained in gnotobiotic animals throughout an 8-wk colonization (Figure 3.1D, F). To investigate maintenance of mucoid populations, we explored *K. pneumoniae*'s biogeography throughout the gastrointestinal tract. The gastrointestinal tracts of ASF mice were divided into 7 sample sites (**Supplemental Figure 3.4A**). Culturable counts of *K. pneumoniae* were taken from the luminal contents and associated mucosa at each site. Total *K. pneumoniae* in luminal contents increased sequentially along the gastrointestinal tract (**Figure 3.11A**). NMV *K. pneumoniae* predominated throughout most of the gastrointestinal tract in both luminal and mucosal sites with the exception of the distal small intestine, where the proportion of mucoid *K. pneumoniae* spiked (**Figure 3.11B**). The distal small intestine also had the highest gene expression of *lysozyme 1* (**Figure 3.11C**) and cryptdins, mouse enteric α-defensins (**Figure 3.11D**), which are antimicrobial peptides (AMPs) released by Paneth cells (196). There was a direct relationship between high mucoid *K. pneumoniae* populations and high host cryptdin expression (Spearman correlation, r=0.39, P=0.015) (**Figure 3.11E**). Mucoid *K. pneumoniae* levels did not follow the expression pattern of AMPs produced by colonic epithelial cells (*mouse β-defensin3*, **Supplemental Figure 3.4B**), suggesting that AMPs produced specifically by Paneth cells may shape *K. pneumoniae* CPS population distribution in the gut.

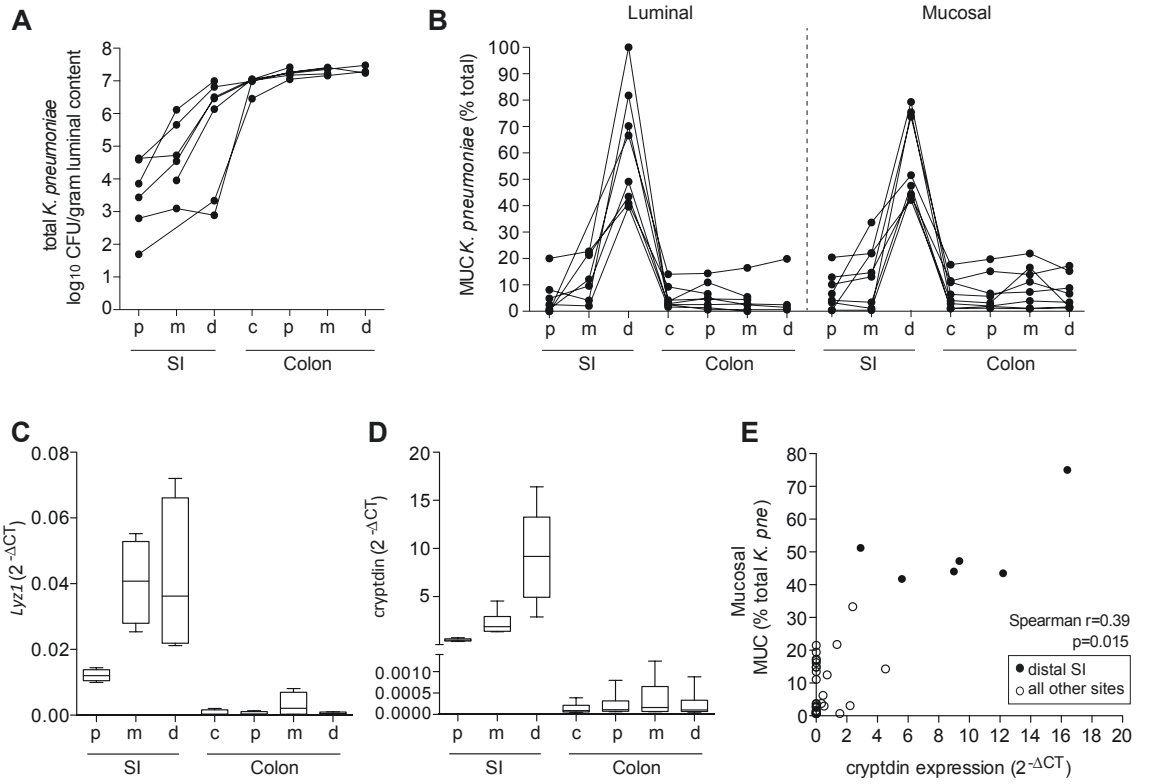

Figure 3.11. Biogeography of mucoid (MUC) *K. pneumoniae* populations correlate with regions of high Paneth cell AMP expression in the gastrointestinal tract. (A) Total *K. pneumoniae* CFU recovered from luminal contents throughout the gastrointestinal tract. Proximal (p), mid (m), distal (d), and cecum (c). Missing data points correspond to gastrointestinal regions with no luminal content at the time of the experiment. **(B)** Luminal and mucosal MUC *K. pneumoniae* populations throughout the Gastrointestinal tract as a percentage of total *K. pneumoniae*. Host Lysozyme1 **(C)** and general cryptdin **(D)** expression along the gastrointestinal tract. **(E)** Positive Spearman correlation between samples sites with high MUC populations and high host cryptdin expression. Shaded symbols represent distal SI site, open symbols represent all other sites. For (A) and (B) symbols connected by lines represent individual mice (n=8), for (C) and (D) box and whiskers show mean ± SD for n=6 mice, in (E) symbols represent single sample sites from n=6 mice.

CPS protects *K. pneumoniae* from killing by Paneth cell α-defensins.

Based on the correlation between mucoid *K. pneumoniae* and high host cryptdin expression, we hypothesized that CPS provides *K. pneumoniae* with an advantage in the presence of α-defensins *in vivo*. We tested the sensitivity of *K. pneumoniae* to α-defensins and found increased killing activity against NMVs compared to mucoid *K. pneumoniae* with cryptdin 23 (Crp23, produced by mouse Paneth cells, **Figure 3.12A**), α-defensin 1 (HNP1, produced by human neutrophils, **Figure 3.12B**), and α-defensin 5 (HD5, produced by human Paneth cells, **Figure 3.12C**) ($P \leq 0.05$ - $P \leq 0.001$), supporting the conclusion that CPS protects *K. pneumoniae* from host α-defensins. Mucoid *K. pneumoniae* is also protected from killing by β-defensins (**Supplemental Figure 3.5**), but as the geography of expression does match mucoid *K. pneumoniae* colonization (**Supplemental Figure 3.4B**), these AMPs may be less of a selective pressure or be present at too low concentrations in the colons of healthy mice to impact *K. pneumoniae* population dynamics.

Small intestinal organoids can be cultured from primary stem cells present in intestinal crypts. They model the complex small intestinal epithelium and contain its full complement of differentiated cells types (196). Using microinjection into organoids to model luminal bacterial exposure within the gastrointestinal tract, Paneth cell α-defensins have been shown to restrict bacterial growth in organoids (197). However, bacterial growth was not restricted in organoids produced from *Mmp7*$^{-/-}$ mice, which lack active Paneth cell α-defensins but are otherwise physiologically normal (198). To address the effects of CPS on *K. pneumoniae* exposed to naturally secreted Paneth cell α-defensins, we compared the growth of mucoid and NMVs after microinjection into wild-type (WT)

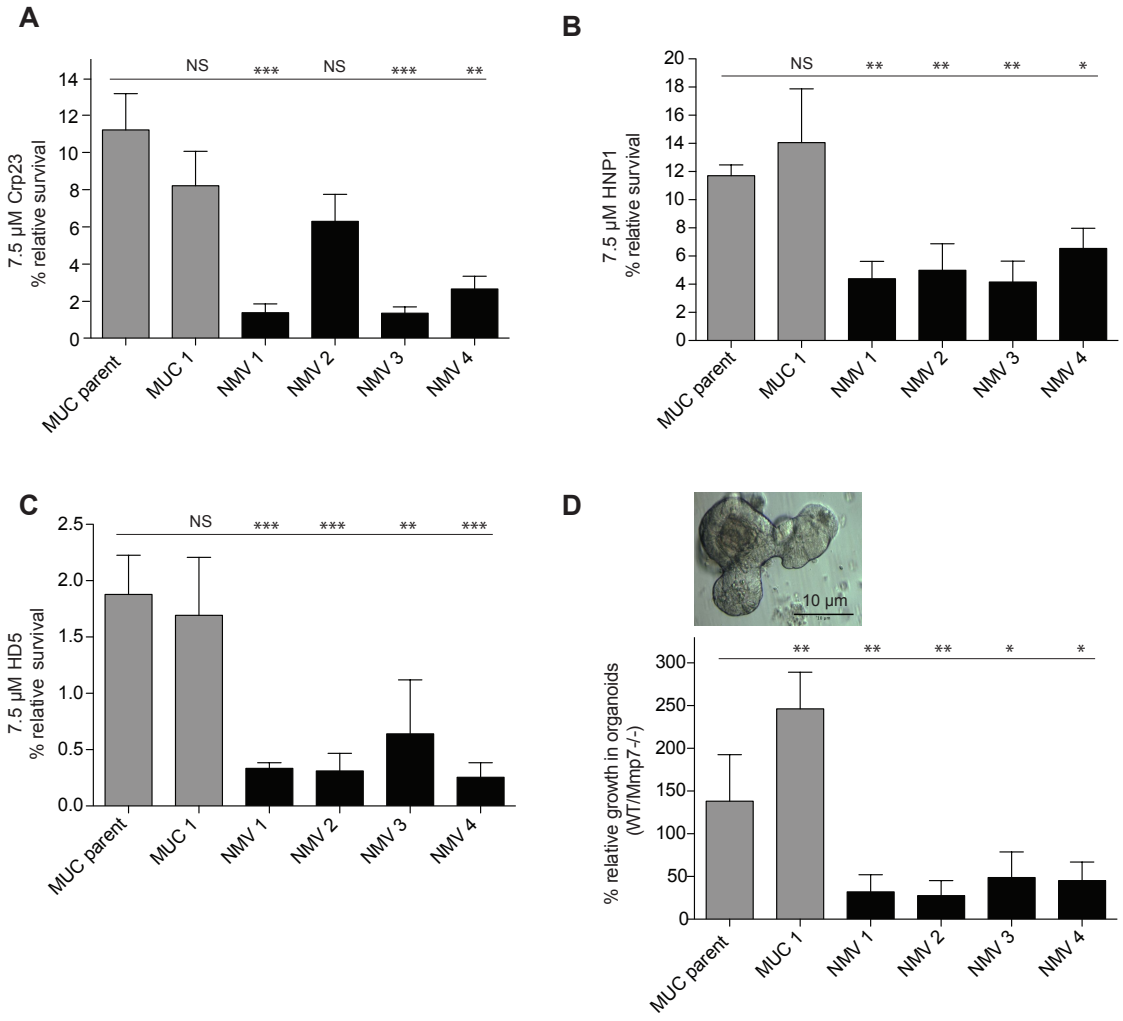

Figure 3.12. CPS protects *K. pneumoniae* against killing by Paneth cell AMPs. Relative survival of mucoid (MUC) and NMV variants in the presence of murine Crp23 **(A)**, human HNP1 **(B)**, and human HD5 **(C)**. Relative survival as compared to untreated samples. **(D)** Image of a small intestinal organoid in culture (top). Relative survival of CPS variants in organoids with Paneth cell cryptdin production (WT) compared with organoids defective in cryptdin production (*Mmp7*$^{-/-}$). *** $P \leq 0.001$, ** $P \leq 0.01$, * $P \leq 0.05$, one-way ANOVA with Dunnett's posttest.

and *Mmp7*$^{-/-}$ small intestinal organoids. A significant (2-4 fold; $P \leq 0.05$ - $P \leq 0.001$) growth inhibition was seen with all NMVs in the WT organoids compared to growth in *Mmp7*$^{-/-}$ organoids (**Figure 3.12D**). In contrast, mucoid *K. pneumoniae* growth actually increased in WT organoids (**Figure 3.12D**). These data support that increased sensitivity of NMVs to AMPs, specifically α-defensins, imposes selective pressure in the mouse small intestine during colonization.

V. DISCUSSION

The diverse and dense microbial environment of the mammalian gastrointestinal tract has made understanding the response of bacterial populations to individual features of the gastrointestinal environment challenging. GF and gnotobiotic mouse models with minimal microbial communities allowed us to disentangle contributions from the host and microbiota in shaping spatial population dynamics of the gut symbiont, *K. pneumoniae*, along the gastrointestinal tract. While the presence of a mucoid CPS coat was a handicap for *K. pneumoniae* when subjected to the harsh gastrointestinal conditions of bile salts and a low pH *in vitro* (**Figure 3.4**), maintenance of mucoid populations in the distal small intestine, and more importantly, absence of NMV populations in the gastrointestinal tracts of conventionally colonized mice, suggested the presence of other significant selective pressures.

In tracing the biogeography of *K. pneumoniae* CPS populations along the gastrointestinal tract, Paneth cells emerged as selective pressure favoring mucoid *K. pneumoniae.* While prior work has demonstrated *in vitro* resistance to cationic AMPs by *K. pneumoniae* and other encapsulated bacteria (176, 177), determining if and how this

shapes *K. pneumoniae* CPS populations *in vivo* has remained elusive. Not only did mucoid *K. pneumoniae* tolerate direct exposure to physiologic levels of purified AMPs better than NMVs (**Figure 3.12A-C**), but mucoid *K. pneumoniae* also displayed enhanced growth in the presence of naturally secreted Paneth cell AMPs in small intestinal organoids (**Figure 3.12D**). This finding speaks to a growing body of research suggesting that microbes actively sense and respond to host immune molecules, with one of the most striking examples being activation of quorum sensing and virulence pathways in *Pseudomonas aeruginosa* upon binding of host interferon γ to the bacterial outer membrane porin OprF (199). With respect to AMPs, polymixin B or neutrophil defensin 1 exposure has been hypothesized to increase *K. pneumoniae* CPS production (176) and to globally alter *K. pneumoniae* gene expression (200). A recent report on the influence of AMPs on gastrointestinal bacterial communities found that several common gut symbiotic bacteria share high levels of resistance to AMPs (201). Additionally, differential α-defensin expression influences the composition of symbiotic bacterial populations in SPF mice (202). Collectively, these studies support the importance of Paneth cells in influencing bacterial colonization of the host (203).

In this study, we also identified an advantage conferred by CPS when *K. pneumoniae* is part of a complex gastrointestinal microbiota (**Figure 3.6**). The selective pressure of a diverse microbiota was best exemplified during *K. pneumoniae* colonization of SPF mice inoculated as neonates (**Figure 3.6C**). Neonatal Paneth cell numbers remain low until post-natal day 28 (204), suggesting that the selective pressure of Paneth cell α-defensins was minimal in these mice and highlighting the strong influence of the microbiota. There have been contradictory data on the role of capsule when *K.*

pneumoniae colonizes the gastrointestinal tract (128, 175). The most recent direct investigation of this question reported equivalent gastrointestinal colonization between mucoid and non-mucoid mutants as measured by fecal bacterial counts in streptomycin treated mice (175), which harbor a markedly perturbed gut microbiota. Streptomycin depletes the gastrointestinal tract of many potential *K. pneumoniae* competitors, such as other members of the γ-*Proteobacteria* (34), including *E. coli*, which we found had an antagonistic relationship with *K. pneumoniae* (**Figure 3.6E**). Additionally, fecal CFU counts of *K. pneumoniae* recovered from streptomycin treated mice in Struve *et al.* are several logs higher than those that we observed in SPF mice and are equivalent to colonization levels we observed in gnotobiotic associations (**Supplemental Table 3.1**). Thus, the data of Struve *et al.* are not in conflict with our observations, but rather, support our findings on NMV expansion in gnotobiotic ASF associations (**Figure 3.1**) and that gut microbial community diversity is a selective pressure for *K. pneumoniae* CPS maintenance.

Further studies are needed to define the precise role that CPS plays in *K. pneumoniae*'s interactions with other bacteria. We hypothesize that CPS may aide *K. pneumoniae* in several ways. Unfortunately, the mechanism of CPS loss in NMVs remains indeterminate. Genomic analyses did not reveal SNPs or large deletions shared among NMVs that could explain CPS loss (**Supplemental Table 3.2**). Genes regulating CPS production, such as *rmpA,* are often carried on plasmids (101); however, NMV plasmid profiles were similar to mucoid profiles (**Figure 3.2**). *K. pneumoniae* with CPS coats grow faster as a biofilm as compared to engineered NMVs (205). Biofilms in the gut have been found attached to food particles, and bacteria residing in gut biofilms are

known to digest complex carbohydrates at different rates than non-aggregated bacteria (206). Perhaps CPS, by aiding in the establishment of a fast-growing biofilm, help *K. pneumoniae* sequester and utilize resources more efficiently than NMV *K. pneumoniae* when competing with many other bacteria for the same pool of resources.

Alternatively CPS may afford *K. pneumoniae* a competitive advantage in a complex microbiota through physical protection from direct bacterial interactions. Given the mechanistic similarities between host AMPs and bacterially produced antimicrobials (207), CPS may protect *K. pneumoniae* against bacterially produced antimicrobials. In support of this concept, we observed increased survival of mucoid *K. pneumoniae* as compared to NMVs during *in vitro* competition experiments with a murine *E. coli* isolate (**Figure 3.6E**). While little research to date has focused on competition between *K. pneumoniae* and *E. coli* specifically, antagonistic relationships can exist between bacteria of the same phylum, family, and often species in polymicrobial environments such as the Gastrointestinal tract (208).

The cache of antimicrobial weaponry employed by bacteria against other bacteria includes microcins, contact-dependent inhibition (CDI), and type VI secretion of protein effectors. Gram-negative bacteria produce many AMPs. For example, the *E. coli* AMP, microcin7, exhibits antimicrobial activity against *K. pneumoniae* (209). In addition to released bacterial toxins such as microcins and colicins, *E. coli* can deliver toxins using methods that require cell-to-cell contact with a targeted bacterium. While type VI secretion (T6SS) were initially described in relation to host-pathogen interactions (210), extensive work in *Vibrio cholera* and *Pseudomonas aeruginosa* has established a role for this system in intra- and inter-species bacterial warfare (211, 212). T6SS loci have been

reported in many species of Proteobacteria, including *E. coli* (213). Investigation of the genome of the *E. coli* used in our studies revealed presence of two T6SS loci and a predicted microcin, which may contribute to the inhibitory interaction we observed against *K. pneumoniae*. Just as CPS can physically protect *K. pneumoniae* from antimicrobials in solution, CPS may restrict access of CDI or T6SS machinery to the cell surface proteins required for CDI, or to the bacterial periplasm necessary for T6SS. Collectively our data suggest that CPS is an important defense mechanism against attack from both host and bacterial cells. In the gastrointestinal tract of conventional mice, the host and the gut microbiota likely act in tandem to select for a mucoid *K. pneumoniae* population. This begins with Paneth cell AMPs in the distal small intestine and is followed by increased microbial density and diversity throughout the colon. By maintaining a mucoid *K. pneumoniae* population in the ileum, the host has selected *K. pneumoniae* to be a more effective competitor in the lower gastrointestinal tract. This host-microbiota co-maintenance of mucoid *K. pneumoniae* populations, which represent the most virulent clinical isolates, may explain why the gastrointestinal tract is a significant reservoir for human *K. pneumoniae* disease. While CPS has classically been studied as a means to evade the host immune system, we define the importance of mucoid CPS for when *K. pneumoniae* becomes part of the polymicrobial environment of the colon. Overall, our study suggests that bacterial-bacterial interactions may be equally, if not more important than host factors in influencing the population dynamics of a single bacterial species within the gastrointestinal tract.

VI. MATERIALS AND METHODS

Bacterial strains and culture conditions

K. pneumoniae WGLW5 (mucoid parent; BEI HM-749) and the murine *E. coli* strain were previously cultured from stool of BALB/c *T-bet*$^{-/-}$ *x Rag2*$^{-/-}$ (TRUC) mice (127). MUC1, NMV1, NMV2, NMV3, and NMV4 are WGLW5 derivatives isolated from stool after a 4-week passage of WGLW5 through a GF mouse. *K. pneumoniae* strains used in competition with *E. coli* were isolated after 1.5-week passage of WGLW5 through a GF mouse. *K. pneumoniae* WGLW2 (BEI HM-751) and WGLW3 (BEI HM-748) are clinical isolates cultured from human sputum and stool respectively. Bacteria were cultured in Luria-Bertani (LB) broth shaking aerobically at 37°C overnight or on MacConkey agar. Growth curves (Fig. 2c) were conducted in 6 mL LB with overnight bacteria diluted 1:500.

ASF strains- *Clostridium* sp. (ASF356), *Lactobacillus* sp. (ASF360), *Lactobacillus murinus* (ASF361), *Mucispirillum schaedleri* (ASF457), *Eubacterium plexicaudatum* (ASF492), *Firmicutes* bacterium (ASF500), *Clostridium* sp. (ASF502), and *Parabacteroides* sp. (ASF519) were obtained from Iowa State University (214).

Animal husbandry

SPF mice were housed in microisolator cages in the Harvard T. H. Chan School of Public Health barrier facility. Mouse studies were approved and carried out in accordance with Harvard Medical School's (HMS) Standing Committee on Animals and the N.I.H. guidelines for animal use and care. GF and gnotobiotic mice were bred and maintained under sterile conditions in gnotobiotic isolators at Children's Hospital Boston.

Female and male BALB/c mice aged 6-12 weeks were used for GF, gnotobiotic, and SPF experiments unless noted. Mice were bred in house unless noted.

Culture-based studies of fecal and mucosal *K. pneumoniae* populations

GF and gnotobiotic-ASF mice we orally inoculated with ~1x10^8 *K. pneumoniae* suspended in PBS (or 50 µl of feces resuspended in PBS). An equal amount was spread on their fur and anus. At indicated time points, stool was collected from individual mice and serially diluted 10-fold using sterile PBS onto MacConkey agar for *K. pneumoniae* culturable counts after 24 h at 37° C. Colonies were counted on plates with bacterial densities of 30-300 CFU. Log_{10} CFU/ g stool bacteria were calculated after accounting for dry and wet fecal weights. Mucoid and NMV populations are presented as percentages of total *K. pneumoniae* CFU.

For the stool desiccation study, pellets were collected from individual mice and half of each sample was plated for CFU enumeration after weight measurements. The remaining stool sample was allowed to dry for 24 hours at room temperature. Following this desiccation period, samples were weighed and serial diluted onto MacConkey agar for the final CFU count.

SPF pup inoculation

Beginning on the day of birth, SPF BALB/c pups (Charles River) were sprinkled with 1.5 x 10^8 CFU *K. pneumoniae* in PBS daily for 7 days. 3-weeks after the final *K. pneumonia*e inoculation, stool was assessed for culturable counts of *K. pneumoniae* and *E. coli*. Individual colonies were re-streaked onto Tryptic Soy Agar (TSA) for 18 h at 37°C and screened for indole production (BD DMACA Indole reagent). Indole (-) *K. pneumoniae* stained pink; indole (+) *E. coli* stained blue.

Gnotobiotic DSS colitis model

ASF-TRUC mice were associated with *K. pneumoniae* WGLW5 for 4 weeks. Stool was collected and plated for culturable *K. pneumoniae* counts on MacConkey agar. Drinking water was amended with 1.5% or 3% DSS (Affymetrix), filter sterilized. After 8 days on DSS, stool was plated and mice were sacrificed. Colons were harvested and processed for histology.

In a second experiment, ASF-TRUC mice were administered 3% DSS in drinking water for 5 days, followed by colonization with *K. pneumoniae* WGLW5. Counts of fecal *K. pneumoniae* were collected for 8 days following colonization. 3% DSS continued for full length of experiment

Histology

At the time of sacrifice, colons were harvested, colonic contents were removed, and tissues were fixed in a solution of PBS with 4% paraformaldehyde. Tissue was paraffin embedded, sectioned into 0.5 um thick sections and stained with hematoxylin and eosin. Blinded slides were scored by Dr. Jonathan Glickman. Colitis scores were assigned based on the cumulative sum of four criteria with a severity ranking between 0-4: mononuclear cell infiltration, polymorphonuclear cell infiltration, epithelial crypt hyperplasia, and epithelial injury. 0-absent, 1-mild, 2-moderate, 3-severe as described previously (166).

Glucuronic acid measurement

K. pneumoniae CPS production was assessed by measuring the glucuronic acid content (215, 216) of extracted bacterial CPS (217). 100 µl of 1% Zwittergent 3-14 (Sigma) in 100 mM citric acid was added to 500 µl of a washed overnight *K. pneumoniae*

culture re-suspended in PBS or to a PBS solution containing an overnight *K. pneumoniae* colony from agar. Following incubation for 30 min at 50° C and centrifugation, 250 µl supernatant was added to 1 mL ethanol. After precipitation at 4° C for 30 min, samples were spun, supernatants were removed, pellets were dried for 20 min on ice, and capsular material was resuspended in 200 µl H_2O. Glucuronic acid was measured by adding 1.2 mL 12.5 mm tetraborate in concentrated H_2SO_4 to 200 µl aliquots of D-glucuronic acid standards (Sigma) and extracted *K. pneumoniae* CPS. Samples were heated at 70° C for 5 min. 20 µl of a 0.15% 3-phenylphenol (Sigma) in 0.5% NaOH were added to cooled tubes. Samples were vortexed, and 520nm absorbances were recorded after 10 min. CPS concentrations were reported as fg glucuronic acid per CFU based on initial culture concentrations.

***K. pneumoniae* genomic analyses**

CPS gene clusters for WGLW2, 3, and 5 were defined by BLAST comparisons of genes in the known vicinity of CPS clusters using whole-genome sequences (WGSs) generated by the *Klebsiella* group Sequencing Project, Broad Institute of Harvard and MIT.

MiSeq WGSs of MUCparent, MUC1, NMV1, NMV2, NMV3, and NMV4 were generated by the HMS Biopolymers Core. Burrows-Wheeler Aligner (BWA) was used to align variant reads to the WGLW5 reference genome. SNPs were identified using Samtools (http://samtools.sourceforge.net). Raw sequence reads have been deposited in NCBI's SRA. **Table 3.3** lists accession IDs.

Table 3.3. *K. pneumoniae* whole-genome sequence submissions.

Isolate	Source	Capsule Phenotype	WGS Sequence Data	Database	Accession
WGLW2	human sputum	mucoid	assembled and annotated	NCBI GenBank	GCA_000300675.1
WGLW3	human stool	mucoid	assembled and annotated	NCBI GenBank	GCA_000300935.1
WGLW5	murine stool	mucoid	assembled and annotated	NCBI GenBank	GCA_000300955.1
MUC parent	passaged WGLW5	mucoid	raw .fastq reads	NCBI SRA	SRR1743357
MUC 1	MUC parent derivative after passage through GF mouse	mucoid	raw .fastq reads	NCBI SRA	SRR1743361
MUC 1 resequenced	MUC parent derivative after passage through GF mouse	mucoid	raw .fastq reads	NCBI SRA	SRR1743377
NMV 1	MUC parent derivative after passage through GF mouse	non-mucoid	raw .fastq reads	NCBI SRA	SRR1743362
NMV 2	MUC parent derivative after passage through GF mouse	non-mucoid	raw .fastq reads	NCBI SRA	SRR1743364
NMV 3	MUC parent derivative after passage through GF mouse	non-mucoid	raw .fastq reads	NCBI SRA	SRR1743365
NMV 4	MUC parent derivative after passage through GF mouse	non-mucoid	raw .fastq reads	NCBI SRA	SRR1743366
NMV 4 resequenced	MUC parent derivative after passage through GF mouse	non-mucoid	raw .fastq reads	NCBI SRA	SRR1743379

Assembly and annotation of strains

150 bp paired-end Illumina reads from each strain (Parent, MUC1, NMV1, NMV2, NMV3, and NMV4) were assembled with SPAdes assembler v 3-5-0 (218). Scaffolds for each strain were annotated with Prokka (187), using the flag "–kingdom Bacteria." All scaffolds, gene annotations, and code are available for download at http://huttenhower.sph.harvard.edu/klebsiella2015/

Ordering of scaffolds

The WGLW5 reference genome (GenBank; GCF_000300955.1) contains 10 scaffolds. To determine their putative placement, we used Contiguator (219) to align them to chromosome 1 of the completed genome *K. pneumoniae* strain MGH78578 (gi|150953431|gb|CP000647.1). In this manner, we partitioned the scaffolds of the WGLW5 genome into four ordered genomic scaffolds and six plasmids (lengths 337582, 139159, 40758, 26040, 24319, and 4470 bp). We used this ordered WGLW5 scaffold created by Contiguator as a reference to order the scaffolds of all other assemblies, then used ProgressiveMauve (180) to assess genomic rearrangement on chromosome 1.

Determination of assembly gaps

For each assembly, bowtie2 (220) was used to align reads to chromosome 1 of the reference genome WGLW5. Bedtools (221) was used to calculate coverage for each alignment, as detailed in the script "bed.sh". The resulting tracks were visualized with Integrative Genome Viewer (7).

Conservation of genomic content

In order to assess whether gene content was conserved between strains, for each gene, we used bowtie2 (220) to align reads from each strain. We then calculated median coverage across all bases for each gene using bedtools (222). We removed low-coverage outlier genes, defined as (coverage < (25^{th} percentile - (2 * interquartile range))) for each genome.

TRUC *E. coli* genomic analyses

The TRUC *E. coli* genome was sequenced on an Illumina MiSeq by the Biopolymers Core of Harvard Medical School. Adapter trimming was performed with Trimmomatic (223). Low quality bases were removed with a trailing score of 20 and a sliding window of 20. Velvet (186) was used for genome assembly with a Kmer of 85 and minmum contig length of 200 base pairs, and PROKKA (187) was used for genome annotation.

Comparison of the TRUC *E. coli* genome to three additional gastrointestinal *E. coli* isolates was undertaken using Progressive Mauve (180). The BLAST Ring Image Generator (BRIG) (192) confirmed genomic relationships between TRUC *E. coli* and 8 additional *E. coli* isolates.

Island Viewer (193) identified genes predicted to fall on genomic islands, and BLAST was used to more fully define and annotate the T6SS loci of TRUC *E. coli*.

***K. pneumoniae* survival assays**

Altered pH and bile acid

Overnight cultures of *K. pneumoniae* were washed in PBS and re-suspended in an equal volume of LB pH 3.0 (amended with hydrochloric acid) or LB with 2% Difco Bile Salts No. 3 (BD). Surviving CFU were enumerated after shaking at 37°C for 2 h. Percentage survival compared to initial bacterial concentrations.

Human and mouse α-defensins

Overnight *K. pneumoniae* cultures were diluted 20x into fresh LB and incubated at 37°C for 1 h with shaking. Cultures were diluted to OD600 0.5 with 10 mM PIPES and

1% tryptic soy broth (PIPES-TSB). Bacteria were washed 2x and resuspended in 1 mL PIPES-TSB. After a 1:10 dilution in PIPES-TSB, 25 µl bacteria were mixed with 7.5 µM HNP1 (Abcam), HD5 (Hycult Biotech), or Crp23 (purified by reverse-phase high-pressure liquid chromatography from oxidative refolding of partially purified linear peptides (224)). Samples were incubated at 37°C for 2 h with shaking before CFU enumeration. Percentage relative survival in comparison to untreated bacterial samples.

E. coli competition killing

Competition assays were performed as previously described (211). Briefly, overnight cultures of *E. coli* and *K. pneumoniae* were washed and diluted 100x into LB. After 2.5 h at 37°C with shaking (OD600 of ~0.8), bacteria were centrifuged at 10,000 X g and resuspended to an OD600 of ~10. *K. pneumoniae* and *E. coli* were mixed 1:1, 5 µl were spotted onto LB agar, and plates were incubated at 37°C for 2 h. Agar spots were resuspended in 1 mL PBS. CFU were enumerated on MacConkey agar. Percent relative survival in comparison to *K. pneumoniae* spotted in the absence of *E. coli*.

Biogeography of *K. pneumoniae* in the gastrointestinal tract

The Gastrointestinal tracts of gnotobiotic mice associated with *K. pneumoniae* WGLW5 for 4-weeks were divided into 7 sections: equal thirds of the small intestine representing the proximal, middle, and distal small intestine; the cecum; and equal thirds of the colon representing the proximal, middle, and distal colon. Luminal contents and host tissue were taken at each site for *K. pneumoniae* counts and RNA extraction (tissues preserved in RNAlater, Ambion). A PBS wash removed residual luminal content from tissue samples. Luminal and washed mucosal samples were homogenized in PBS and plated for enumeration.

Real-time (RT)-qPCR

Tissue in RNAlater was washed with PBS prior to physical homogenization in Qiazol. RNA was extracted (Qiagan RNeasy Mini Kit), DNase treated, and reverse transcribed into cDNA (Bio-Rad iScript cDNA Synthesis Kit). RT-qPCR was performed using the SYBR FAST Universal qPCR Kit (KAPA Biosystems). Gene expression was normalized to *β–actin* expression. Primer sequences are shown in **Table 3.4**.

Table 3.4. Primer sequences used in RT-qPCR expression studies.

Primer	Sequence 5'-3'
ActB 987 (forward)[1]	TACCACCATGTACCCAGGCA
ActB 1083 (reverse) {Martinon:2010kt}	CTCAGGAGGAGCAATGATCTTGAT
Cryptdin[a] (forward) {Hashimoto:2012bx}	TCCTCCTCTCTGCCCTYGTCCTG
Cryptdin[a] (reverse) {Hashimoto:2012bx}	CTCTTCTCCTGGCTGCTCCTC
LYZ1 (forward) {Hashimoto:2012bx}	GCCAAGGTCTACAATCGTTGTGAGTTG
LYZ1 (reverse) {Hashimoto:2012bx}	CAGTCAGCCAGCTTGACACCACG
mBD3 (forward) {RivasSantiago:2006fd}	TCTGTTTGCATTTCTCCTGGTG
mBD3 (reverse) {RivasSantiago:2006fd}	TAAACTTCCAACAGCTGGAGTGG

[a] These primers are labeled DEFA1 (225); however, because they recognize many Crp isoforms, we consider them a general measure of Crp expression.

Small intestinal organoid production, maintenance, and microinjection

Organoids from WT and *Mmp7*$^{-/-}$ mice, both on a C57BL/6NHsd background (224), were cultured in growth factor reduced Matrigel (BD Biosciences) and Complete Crypt Culture Medium (CCCM) and microinjected as previously described (197). 3 days prior to microinjection, organoids were subcultured, deposited in 30 µl Matrigel on glass coverslips in 12-well tissue culture dishes, and overlaid with 1 mL CCCM without

antibiotics. On the day of the experiment, overnight cultures in LB were diluted 1:20 to a final volume of 10 mL in LB. After 1 h at 37°C with shaking, 1 mL was washed 2x and resuspended in 100 µl of PBS. One needle was used to microinject 20 organoids of each genotype, which comprised a single sample. Each organoid received ~$5x10^2$ CFU. Samples were incubated in CCCM without antibiotics for 1 h, followed by 1 h with 100 µg/mL gentamicin. Organoids were washed 2x with Advanced DMEM/F12 and grown in CCCM without antibiotics. At 9 h post-injection, organoids were removed from Matrigel using Cell Dissociation Solution (BD Biosciences) at 4° C for 30 min, pelleted at 300 x g for 5 min, and resuspended in 100 µl sterile water for 5 min to lyse eukaryotic cells. Samples were vortexed for 15 sec before serial dilution onto LB agar. Relative survival as a percentage of CFU recovered from WT organoids divided by *Mmp7*$^{-/-}$ organoids.

Statistical Analyses

Statistical calculations were performed using GraphPad Prism® software. Utilized tests include Mann-Whitney, one-way ANOVA with Dunnett's post-test, two-way ANOVA with Bonferroni post-tests, and Spearman correlation.

CHAPTER 4

CONCLUSIONS AND FUTURE DIRECTIONS

I. CONCLUSIONS

Klebsiella pneumoniae is a clinically important bacterium that causes many infections in susceptible patients and is a growing cause for concern for patients and infectious disease specialists because of its ever-increasing antibiotic resistance. One of the reasons *K. pneumoniae* can spread so quickly in hospital and community settings is because this bacterium can be carried as part of the gastrointestinal microbiota of healthy individuals. This thesis explores *K. pneumoniae* in the setting of its principal reservoir for human disease- the gastrointestinal tract.

Expanding on previous work with murine-derived *K. pneumoniae* (127), we find that human clinical isolates are also able to drive colonic inflammation in mice regardless of their original organ of isolation. Although all isolates could drive inflammation, only WGLW5, an isolate of mouse origin, was able to move beyond the gastrointestinal tract, as reflected by presence of this bacterium in mesenteric lymph nodes. Through gnotobiotic associations we also observed a previously unidentified sexual dimorphism in colitis severity in the *Tbet*$^{-/-}$ *Rag2*$^{-/-}$ mouse model of ulcerative colitis. Colitis was found to be more severe in male mice.

Many virulent *K. pneumoniae* isolates possess a mucoid capsule. This thesis assesses the importance of capsule for *K. pneumoniae* survival in the gastrointestinal tract. Our data suggest that Paneth cell antimicrobial peptides exert selective pressure that favors mucoid *K. pneumoniae* populations. In addition to defining host factors that influence *K. pneumoniae* populations, this study reveals that *K. pneumoniae's* capsule provides it with a competitive advantage against other bacteria in the gastrointestinal

tract, providing compelling evidence for biological relevance of capsule beyond traditional virulence functions.

II. LIMITATIONS AND FUTURE DIRECTIONS

Small panel of *K. pneumoniae* isolates

One limitation of these studies is the small panel of *K. pneumoniae* isolates tested (**Chapter 2**). Ideally, comparative genomic approaches should reveal genome signatures of virulence depending on host adaptation and original site of *K. pneumoniae* isolation. However, with only 1 murine isolate, it is difficult to draw conclusions about gene selection specific to host species. Additionally, since our isolates were taken from diverse tissue sites, we could not relate auxiliary genome content to selection for specific environments (eg. colon vs. nasopharynx vs. urinary tract). This issue was further complicated by the finding the *K. pneumoniae* WGLW5, taken from murine stool, is more genetically similar to the human sputum isolate than the human stool isolate. Future studies would benefit from inclusions of larger pool of *K. pneumoniae* isolates collected from different hospitals and diverse organ sites.

Minimal microbial community necessary for *K. pneumoniae* driven inflammation

Another limitation of this work lies in the inability to define the minimal microbial community necessary for *K. pneumoniae* to drive colonic inflammation (**Chapter 2**). As addressed previously, the ASF likely represents too minimal of a gnotobiotic microbial community to recapitulate the results of feeding *K. pneumoniae* to SPF mice. This could be due to lack of essential interactions between *K. pneumoniae* and

other bacteria in the microbiome, or due to a deficiency in immune development and response driven by gnotobiotic communities.

Moving forward, several approaches could be utilized to further define microbial community requirements for *K. pneumoniae* driven disease. Continuing to leverage gnotobiotics, individual bacterial species can be added to the ASF. Taking inspiration from Andrew Goodman's consortium (74) and from a lack of *Bacteroidetes* in the ASF, *Bacteroides thetaiotamicron* and *Bacteroides vulgatus* represent promising initial candidates. Observations from this thesis suggest that *K. pneumoniae* interacts with closely related species of *Proteobacteria* in the gastrointestinal tract (**Figure 2.3C, Figure 3.6D, E**). For this reason, inclusion of another *Proteobacteria,* such as *E. coli*, to gnotobiotic ASF mice may change *K. pneumoniae*'s behavior in the gastrointestinal tract in a way that promotes inflammation of host tissue.

Conversely, instead of building a microbiota from scratch in gnotobiotic mice, a full microbiota can be systematically depleted of bacterial groups with antibiotics *in vivo*. After identifying differential combinations of antibiotics that allow or prevent *K. pneumoniae* associated colonic inflammation, 16S rRNA amplicon sequencing of DNA from stool will help identify necessary strains.

Method of CPS variation

A significant limitation of the work presented in **Chapter 3** is an incomplete understanding of the nature of capsule loss in NMVs of *K. pneumoniae*. While stability of the NMV phenotype both *in vitro* and *in vivo* argues for a genetic basis of decreased capsule production, comparison of genome sequences in a SNP analysis, gene presence and absence screen, and an assessment of genome rearrangements did not reveal any

shared or likely mechanisms that could explain the NMV phenotype. Given that NMVs appear gradually over time in gnotobiotic mice and that the NMV phenotype manifests in heterogeneous colony morphology, one interpretation of our results is that there are likely many genomic events that could lead to capsule loss. If each of the 4 NMV isolates is producing less capsule due to independent mutations, our approach of using comparative genomics and looking for shared genome changes will not provide answers. While we attempted to account for this by expanding our analysis to search for mutations in shared functional pathways, this was not an exhaustive strategy.

Another interpretation of our findings is that the NMV phenotype is driven by changes in gene expression rather than gene loss or mutation. While stability of the NMV phenotype seems to argue against phase variation or expression changes, it is possible that with complex regulation we have not been able to mimic the environment necessary to induce capsule re-expression in CPS variants. Several experimental procedures could be attempted in the future to assess the contribution of gene expression to capsule loss in NMV *K. pneumoniae*.

RNAseq could be used on capsule variants to measure differential gene expression and look for commonalities among NMV variants. A caveat to this approach is that the regulatory network involved in capsule production for *K. pneumoniae* is not fully worked out. While well studied transcription factors such as *rmpA* and *rmpA2* are known to increase capsule expression, most *K. pneumoniae* isolates do not carry the plasmids containing these regulatory elements and, yet, still maintain high CPS expression (101). Coupled with the heterogeneity of the NMV phenotype and possibility

of several mechanisms contributing to CPS loss, RNAseq results have the potential to be difficult to interpret.

In order to assess epigenetic control of capsule production in NMV *K. pneumoniae*, the methylation status of the genome could also be addressed. Sequencing with the Pacific Bioscience (PacBio) SMRT sequencing technology can identify modified pieces of bacterial DNA (226). PacBio sequencing reveals carbon-5-methylated cytosines, nitrogen-6-mehtylated adenines, and nitrogen-4-methylated cytosines (227). Methylation has been shown to be involved in the regulation of pili expression in *E. coli* (228), LPS expression in *Legionella pneumophila* (229), and could represent an as yet unidentified regulatory mechanism for CPS expression in *K. pneumoniae*.

An important control to use in studies of *K. pneumoniae* CPS moving forward is an isogenic isolate with CPS deficiency resulting from a defined mutation. Deletion of highly conserved genes in the CPS gene cluster, such as *gnd* or *galF*, using the lambda Red recombination system (230) may generate such a strain.

Paneth cell deficient mice

In **Chapter 3**, we use small intestinal organoids from mice that either lack or produce mature cryptdins to show that MUC *K. pneumoniae* has a growth advantage in the presence of physiological concentrations of host antimicrobial peptides. While a better experimental system than *in vitro* killing assays, organoids do not fully replicate the conditions that *K. pneumoniae* would be experiencing in a live animal. Future experiments would benefit from the use of gnotobiotic mouse models with Paneth cell AMP deficiencies. These models include both the *Mmp7*$^{-/-}$ mice (198) that were used for organoid generation in **Chapter 3** and ATG16L1^{HM} mice. These mice are hypomorphic

for a Crohn's disease susceptibility risk allele and have been shown to be deficient in Paneth cell release of AMPs (14). If capsule is truly protective against host AMPs, in an absence of functional Paneth cells NMV *K. pneumoniae* would be expected to fully overtake MUC *K. pneumoniae* in the small intestine of GF or gnotobiotic ASF mice.

Summary

This thesis explores the relationship between the capsule of *K. pneumoniae,* other bacteria, and the host throughout the gastrointestinal tract. We implicate capsule in protecting *K. pneumoniae* from direct killing by antimicrobial peptides produced by Paneth cells in the small intestine and from killing by *E. coli*. Studies diving deeper into the mechanism of antagonism between *K. pneumoniae* and *E. coli* will further define the importance of capsule in interactions between bacteria. Given the clinical burden of *K. pneumoniae*, complete knowledge of this bacterium's colonization factors could aide in novel preventative and therapeutic approaches to eliminate *K. pneumoniae* from the gastrointestinal tract of carriers.

APPENDIX I

SUPPLEMENTARY MATERIALS

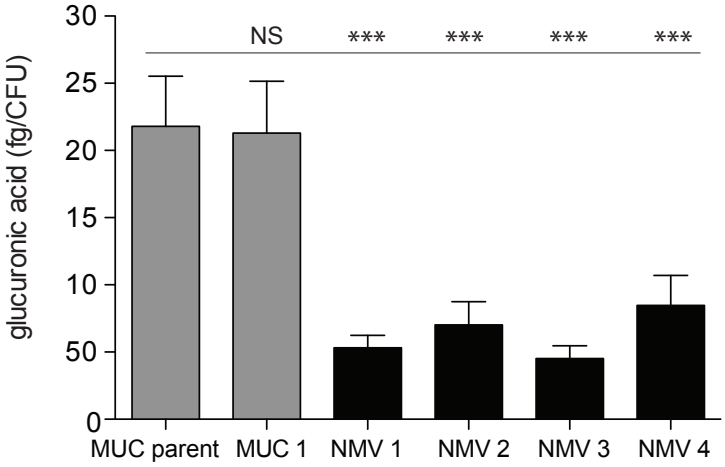

Supplemental Figure 3.1. Reduced glucuronic acid content of NMV *K. pneumoniae* isolates. Membrane fractions were isolated from overnight mucoid (MUC) and NMV variants in liquid LB culture and assessed for glucuronic acid concentration via acid hydrolysis. Bars represent mean ± SD of 3 biological replicates. ***, $P \leq 0.001$, one-way ANOVA with Dunnett's post-test.

A

B

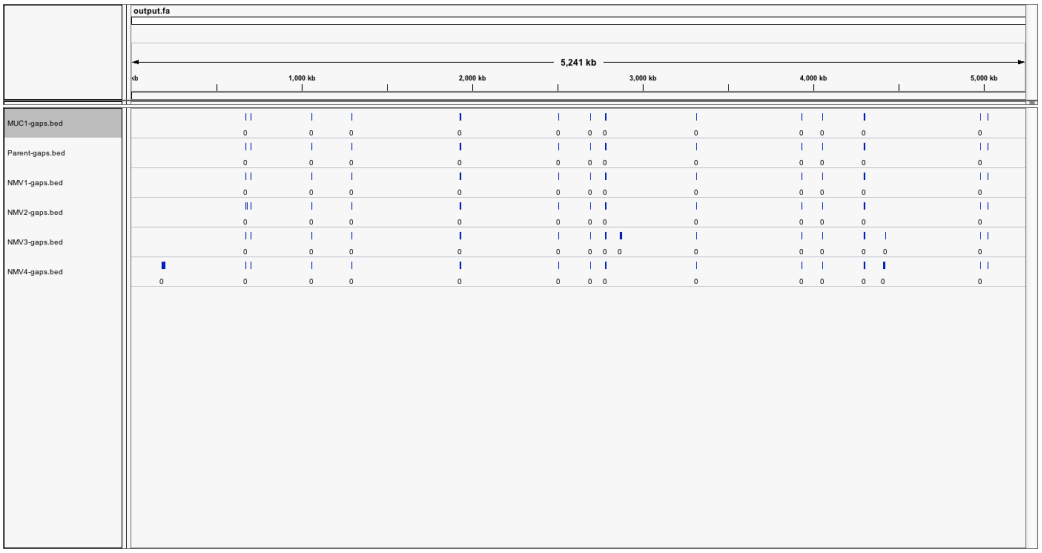

Supplemental Figure 3.2. Comparative genomic analyses of *K. pneumoniae* variants. (A) ProgressiveMauve alignments of the scaffolds of *K. pneumoniae* variants MUC1, NMV1, NMV2, NMV3, NMV4, and Parent. **(B)** The distribution of gaps in chromosome 1 of the genomes of *K. pneumoniae* variants MUC1, NMV1, NMV2, NMV3, NMV4, and Parent, relative to WGLW5 reference genome.

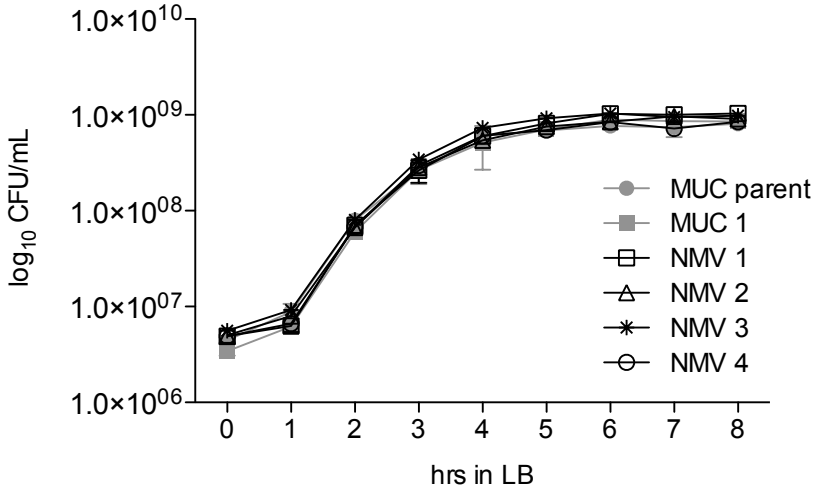

Supplemental Figure 3.3. Growth curve of *K. pneumoniae* variants in LB broth. Overnight cultures diluted 1:500 into 6mL fresh LB and grown shaking at 37°C. Aliquots serial diluted onto MacConkey agar for CFU counts every hour for 8 hours.

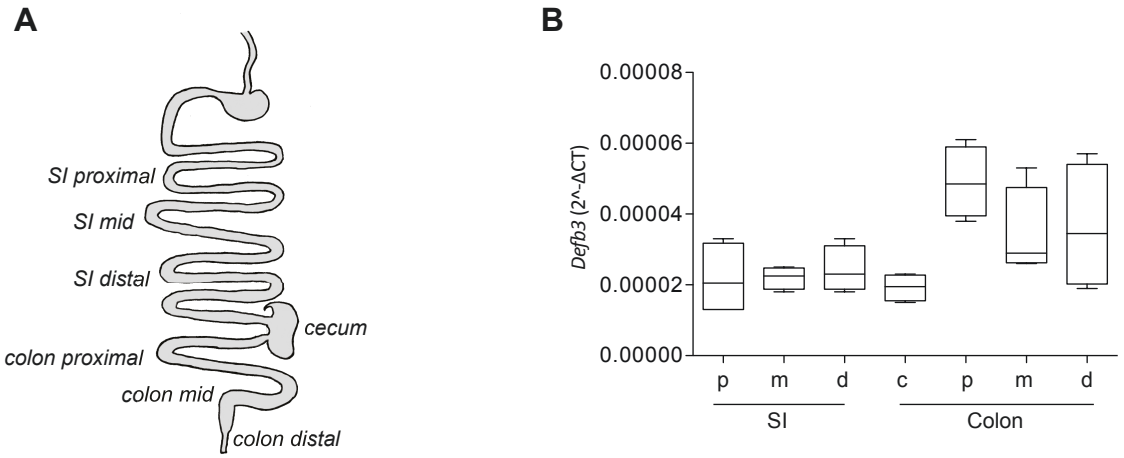

Supplemental Figure 3.4. Biogeography of *K. pneumoniae* and host AMP expression throughout the gastrointestinal tract. (A) Experimental schema for biogeography assessments. At 7 samples sites along the gastrointestinal tract of ASF mice, luminal contents and mucosal tissue were harvested for *K. pneumoniae* CFU counts and host tissue expression studies. (B) β-defensin3 expression throughout the gastrointestinal tract of n=6 mice.

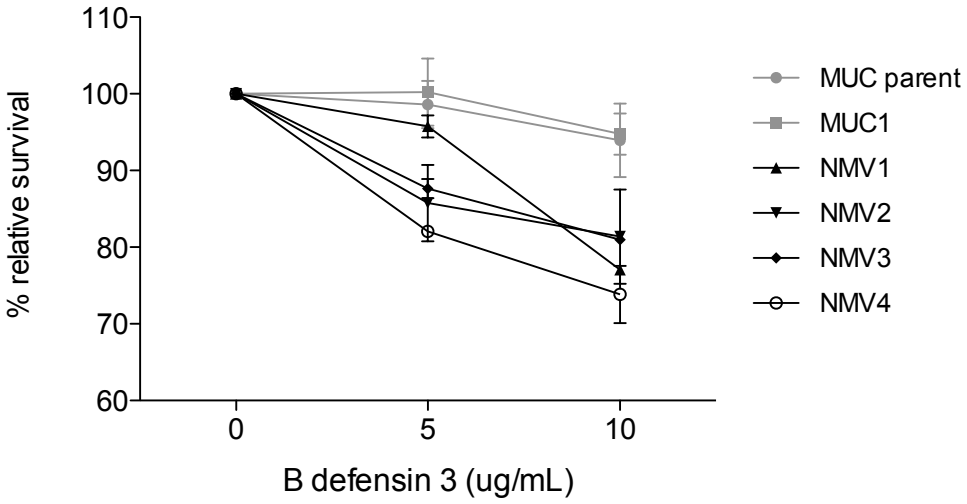

Supplemental Figure 3.5. **β-defensin killing of *K. pneumoniae* variants**. Relative survival of MUC (gray) and NMV (black) *K. pneumoniae* variants in response to 2-hr killing assays with β-defensin 3 at increasing concentrations.

Supplemental Table 3.1. Average log_{10}CFU/g stool and SD of *K. pneumoniae* in stool from gnotobiotic and specified pathogen free associations.

Microbiota	collection time point (weeks)	corrected log_{10}CFU/g stool
K. pneumoniae WGLW5	8	8.9 ± 0.1
ASF + *K. pneumoniae* WGLW5	8	7.6 ± 0.5
ASF + *K. pneumoniae* WGLW5 + SPF stool	8	6.3 ± 0.6
SPF + *K. pneumoniae* WGLW5 sprinkling	4	4.4 ± 0.5
SPF + *K. pneumoniae* MUC1 sprinkling	4	4.7 ± 0.7
ASF + *K. pneumoniae* WGLW2	8	7.6 ± 0.9
ASF + *K. pneumoniae* WGLW3	8	8.5 ± 0.05

Supplemental Table 3.2. Samtools SNP output of *K. pneumoniae* variant whole-genome sequences aligned to reference genome WGLW5.

***K. pneumoniae* variant**	**# SNPs (aligned to WGLW5 reference)**	**# SNPs within CPS cluster**	**# genes with SNPs shared among NMVs**	**# KEGG pathways with SNPs shared among NMVs**
MUC parent	130	0	NA	NA
MUC 1	176	0	NA	NA
NMV 1	137	0	0	0
NMV 2	137	0	0	0
NMV 3	132	1[a]	0	0
NMV 4	162	0	0	0

[a] Synonymous substitution in *wcaJ*

Supplemental Table 3.3. Gene coverage similarity between *K. pneumoniae* variants. Each column represents one variant. Each row shows the number of genes in the column variant that are not found in the genome of the row variant.

	PARENT (5316 genes)	**MUC1 (5366 genes)**	**NMV1 (5308 genes)**	**NMV2 (5388 genes)**	**NMV3 (5310 genes)**	**NMV4 (5267 genes)**
notPARENT	0	14	14	25	14	13
notMUC1	0	0	4	11	4	2
notNMV1	20	28	0	31	22	22
notNMV2	2	2	2	0	2	0
notNMV3	12	14	14	21	0	15
notNMV4	54	58	57	65	60	0

REFERENCES

1. **Venema K**. 2010. Role of gut microbiota in the control of energy and carbohydrate metabolism. Curr Opin Clin Nutr Metab Care **13**:432–438.

2. **Maranduba CMDC**, **De Castro SBR**, **de Souza GT**, **Rossato C**, **da Guia FC**, **Valente MAS**, **Rettore JVP**, **Maranduba CP**, **de Souza CM**, **do Carmo AMR**, **Macedo GC**, **Silva F de S**. 2015. Intestinal microbiota as modulators of the immune system and neuroimmune system: impact on the host health and homeostasis. J Immunol Res **2015**:931574–14.

3. **Frank DN**, **Pace NR**. 2008. Gastrointestinal microbiology enters the metagenomics era. Curr Opin Gastroenterol **24**:4–10.

4. **Turnbaugh PJ**, **Hamady M**, **Yatsunenko T**, **Cantarel BL**, **Duncan A**, **Ley RE**, **Sogin ML**, **Jones WJ**, **Roe BA**, **Affourtit JP**, **Egholm M**, **Henrissat B**, **Heath AC**, **Knight R**, **Gordon JI**. 2009. A core gut microbiome in obese and lean twins. Nature **457**:480–484.

5. **Qin J**, **Li R**, **Raes J**, **Arumugam M**, **Burgdorf KS**, **Manichanh C**, **Nielsen T**, **Pons N**, **Levenez F**, **Yamada T**, **Mende DR**, **Li J**, **Xu J**, **Li S**, **Li D**, **Cao J**, **Wang B**, **Liang H**, **Zheng H**, **Xie Y**, **Tap J**, **Lepage P**, **Bertalan M**, **Batto J-M**, **Hansen T**, **Le Paslier D**, **Linneberg A**, **Nielsen HB**, **Pelletier E**, **Renault P**, **Sicheritz-Ponten T**, **Turner K**, **Zhu H**, **Yu C**, **Li S**, **Jian M**, **Zhou Y**, **Li Y**, **Zhang X**, **Li S**, **Qin N**, **Yang H**, **Wang J**, **Brunak S**, **Doré J**, **Guarner F**, **Kristiansen K**, **Pedersen O**, **Parkhill J**, **Weissenbach J**, **MetaHIT Consortium**, **Bork P**, **Ehrlich SD**, **Wang J**. 2010. A human gut microbial gene catalogue established by metagenomic sequencing. Nature **464**:59–65.

6. **Wen L**, **Ley RE**, **Volchkov PY**, **Stranges PB**, **Avanesyan L**, **Stonebraker AC**, **Hu C**, **Wong FS**, **Szot GL**, **Bluestone JA**, **Gordon JI**, **Chervonsky AV**. 2008. Innate immunity and intestinal microbiota in the development of Type 1 diabetes. Nature **455**:1109–1113.

7. **Vijay-Kumar M**, **Aitken JD**, **Carvalho FA**, **Cullender TC**, **Mwangi S**, **Srinivasan S**, **Sitaraman SV**, **Knight R**, **Ley RE**, **Gewirtz AT**. 2010. Metabolic syndrome and altered gut microbiota in mice lacking Toll-like receptor 5. Science **328**:228–231.

8. **Barker N**. 2014. Adult intestinal stem cells: critical drivers of epithelial homeostasis and regeneration. Nat Rev Mol Cell Biol **15**:19–33.

9. **Turner JR**. 2009. Intestinal mucosal barrier function in health and disease. Nat Rev Immunol **9**:799–809.

10. **Karlsson J**, **Pütsep K**, **Chu H**, **Kays RJ**, **Bevins CL**, **Andersson M**. 2008. Regional variations in Paneth cell antimicrobial peptide expression along the mouse intestinal tract. BMC Immunol **9**:37.

11. **Salzman NH**. 2010. Paneth cell defensins and the regulation of the microbiome: détente at mucosal surfaces. Gut Microbes **1**:401–406.

12. **Salzman NH**, **Underwood MA**, **Bevins CL**. 2007. Paneth cells, defensins, and the commensal microbiota: a hypothesis on intimate interplay at the intestinal mucosa. Seminars in Immunology **19**:70–83.

13. **Clevers HC**, **Bevins CL**. 2013. Paneth Cells: Maestros of the Small Intestinal Crypts. Annu Rev Physiol **75**:289–311.

14. **Cadwell K**, **Liu JY**, **Brown SL**, **Miyoshi H**, **Loh J**, **Lennerz JK**, **Kishi C**, **Kc W**, **Carrero JA**, **Hunt S**, **Stone CD**, **Brunt EM**, **Xavier RJ**, **Sleckman BP**, **Li E**, **Mizushima N**, **Stappenbeck TS**, **Virgin HW IV**. 2008. A key role for autophagy and the autophagy gene Atg16l1 in mouse and human intestinal Paneth cells. Nature **456**:259–263.

15. **Wu WM**, **Yang YS**, **Peng LH**. 2014. Microbiota in the stomach: new insights. J Dig Dis **15**:54–61.

16. **Stearns JC**, **Lynch MDJ**, **Senadheera DB**, **Tenenbaum HC**, **Goldberg MB**, **Cvitkovitch DG**, **Croitoru K**, **Moreno-Hagelsieb G**, **Neufeld JD**. 2011. Bacterial biogeography of the human digestive tract. Sci Rep **1**:170.

17. **Salzman NH**. 2011. Microbiota-immune system interaction: an uneasy alliance. Curr Opin Microbiol **14**:99–105.

18. **Maltby R**, **Leatham-Jensen MP**, **Gibson T**, **Cohen PS**, **Conway T**. 2013. Nutritional basis for colonization resistance by human commensal Escherichia coli strains HS and Nissle 1917 against E. coli O157:H7 in the mouse intestine. PLoS ONE **8**:e53957.

19. **Lawley TD**, **Walker AW**. 2013. Intestinal colonization resistance. Immunology **138**:1–11.

20. **Hertzberger R**, **Arents J**, **Dekker HL**, **Pridmore RD**, **Gysler C**, **Kleerebezem M**, **de Mattos MJT**. 2014. H(2)O(2) production in species of the Lactobacillus acidophilus group: a central role for a novel NADH-dependent flavin reductase. Applied and Environmental Microbiology **80**:2229–2239.

21. **Cotter PD**, **Ross RP**, **Hill C**. 2013. Bacteriocins, a viable alternative to antibiotics? Nat Rev Micro **11**:95–105.

22. **Stecher B**, **Chaffron S**, **Käppeli R**, **Hapfelmeier S**, **Freedrich S**, **Weber TC**, **Kirundi J**, **Suar M**, **McCoy KD**, **Mering von C**, **Macpherson AJ**, **Hardt W-D**. 2010. Like will to like: abundances of closely related species can predict susceptibility to intestinal colonization by pathogenic and commensal bacteria. PLoS Pathog **6**:e1000711.

23. **Cash HL**, **Whitham CV**, **Behrendt CL**, **Hooper LV**. 2006. Symbiotic bacteria direct expression of an intestinal bactericidal lectin. Science **313**:1126–1130.

24. **Endt K**, **Stecher B**, **Chaffron S**, **Slack E**, **Tchitchek N**, **Benecke A**, **Van Maele L**, **Sirard J-C**, **Mueller AJ**, **Heikenwalder M**, **Macpherson AJ**, **Strugnell R**, **Mering von C**, **Hardt W-D**. 2010. The microbiota mediates pathogen clearance from the gut lumen after non-typhoidal Salmonella diarrhea. PLoS Pathog **6**:e1001097.

25. **Macpherson AJ**, **Harris NL**. 2004. Interactions between commensal intestinal bacteria and the immune system. Nat Rev Immunol **4**:478–485.

26. **Round JL**, **Mazmanian SK**. 2009. The gut microbiota shapes intestinal immune responses during health and disease. Nat Rev Immunol **9**:313–323.

27. **Mazmanian SK**, **Round JL**, **Kasper DL**. 2008. A microbial symbiosis factor prevents intestinal inflammatory disease. Nature **453**:620–625.

28. **Ochoa-Repáraz J**, **Mielcarz DW**, **Wang Y**, **Begum-Haque S**, **Dasgupta S**, **Kasper DL**, **Kasper LH**. 2010. A polysaccharide from the human commensal Bacteroides fragilis protects against CNS demyelinating disease. Mucosal Immunol **3**:487–495.

29. **Korn T**, **Bettelli E**, **Oukka M**, **Kuchroo VK**. 2009. IL-17 and Th17 Cells. Annu Rev Immunol **27**:485–517.

30. **Ivanov II**, **Atarashi K**, **Manel N**, **Brodie EL**, **Shima T**, **Karaoz U**, **Wei D**, **Goldfarb KC**, **Santee CA**, **Lynch SV**, **Tanoue T**, **Imaoka A**, **Itoh K**, **Takeda K**, **Umesaki Y**, **Honda K**, **Littman DR**. 2009. Induction of intestinal Th17 cells by segmented filamentous bacteria. Cell **139**:485–498.

31. **Kinnebrew MA**, **Ubeda C**, **Zenewicz LA**, **Smith N**, **Flavell RA**, **Pamer EG**. 2010. Bacterial flagellin stimulates Toll-like receptor 5-dependent defense against vancomycin-resistant Enterococcus infection. J Infect Dis **201**:534–543.

32. **Clarke TB**, **Davis KM**, **Lysenko ES**, **Zhou AY**, **Yu Y**, **Weiser JN**. 2010. Recognition of peptidoglycan from the microbiota by Nod1 enhances systemic innate immunity. Nat Med **16**:228–231.

33. **Dethlefsen L**, **Huse S**, **Sogin ML**, **Relman DA**. 2008. The pervasive effects of an antibiotic on the human gut microbiota, as revealed by deep 16S rRNA sequencing. PLoS Biol **6**:e280.

34. **Sekirov I**, **Tam NM**, **Jogova M**, **Robertson ML**, **Li Y**, **Lupp C**, **Finlay BB**. 2008. Antibiotic-induced perturbations of the intestinal microbiota alter host susceptibility to enteric infection. Infection and Immunity **76**:4726–4736.

35. **Hill DA**, **Hoffmann C**, **Abt MC**, **Du Y**, **Kobuley D**, **Kirn TJ**, **Bushman FD**, **Artis D**. 2010. Metagenomic analyses reveal antibiotic-induced temporal and spatial changes in intestinal microbiota with associated alterations in immune cell homeostasis. Mucosal Immunol **3**:148–158.

36. **Giongo A**, **Gano KA**, **Crabb DB**, **Mukherjee N**, **Novelo LL**, **Casella G**, **Drew JC**, **Ilonen J**, **Knip M**, **Hyöty H**, **Veijola R**, **Simell T**, **Simell O**, **Neu J**, **Wasserfall CH**, **Schatz D**, **Atkinson MA**, **Triplett EW**. 2011. Toward defining the autoimmune microbiome for type 1 diabetes. The ISME Journal **5**:82–91.

37. **Onderdonk AB**, **Garrett WS**. 2010. Gas Gangrene and Other Clostridium-Associated Diseases, pp. 3103–3109. *In* Mandell, Douglas, and Bennetts Principles and Practice of Infectious Disease, 7 ed. Philadelphia.

38. **Walk ST**, **Young VB**. 2008. Emerging Insights into Antibiotic-Associated Diarrhea and Clostridium difficile Infection through the Lens of Microbial Ecology. Interdiscip Perspect Infect Dis **2008**:125081–7.

39. **Giel JL**, **Sorg JA**, **Sonenshein AL**, **Zhu J**. 2010. Metabolism of bile salts in mice influences spore germination in Clostridium difficile. PLoS ONE **5**:e8740.

40. **Sekirov I**, **Finlay BB**. 2009. The role of the intestinal microbiota in enteric infection. J Physiol (Lond) **587**:4159–4167.

41. **Marshall BM**, **Ochieng DJ**, **Levy SB**. 2010. Commensals: underappreciated reservoir of antibiotic resistance. Microbe Magazine.

42. **Allen HK**, **Donato J**, **Wang HH**, **Cloud-Hansen KA**, **Davies J**, **Handelsman J**. 2010. Call of the wild: antibiotic resistance genes in natural environments. Nat Rev Micro **8**:251–259.

43. **Sjölund M**, **Wreiber K**, **Andersson DI**, **Blaser MJ**, **Engstrand L**. 2003. Long-term persistence of resistant Enterococcus species after antibiotics to eradicate Helicobacter pylori. Ann Intern Med **139**:483–487.

44. **Sommer MOA**, **Dantas G**, **Church GM**. 2009. Functional characterization of the antibiotic resistance reservoir in the human microflora. Science **325**:1128–1131.

45. **Bobak DA**, **Guerrant RL**. 2010. Nausea, Vomiting, and Noninflammatory Diarrhea, pp. 1359–1373. *In* Mandell GL, Bennett JE, Dolin R, editors. Mandell, Douglas, and Bennetts Principles and Practice of Infectious Disease, 7 ed. Philadelphia.

46. **Fankhauser RL**, **Monroe SS**, **Noel JS**, **Humphrey CD**, **Bresee JS**, **Parashar UD**, **Ando T**, **Glass RI**. 2002. Epidemiologic and molecular trends of "Norwalk-like viruses" associated with outbreaks of gastroenteritis in the United States. J Infect Dis **186**:1–7.

47. **Lyman WH**, **Walsh JF**, **Kotch JB**, **Weber DJ**, **Gunn E**, **Vinjé J**. 2009. Prospective Study of Etiologic Agents of Acute Gastroenteritis Outbreaks in Child Care Centers. The Journal of Pediatrics **154**:253–257.

48. **Moser LA**, **Carter M**, **Schultz-Cherry S**. 2007. Astrovirus increases epithelial barrier permeability independently of viral replication. J Virol **81**:11937–11945.

49. **Fang S-B**, **Lee H-C**, **Hu J-J**, **Hou S-Y**, **Liu H-L**, **Fang H-W**. 2009. Dose-dependent effect of Lactobacillus rhamnosus on quantitative reduction of faecal rotavirus shedding in children. J Trop Pediatr **55**:297–301.

50. **Vandenplas Y**, **Salvatore S**, **Viera M**, **Devreker T**, **Hauser B**. 2007. Probiotics in infectious diarrhoea in children: are they indicated? Eur J Pediatr **166**:1211–1218.

51. **Frank DN**, **St Amand AL**, **Feldman RA**, **Boedeker EC**, **Harpaz N**, **Pace NR**. 2007. Molecular-phylogenetic characterization of microbial community imbalances in human inflammatory bowel diseases. Proc Natl Acad Sci USA **104**:13780–13785.

52. **Barrett JC**, **Hansoul S**, **Nicolae DL**, **Cho JH**, **Duerr RH**, **Rioux JD**, **Brant SR**, **Silverberg MS**, **Taylor KD**, **Barmada MM**, **Bitton A**, **Dassopoulos T**, **Datta LW**, **Green T**, **Griffiths AM**, **Kistner EO**, **Murtha MT**, **Regueiro MD**, **Rotter JI**, **Schumm LP**, **Steinhart AH**, **Targan SR**, **Xavier RJ**, **Libioulle C**, **Sandor C**, **Lathrop M**, **Belaiche J**, **Dewit O**, **Gut I**, **Heath S**, **Laukens D**, **Mni M**, **Rutgeerts P**, **Van Gossum A**, **Zelenika D**,

Franchimont D, **Hugot J-P**, **De Vos M**, **Vermeire S**, **Louis E**, **Cardon LR**, **Anderson CA**, **Drummond H**, **Nimmo E**, **Ahmad T**, **Prescott NJ**, **Onnie CM**, **Fisher SA**, **Marchini J**, **Ghori J**, **Bumpstead S**, **Gwilliam R**, **Tremelling M**, **Deloukas P**, **Mansfield J**, **Jewell D**, **Satsangi J**, **Mathew CG**, **Parkes M**, **Georges M**, **Daly MJ**. 2008. Genome-wide association defines more than 30 distinct susceptibility loci for Crohn's disease. Nat Genet **40**:955–962.

53. **Cadwell K**, **Patel KK**, **Maloney NS**, **Liu T-C**, **Ng ACY**, **Storer CE**, **Head RD**, **Xavier R**, **Stappenbeck TS**, **Virgin HW**. 2010. Virus-Plus-Susceptibility Gene Interaction Determines Crohn's Disease Gene Atg16L1 Phenotypes in Intestine. Cell **141**:1135–1145.

54. **Letarov A**, **Kulikov E**. 2009. The bacteriophages in human- and animal body-associated microbial communities. Journal of Applied Microbiology **107**:1–13.

55. **Reyes A**, **Haynes M**, **Hanson N**, **Angly FE**, **Heath AC**, **Rohwer F**, **Gordon JI**. 2010. Viruses in the faecal microbiota of monozygotic twins and their mothers. Nature **466**:334–338.

56. **Saleh M**, **Elson CO**. 2011. Experimental Inflammatory Bowel Disease: Insights into the Host-Microbiota Dialog. Immunity **34**:293–302.

57. 2011. Key questions to guide a better understanding of host–commensal microbiota interactions in intestinal inflammation **4**:127–132.

58. **Danese S**, **Fiocchi C**. 2011. Ulcerative colitis. N Engl J Med **365**:1713–1725.

59. **Podolsky DK**. 2002. Inflammatory bowel disease. N Engl J Med **347**:417–429.

60. **Talley NJ**, **Abreu MT**, **Achkar J-P**, **Bernstein CN**, **Dubinsky MC**, **Hanauer SB**, **Kane SV**, **Sandborn WJ**, **Ullman TA**, **Moayyedi P**, **American College of Gastroenterology IBD Task Force**. 2011. An evidence-based systematic review on medical therapies for inflammatory bowel disease. Am J Gastroenterol **106 Suppl 1**:S2–25.

61. **Hanauer SB**. 2006. Inflammatory bowel disease: epidemiology, pathogenesis, and therapeutic opportunities. Inflammatory Bowel Diseases **12 Suppl 1**:S3–9.

62. **Anderson CA**, **Boucher G**, **Lees CW**, **Franke A**, **D'Amato M**, **Taylor KD**, **Lee JC**, **Goyette P**, **Imielinski M**, **Latiano A**, **Lagacé C**, **Scott R**, **Amininejad L**, **Bumpstead S**, **Baidoo L**, **Baldassano RN**, **Barclay M**, **Bayless TM**, **Brand S**, **Büning C**, **Colombel J-F**, **Denson LA**, **De Vos M**, **Dubinsky M**, **Edwards C**, **Ellinghaus D**, **Fehrmann RSN**, **Floyd JAB**, **Florin T**, **Franchimont D**, **Franke L**, **Georges M**, **Glas J**, **Glazer NL**, **Guthery SL**, **Haritunians T**, **Hayward NK**, **Hugot J-P**, **Jobin G**, **Laukens D**, **Lawrance I**, **Lémann M**, **Levine A**, **Libioulle C**, **Louis E**, **McGovern DP**, **Milla M**, **Montgomery GW**, **Morley KI**, **Mowat C**, **Ng A**, **Newman W**, **Ophoff RA**, **Papi L**, **Palmieri O**, **Peyrin-Biroulet L**, **Panés J**, **Phillips A**, **Prescott NJ**, **Proctor DD**, **Roberts R**, **Russell R**, **Rutgeerts P**, **Sanderson J**, **Sans M**, **Schumm P**, **Seibold F**, **Sharma Y**, **Simms LA**, **Seielstad M**, **Steinhart AH**, **Targan SR**, **van den Berg LH**, **Vatn M**, **Verspaget H**, **Walters T**, **Wijmenga C**, **Wilson DC**, **Westra H-J**, **Xavier RJ**, **Zhao ZZ**, **Ponsioen CY**, **Andersen V**, **Torkvist L**, **Gazouli M**, **Anagnou NP**, **Karlsen TH**, **Kupcinskas L**, **Sventoraityte J**, **Mansfield JC**, **Kugathasan S**, **Silverberg MS**, **Halfvarson J**, **Rotter JI**, **Mathew CG**, **Griffiths AM**, **Gearry R**, **Ahmad T**, **Brant SR**, **Chamaillard M**, **Satsangi**

J, **Cho JH**, **Schreiber S**, **Daly MJ**, **Barrett JC**, **Parkes M**, **Annese V**, **Hakonarson H**, **Radford-Smith G**, **Duerr RH**, **Vermeire S**, **Weersma RK**, **Rioux JD**. 2011. Meta-analysis identifies 29 additional ulcerative colitis risk loci, increasing the number of confirmed associations to 47. Nat Genet **43**:246–252.

63. **Dieleman LA**, **Ridwan BU**, **Tennyson GS**, **Beagley KW**, **Bucy RP**, **Elson CO**. 1994. Dextran sulfate sodium-induced colitis occurs in severe combined immunodeficient mice. Gastroenterology **107**:1643–1652.

64. **Kühn R**, **Löhler J**, **Rennick D**, **Rajewsky K**, **Müller W**. 1993. Interleukin-10-deficient mice develop chronic enterocolitis. Cell **75**:263–274.

65. **Uhlig HH**, **Coombes J**, **Mottet C**, **Izcue A**, **Thompson C**, **Fanger A**, **Tannapfel A**, **Fontenot JD**, **Ramsdell F**, **Powrie F**. 2006. Characterization of Foxp3+CD4+CD25+ and IL-10-secreting CD4+CD25+ T cells during cure of colitis. The Journal of Immunology **177**:5852–5860.

66. **Garrett WS**, **Lord GM**, **Punit S**, **Lugo-Villarino G**, **Mazmanian SK**, **Ito S**, **Glickman JN**, **Glimcher LH**. 2007. Communicable ulcerative colitis induced by T-bet deficiency in the innate immune system. Cell **131**:33–45.

67. **Curry JD**, **Schlissel MS**. 2008. RAG2's non-core domain contributes to the ordered regulation of VDJ recombination. Nucleic Acids Res **36**:5750–5762.

68. **Glimcher LH**. 2007. Trawling for treasure: tales of T-bet. Nat Immunol **8**:448–450.

69. **Thompson GR**, **Trexler PC**. 1971. Gastrointestinal structure and function in germ-free or gnotobiotic animals. Gut **12**:230–235.

70. **Rabot S**, **Membrez M**, **Bruneau A**, **Gérard P**, **Harach T**, **Moser M**, **Raymond F**, **Mansourian R**, **Chou CJ**. 2010. Germ-free C57BL/6J mice are resistant to high-fat-diet-induced insulin resistance and have altered cholesterol metabolism. FASEB J **24**:4948–4959.

71. **Schaedler RW**, **Dubos R**, **Costello R**. 1965. Association of germfree mice with bacteria isolated from normal mice. J Exp Med **122**:77–82.

72. **Dewhirst FE**, **Chien CC**, **Paster BJ**, **Ericson RL**, **Orcutt RP**, **Schauer DB**, **Fox JG**. 1999. Phylogeny of the defined murine microbiota: altered Schaedler flora. Applied and Environmental Microbiology **65**:3287–3292.

73. **Geuking MB**, **Cahenzli J**, **Lawson MAE**, **Ng DCK**, **Slack E**, **Hapfelmeier S**, **McCoy KD**, **Macpherson AJ**. 2011. Intestinal bacterial colonization induces mutualistic regulatory T cell responses. Immunity **34**:794–806.

74. **Goodman AL**, **McNulty NP**, **Zhao Y**, **Leip D**, **Mitra RD**, **Lozupone CA**, **Knight R**, **Gordon JI**. 2009. Identifying Genetic Determinants Needed to Establish a Human Gut Symbiont in Its Habitat. Cell Host Microbe **6**:279–289.

75. **Atarashi K**, **Tanoue T**, **Oshima K**, **Suda W**, **Nagano Y**, **Nishikawa H**, **Fukuda S**, **Saito T**, **Narushima S**, **Hase K**, **Kim S**, **Fritz JV**, **Wilmes P**, **Ueha S**, **Matsushima K**, **Ohno H**,

Olle B, **Sakaguchi S**, **Taniguchi T**, **Morita H**, **Hattori M**, **Honda K**. 2013. Treg induction by a rationally selected mixture of Clostridia strains from the human microbiota. Nature **500**:232–236.

76. **Goodman AL**, **Kallstrom G**, **Faith JJ**, **Reyes A**, **Moore A**, **Dantas G**, **Gordon JI**. 2011. Extensive personal human gut microbiota culture collections characterized and manipulated in gnotobiotic mice. Proc Natl Acad Sci USA **108**:6252–6257.

77. **Schmidt TM**, **DeLong EF**, **Pace NR**. 1991. Analysis of a marine picoplankton community by 16S rRNA gene cloning and sequencing. Journal of Bacteriology **173**:4371–4378.

78. **Woese CR**, **Fox GE**. 1977. Phylogenetic structure of the prokaryotic domain: the primary kingdoms. Proc Natl Acad Sci USA **74**:5088–5090.

79. **Chakravorty S**, **Helb D**, **Burday M**, **Connell N**, **Alland D**. 2007. A detailed analysis of 16S ribosomal RNA gene segments for the diagnosis of pathogenic bacteria. J Microbiol Methods **69**:330–339.

80. **Nelson MC**, **Morrison HG**, **Benjamino J**, **Grim SL**, **Graf J**. 2014. Analysis, optimization and verification of Illumina-generated 16S rRNA gene amplicon surveys. PLoS ONE **9**:e94249.

81. **Caporaso JG**, **Kuczynski J**, **Stombaugh J**, **Bittinger K**, **Bushman FD**, **Costello EK**, **Fierer N**, **Peña AG**, **Goodrich JK**, **Gordon JI**, **Huttley GA**, **Kelley ST**, **Knights D**, **Koenig JE**, **Ley RE**, **Lozupone CA**, **McDonald D**, **Muegge BD**, **Pirrung M**, **Reeder J**, **Sevinsky JR**, **Turnbaugh PJ**, **Walters WA**, **Widmann J**, **Yatsunenko T**, **Zaneveld J**, **Knight R**. 2010. QIIME allows analysis of high-throughput community sequencing data. Nat Methods **7**:335–336.

82. **Langille MGI**, **Zaneveld J**, **Caporaso JG**, **McDonald D**, **Knights D**, **Reyes JA**, **Clemente JC**, **Burkepile DE**, **Vega Thurber RL**, **Knight R**, **Beiko RG**, **Huttenhower C**. 2013. Predictive functional profiling of microbial communities using 16S rRNA marker gene sequences. Nat Biotechnol **31**:814–821.

83. **Segata N**, **Izard J**, **Waldron L**, **Gevers D**, **Miropolsky L**, **Garrett WS**, **Huttenhower C**. 2011. Metagenomic biomarker discovery and explanation. Genome Biol **12**:R60.

84. **Friedländer C**. 1882. Ueber die Schizomyceten bei der acuten fibrösen Pneumonie. Virchows Arch pathol Anat u Physiol **87**:319–324.

85. **Podschun R**, **Ullmann U**. 1998. Klebsiella spp. as nosocomial pathogens: epidemiology, taxonomy, typing methods, and pathogenicity factors. Clin Microbiol Rev **11**:589–603.

86. **Iniguez AL**, **Dong Y**, **Triplett EW**. 2004. Nitrogen fixation in wheat provided by Klebsiella pneumoniae 342. Mol Plant Microbe Interact **17**:1078–1085.

87. **Li B**, **Zhao Y**, **Liu C**, **Chen Z**, **Zhou D**. 2014. Molecular pathogenesis of Klebsiella pneumoniae. Future Microbiol **9**:1071–1081.

88. **Qiao S**, **Luo Q**, **Zhao Y**, **Zhang XC**, **Huang Y**. 2014. Structural basis for lipopolysaccharide insertion in the bacterial outer membrane. Nature **511**:108–111.

89. **Kozak W**, **Conn CA**, **Kluger MJ**. 1994. Lipopolysaccharide induces fever and depresses locomotor activity in unrestrained mice. Am J Physiol **266**:R125–35.

90. **Coutinho RL**, **Visconde MF**, **Descio FJ**, **Nicoletti AG**, **Pinto FCL**, **Silva ACRD**, **Rodrigues-Costa F**, **Gales AC**, **Furtado GHC**. 2014. Community-acquired invasive liver abscess syndrome caused by a K1 serotype Klebsiella pneumoniae isolate in Brazil: a case report of hypervirulent ST23. Mem Inst Oswaldo Cruz **109**:970–971.

91. **Lin J-C**, **Koh TH**, **Lee N**, **Fung C-P**, **Chang F-Y**, **Tsai Y-K**, **Ip M**, **Siu LK**. 2014. Genotypes and virulence in serotype K2 Klebsiella pneumoniae from liver abscess and non-infectious carriers in Hong Kong, Singapore and Taiwan. Gut Pathog **6**:21.

92. **Yang F-L**, **Yang Y-L**, **Liao P-C**, **Chou J-C**, **Tsai K-C**, **Yang A-S**, **Sheu F**, **Lin T-L**, **Hsieh P-F**, **Wang J-T**, **Hua K-F**, **Wu S-H**. 2011. Structure and immunological characterization of the capsular polysaccharide of a pyrogenic liver abscess caused by Klebsiella pneumoniae: activation of macrophages through Toll-like receptor 4. J Biol Chem **286**:21041–21051.

93. **Shu H-Y**, **Fung C-P**, **Liu Y-M**, **Wu K-M**, **Chen Y-T**, **Li L-H**, **Liu T-T**, **Kirby R**, **Tsai S-F**. 2009. Genetic diversity of capsular polysaccharide biosynthesis in Klebsiella pneumoniae clinical isolates. Microbiology (Reading, Engl) **155**:4170–4183.

94. **Cortés G**, **Alvarez D**, **Saus C**, **Albertí S**. 2002. Role of lung epithelial cells in defense against Klebsiella pneumoniae pneumonia. Infection and Immunity **70**:1075–1080.

95. **Matatov R**, **Goldhar J**, **Skutelsky E**, **Sechter I**, **Perry R**, **Podschun R**, **Sahly H**, **Thankavel K**, **Abraham SN**, **Ofek I**. 1999. Inability of encapsulated Klebsiella pneumoniae to assemble functional type 1 fimbriae on their surface. FEMS Microbiol Lett **179**:123–130.

96. **DeLeo FR**, **Chen L**, **Porcella SF**, **Martens CA**, **Kobayashi SD**, **Porter AR**, **Chavda KD**, **Jacobs MR**, **Mathema B**, **Olsen RJ**, **Bonomo RA**, **Musser JM**, **Kreiswirth BN**. 2014. Molecular dissection of the evolution of carbapenem-resistant multilocus sequence type 258 Klebsiella pneumoniae. Proc Natl Acad Sci USA **111**:4988–4993.

97. **Whitfield C**. 2006. Biosynthesis and Assembly of Capsular Polysaccharides in Escherichia coli. Annual Reviews Microbiology **75**:39–68.

98. **Ho J-Y**, **Lin T-L**, **Li C-Y**, **Lee A**, **Cheng A-N**, **Chen M-C**, **Wu S-H**, **Wang J-T**, **Li T-L**, **Tsai M-D**. 2011. Functions of Some Capsular Polysaccharide Biosynthetic Genes in Klebsiella pneumoniae NTUH K-2044. PLoS ONE **6**:e21664.

99. **Fevre C**, **Passet V**, **Deletoile A**, **Barbe V**, **Frangeul L**, **Almeida AS**, **Sansonetti P**, **Tournebize R**, **Brisse S**. 2011. PCR-Based Identification of Klebsiella pneumoniae subsp. rhinoscleromatis , the Agent of Rhinoscleroma. PLOS Negl Trop Dis **5**:e1052.

100. **Wu C-C**, **Wang C-K**, **Chen Y-C**, **Lin T-H**, **Jinn T-R**, **Lin C-T**. 2014. IscR Regulation of Capsular Polysaccharide Biosynthesis and Iron-Acquisition Systems in Klebsiella pneumoniae CG43. PLoS ONE **9**:e107812.

101. **Cheng HY**, **Chen YS**, **Wu CY**, **Chang HY**, **Lai YC**, **Peng HL**. 2010. RmpA regulation of

capsular polysaccharide biosynthesis in Klebsiella pneumoniae CG43. Journal of Bacteriology **192**:3144–3158.

102. **Chen F-J**, **Chan C-H**, **Huang Y-J**, **Liu K-L**, **Peng H-L**, **Chang H-Y**, **Liou G-G**, **Yew T-R**, **Liu C-H**, **Hsu KY**, **Hsu L**. 2011. Structural and mechanical properties of Klebsiella pneumoniae type 3 Fimbriae. Journal of Bacteriology **193**:1718–1725.

103. **Livrelli V**, **De Champs C**, **Di Martino P**, **Darfeuille-Michaud A**, **Forestier C**, **Joly B**. 1996. Adhesive properties and antibiotic resistance of Klebsiella, Enterobacter, and Serratia clinical isolates involved in nosocomial infections. Journal of Clinical Microbiology **34**:1963–1969.

104. **Klemm P**, **Schembri MA**. 2000. Bacterial adhesins: function and structure. International Journal of Medical Microbiology **290**:27–35.

105. **Murphy CN**, **Mortensen MS**, **Krogfelt KA**, **Clegg S**. 2013. Role of Klebsiella pneumoniae type 1 and type 3 fimbriae in colonizing silicone tubes implanted into the bladders of mice as a model of catheter-associated urinary tract infections. Infection and Immunity **81**:3009–3017.

106. **Schembri MA**, **Blom J**, **Krogfelt KA**, **Klemm P**. 2005. Capsule and fimbria interaction in Klebsiella pneumoniae. Infection and Immunity **73**:4626–4633.

107. **Struve C**, **Bojer M**, **Krogfelt KA**. 2008. Characterization of Klebsiella pneumoniae type 1 fimbriae by detection of phase variation during colonization and infection and impact on virulence. Infection and Immunity **76**:4055–4065.

108. **Miethke M**, **Marahiel MA**. 2007. Siderophore-based iron acquisition and pathogen control. Microbiol Mol Biol Rev **71**:413–451.

109. **Podschun R**, **Fischer A**, **Ullmann U**. 1992. Siderophore production of Klebsiella species isolated from different sources. Zentralbl Bakteriol **276**:481–486.

110. **Russo TA**, **Olson R**, **MacDonald U**, **Beanan J**, **Davidson BA**. 2015. Aerobactin, but not yersiniabactin, salmochelin, or enterobactin, enables the growth/survival of hypervirulent (hypermucoviscous) Klebsiella pneumoniae ex vivo and in vivo. Infection and Immunity **83**:3325–3333.

111. **Holt KE**, **Wertheim H**, **Zadoks RN**, **Baker S**, **Whitehouse CA**, **Dance D**, **Jenney A**, **Connor TR**, **Hsu LY**, **Severin J**, **Brisse S**, **Cao H**, **Wilksch J**, **Gorrie C**, **Schultz MB**, **Edwards DJ**, **Nguyen KV**, **Nguyen TV**, **Dao TT**, **Mensink M**, **Minh VL**, **Nhu NTK**, **Schultsz C**, **Kuntaman K**, **Newton PN**, **Moore CE**, **Strugnell RA**, **Thomson NR**. 2015. Genomic analysis of diversity, population structure, virulence, and antimicrobial resistance in Klebsiella pneumoniae, an urgent threat to public health. Proc Natl Acad Sci USA **112**:E3574–81.

112. **Wu K-M**, **Li L-H**, **Yan J-J**, **Tsao N**, **Liao T-L**, **Tsai H-C**, **Fung C-P**, **Chen H-J**, **Liu Y-M**, **Wang J-T**, **Fang C-T**, **Chang S-C**, **Shu H-Y**, **Liu T-T**, **Chen Y-T**, **Shiau Y-R**, **Lauderdale T-L**, **Su I-J**, **Kirby R**, **Tsai S-F**. 2009. Genome sequencing and comparative analysis of Klebsiella pneumoniae NTUH-K2044, a strain causing liver abscess and meningitis. Journal of Bacteriology **191**:4492–4501.

113. **Li L**, **Stoeckert CJ**, **Roos DS**. 2003. OrthoMCL: identification of ortholog groups for eukaryotic genomes. Genome Res **13**:2178–2189.

114. **Ying J**, **Wu S**, **Zhang K**, **Wang Z**, **Zhu W**, **Zhu M**, **Zhang Y**, **Cheng C**, **Wang H**, **Tou H**, **Zhu C**, **Li P**, **Ying J**, **Xu T**, **Yi H**, **Li J**, **Ni L**, **Xu Z**, **Bao Q**, **Lu J**. 2015. Comparative genomics analysis of pKF3-94 in Klebsiella pneumoniae reveals plasmid compatibility and horizontal gene transfer. Front Microbiol **6**:831.

115. **McKenna M**. 2013. THE LAST RESORT: *Health officials are watching in horror as bacteria become resistant to powerful carbapenem antibiotics — one of the last drugs on the shelf*

. Nature **499**:394–396.

116. **Wu H-S**, **Chen T-L**, **Chen IC-J**, **Huang M-S**, **Wang F-D**, **Fung C-P**, **Lee S-D**. 2010. First identification of a patient colonized with Klebsiella pneumoniae carrying blaNDM-1 in Taiwan. J Chin Med Assoc **73**:596–598.

117. **Xu Y**, **Gu B**, **Huang M**, **Liu H**, **Xu T**, **Xia W**, **Wang T**. 2015. Epidemiology of carbapenem resistant Enterobacteriaceae (CRE) during 2000-2012 in Asia. J Thorac Dis **7**:376–385.

118. **Guh AY**, **Bulens SN**, **Mu Y**, **Jacob JT**, **Reno J**, **Scott J**, **Wilson LE**, **Vaeth E**, **Lynfield R**, **Shaw KM**, **Vagnone PMS**, **Bamberg WM**, **Janelle SJ**, **Dumyati G**, **Concannon C**, **Beldavs Z**, **Cunningham M**, **Cassidy PM**, **Phipps EC**, **Kenslow N**, **Travis T**, **Lonsway D**, **Rasheed JK**, **Limbago BM**, **Kallen AJ**. 2015. Epidemiology of Carbapenem-Resistant Enterobacteriaceae in 7 US Communities, 2012-2013. JAMA **314**:1479–1487.

119. **Snitkin ES**, **Zelazny AM**, **Thomas PJ**, **Stock F**, **NISC Comparative Sequencing Program Group**, **Henderson DK**, **Palmore TN**, **Segre JA**. 2012. Tracking a hospital outbreak of carbapenem-resistant Klebsiella pneumoniae with whole-genome sequencing. Sci Transl Med **4**:148ra116–148ra116.

120. **Tascini C**, **Lipsky BA**, **Iacopi E**, **Ripoli A**, **Sbrana F**, **Coppelli A**, **Goretti C**, **Piaggesi A**, **Menichetti F**. 2015. KPC-producing Klebsiella pneumoniae rectal colonization is a risk factor for mortality in patients with diabetic foot infections. Clin Microbiol Infect **21**:790.e1–3.

121. **Liu Y**, **Wang J-Y**, **Jiang W**. 2013. An Increasing Prominent Disease of Klebsiella pneumoniae Liver Abscess: Etiology, Diagnosis, and Treatment. Gastroenterol Res Pract **2013**:258514.

122. **Fung C-P**, **Lin Y-T**, **Lin J-C**, **Chen T-L**, **Yeh K-M**, **Chang F-Y**, **Chuang H-C**, **Wu H-S**, **Tseng C-P**, **Siu LK**. 2012. Klebsiella pneumoniae in gastrointestinal tract and pyogenic liver abscess. Emerging Infect Dis **18**:1322–1325.

123. **Taur Y**, **Xavier JB**, **Lipuma L**, **Ubeda C**, **Goldberg J**, **Gobourne A**, **Lee YJ**, **Dubin KA**, **Socci ND**, **Viale A**, **Perales M-A**, **Jenq RR**, **van den Brink MRM**, **Pamer EG**. 2012. Intestinal domination and the risk of bacteremia in patients undergoing allogeneic hematopoietic stem cell transplantation. CLIN INFECT DIS **55**:905–914.

124. **Tiwana H**, **Natt RS**, **Benitez-Brito R**, **Shah S**, **Wilson C**, **Bridger S**, **Harbord M**, **Sarner M**, **Ebringer A**. 2001. Correlation between the immune responses to collagens type I, III, IV and V and Klebsiella pneumoniae in patients with Crohn's disease and ankylosing spondylitis. Rheumatology (Oxford) **40**:15–23.

125. **Maroncle N**, **Balestrino D**, **Rich C**, **Forestier C**. 2002. Identification of Klebsiella pneumoniae genes involved in intestinal colonization and adhesion using signature-tagged mutagenesis. Infection and Immunity **70**:4729–4734.

126. **Caballero S**, **Carter R**, **Ke X**, **Sušac B**, **Leiner IM**, **Kim GJ**, **Miller L**, **Ling L**, **Manova K**, **Pamer EG**. 2015. Distinct but Spatially Overlapping Intestinal Niches for Vancomycin-Resistant Enterococcus faecium and Carbapenem-Resistant Klebsiella pneumoniae. PLoS Pathog **11**:e1005132.

127. **Garrett WS**, **Gallini CA**, **Yatsunenko T**, **Michaud M**, **DuBois A**, **Delaney ML**, **Punit S**, **Karlsson M**, **Bry L**, **Glickman JN**, **Gordon JI**, **Onderdonk AB**, **Glimcher LH**. 2010. Enterobacteriaceae Act in Concert with the Gut Microbiota to Induce Spontaneous and Maternally Transmitted Colitis. Cell Host Microbe **8**:292–300.

128. **Camprubí S**, **Merino S**, **Guillot JF**, **Tomás JM**. 1993. The role of the O-antigen lipopolysaccharide on the colonization in vivo of the germfree chicken gut by Klebsiella pneumoniae. Microb Pathog **14**:433–440.

129. **Favre-Bonté S**, **Licht TR**, **Forestier C**, **Krogfelt KA**. 1999. Klebsiella pneumoniae capsule expression is necessary for colonization of large intestines of streptomycin-treated mice. Infection and Immunity **67**:6152–6156.

130. **Struve C**, **Forestier C**, **Krogfelt KA**. 2003. Application of a novel multi-screening signature-tagged mutagenesis assay for identification of Klebsiella pneumoniae genes essential in colonization and infection. Microbiology (Reading, Engl) **149**:167–176.

131. **Kumar V**, **Sun P**, **Vamathevan J**, **Li Y**, **Ingraham K**, **Palmer L**, **Huang J**, **Brown JR**. 2011. Comparative genomics of Klebsiella pneumoniae strains with different antibiotic resistance profiles. Antimicrob Agents Chemother **55**:4267–4276.

132. **Fitzgibbons SC**, **Ching Y**, **Yu D**, **Carpenter J**, **Kenny M**, **Weldon C**, **Lillehei C**, **Valim C**, **Horbar JD**, **Jaksic T**. 2009. Mortality of necrotizing enterocolitis expressed by birth weight categories. J Pediatr Surg **44**:1072–5– discussion 1075–6.

133. **Nanthakumar NN**, **Fusunyan RD**, **Sanderson I**, **Walker WA**. 2000. Inflammation in the developing human intestine: A possible pathophysiologic contribution to necrotizing enterocolitis. Proc Natl Acad Sci USA **97**:6043–6048.

134. **Lin PW**, **Nasr TR**, **Stoll BJ**. 2008. Necrotizing enterocolitis: recent scientific advances in pathophysiology and prevention. Semin Perinatol **32**:70–82.

135. **Osrin D**, **Vergnano S**, **Costello A**. 2004. Serious bacterial infections in newborn infants in developing countries. Curr Opin Infect Dis **17**:217–224.

136. **Zhang C**, **Sherman MP**, **Prince LS**, **Bader D**, **Weitkamp J-H**, **Slaughter JC**, **McElroy SJ**. 2012. Paneth cell ablation in the presence of Klebsiella pneumoniae induces necrotizing

enterocolitis (NEC)-like injury in the small intestine of immature mice. Dis Model Mech **5**:522–532.

137. **Gophna U**, **Sommerfeld K**, **Gophna S**, **Doolittle WF**, **Veldhuyzen van Zanten SJO**. 2006. Differences between tissue-associated intestinal microfloras of patients with Crohn's disease and ulcerative colitis. Journal of Clinical Microbiology **44**:4136–4141.

138. **Lederman ER**, **Crum NF**. 2005. Pyogenic liver abscess with a focus on Klebsiella pneumoniae as a primary pathogen: an emerging disease with unique clinical characteristics. Am J Gastroenterol **100**:322–331.

139. **Lee C-H**, **Liu J-W**, **Su L-H**, **Chien C-C**, **Li C-C**, **Yang K-D**. 2010. Hypermucoviscosity associated with Klebsiella pneumoniae-mediated invasive syndrome: a prospective cross-sectional study in Taiwan. Int J Infect Dis **14**:e688–92.

140. **Hyatt D**, **Chen G-L**, **Locascio PF**, **Land ML**, **Larimer FW**, **Hauser LJ**. 2010. Prodigal: prokaryotic gene recognition and translation initiation site identification. BMC Bioinformatics **11**:119.

141. **Fischer S**, **Brunk BP**, **Chen F**, **Gao X**, **Harb OS**, **Iodice JB**, **Shanmugam D**, **Roos DS**, **Stoeckert CJ Jr.** 2002. Using OrthoMCL to Assign Proteins to OrthoMCL-DB Groups or to Cluster Proteomes Into New Ortholog Groups. John Wiley & Sons, Inc., Hoboken, NJ, USA.

142. **Stamatakis A**. 2006. RAxML-VI-HPC: maximum likelihood-based phylogenetic analyses with thousands of taxa and mixed models. Bioinformatics **22**:2688–2690.

143. **García-Gómez E**, **González-Pedrajo B**, **Camacho-Arroyo I**. 2013. Role of sex steroid hormones in bacterial-host interactions. Biomed Res Int **2013**:928290–10.

144. **Neyrolles O**, **Quintana-Murci L**. 2009. Sexual inequality in tuberculosis. PLoS Med **6**:e1000199.

145. **Aebischer T**, **Laforsch S**, **Hurwitz R**, **Brombacher F**, **Meyer TF**. 2001. Immunity against Helicobacter pylori: significance of interleukin-4 receptor alpha chain status and gender of infected mice. Infection and Immunity **69**:556–558.

146. **Zhao J**, **Ng SC**, **Lei Y**, **Yi F**, **Li J**, **Yu L**, **Zou K**, **Dan Z**, **Dai M**, **Ding Y**, **Song M**, **Mei Q**, **Fang X**, **Liu H**, **Shi Z**, **Zhou R**, **Xia M**, **Wu Q**, **Xiong Z**, **Zhu W**, **Deng L**, **Kamm MA**, **Xia B**. 2013. First prospective, population-based inflammatory bowel disease incidence study in mainland of China: the emergence of “western” disease. Inflammatory Bowel Diseases **19**:1839–1845.

147. **Ng SC**, **Tang W**, **Ching JY**, **Wong M**, **Chow CM**, **Hui AJ**, **Wong TC**, **Leung VK**, **Tsang SW**, **Yu HH**, **Li MF**, **Ng KK**, **Kamm MA**, **Studd C**, **Bell S**, **Leong R**, **de Silva HJ**, **Kasturiratne A**, **Mufeena MNF**, **Ling KL**, **Ooi CJ**, **Tan PS**, **Ong D**, **Goh KL**, **Hilmi I**, **Pisespongsa P**, **Manatsathit S**, **Rerknimitr R**, **Aniwan S**, **Wang YF**, **Ouyang Q**, **Zeng Z**, **Zhu Z**, **Chen MH**, **Hu PJ**, **Wu K**, **Wang X**, **Simadibrata M**, **Abdullah M**, **Wu JC**, **Sung JJY**, **Chan FKL**. 2013. Incidence and Phenotype of Inflammatory Bowel Disease Based on Results From the Asia-Pacific Crohn's and Colitis Epidemiology Study. Gastroenterology **145**:158–165.e2.

148. **Nerich V**, **Monnet E**, **Etienne A**, **Louafi S**, **Ramée C**, **Rican S**, **Weill A**, **Vallier N**, **Vanbockstael V**, **Auleley G-R**, **Allemand H**, **Carbonnel F**. 2006. Geographical variations of inflammatory bowel disease in France: a study based on national health insurance data. Inflammatory Bowel Diseases **12**:218–226.

149. **Asakura K**, **Nishiwaki Y**, **Inoue N**, **Hibi T**, **Watanabe M**, **Takebayashi T**. 2009. Prevalence of ulcerative colitis and Crohn's disease in Japan. J Gastroenterol **44**:659–665.

150. **Loftus EV**, **Silverstein MD**, **Sandborn WJ**, **Tremaine WJ**, **Harmsen WS**, **Zinsmeister AR**. 2000. Ulcerative colitis in Olmsted County, Minnesota, 1940-1993: incidence, prevalence, and survival. Gut **46**:336–343.

151. **Bloom SM**, **Bijanki VN**, **Nava GM**, **Sun L**, **Malvin NP**, **Donermeyer DL**, **Dunne WM**, **Allen PM**, **Stappenbeck TS**. 2011. Commensal Bacteroides species induce colitis in host-genotype-specific fashion in a mouse model of inflammatory bowel disease. Cell Host Microbe **9**:390–403.

152. **Papa E**, **Docktor M**, **Smillie C**, **Weber S**, **Preheim SP**, **Gevers D**, **Giannoukos G**, **Ciulla D**, **Tabbaa D**, **Ingram J**, **Schauer DB**, **Ward DV**, **Korzenik JR**, **Xavier RJ**, **Bousvaros A**, **Alm EJ**. 2012. Non-invasive mapping of the gastrointestinal microbiota identifies children with inflammatory bowel disease. PLoS ONE **7**:e39242.

153. **Zenewicz LA**, **Yin X**, **Wang G**, **Elinav E**, **Hao L**, **Zhao L**, **Flavell RA**. 2013. IL-22 deficiency alters colonic microbiota to be transmissible and colitogenic. J Immunol **190**:5306–5312.

154. **Schwab C**, **Berry D**, **Rauch I**, **Rennisch I**, **Ramesmayer J**, **Hainzl E**, **Heider S**, **Decker T**, **Kenner L**, **Müller M**, **Strobl B**, **Wagner M**, **Schleper C**, **Loy A**, **Urich T**. 2014. Longitudinal study of murine microbiota activity and interactions with the host during acute inflammation and recovery. The ISME Journal **8**:1101–1114.

155. **Rowan F**, **Docherty NG**, **Murphy M**, **Murphy B**, **Calvin Coffey J**, **O'Connell PR**. 2010. Desulfovibrio bacterial species are increased in ulcerative colitis. Dis Colon Rectum **53**:1530–1536.

156. **Jergens AE**, **Dorn A**, **Wilson J**, **Dingbaum K**, **Henderson A**, **Liu Z**, **Hostetter J**, **Evans RB**, **Wannemuehler MJ**. 2006. Induction of differential immune reactivity to members of the flora of gnotobiotic mice following colonization with Helicobacter bilis or Brachyspira hyodysenteriae. Microbes and Infection **8**:1602–1610.

157. **Rashid T**, **Ebringer A**, **Wilson C**. 2013. The role of Klebsiella in Crohn's disease with a potential for the use of antimicrobial measures. Int J Rheumatol **2013**:610393–8.

158. **Markle JGM**, **Frank DN**, **Mortin-Toth S**, **Robertson CE**, **Feazel LM**, **Rolle-Kampczyk U**, **Bergen von M**, **McCoy KD**, **Macpherson AJ**, **Danska JS**. 2013. Sex differences in the gut microbiome drive hormone-dependent regulation of autoimmunity. Science **339**:1084–1088.

159. **Ussar S**, **Griffin NW**, **Bezy O**, **Fujisaka S**, **Vienberg S**, **Softic S**, **Deng L**, **Bry L**, **Gordon JI**, **Kahn CR**. 2015. Interactions between Gut Microbiota, Host Genetics and Diet Modulate the Predisposition to Obesity and Metabolic Syndrome. Cell Metabolism **22**:516–

530.

160. **Kasai C**, **Sugimoto K**, **Moritani I**, **Tanaka J**, **Oya Y**, **Inoue H**, **Tameda M**, **Shiraki K**, **Ito M**, **Takei Y**, **Takase K**. 2015. Comparison of the gut microbiota composition between obese and non-obese individuals in a Japanese population, as analyzed by terminal restriction fragment length polymorphism and next-generation sequencing. BMC Gastroenterol **15**:100.

161. **Murri M**, **Leiva I**, **Gomez-Zumaquero JM**, **Tinahones FJ**, **Cardona F**, **Soriguer F**, **Queipo-Ortuño MI**. 2013. Gut microbiota in children with type 1 diabetes differs from that in healthy children: a case-control study. BMC Medicine **11**:46.

162. **Sartor RB**, **Mazmanian SK**. 2012. Intestinal Microbes in Inflammatory Bowel Diseases. The American Journal of Gastroenterology Supplements **1**:15–21.

163. **Salter SJ**, **Cox MJ**, **Turek EM**, **Calus ST**, **Cookson WO**, **Moffatt MF**, **Turner P**, **Parkhill J**, **Loman NJ**, **Walker AW**. 2014. Reagent and laboratory contamination can critically impact sequence-based microbiome analyses. BMC Biology **12**:87.

164. **Kennedy NA**, **Walker AW**, **Berry SH**, **Duncan SH**, **Farquarson FM**, **Louis P**, **Thomson JM**. 2014. The Impact of Different DNA Extraction Kits and Laboratories upon the Assessment of Human Gut Microbiota Composition by 16S rRNA Gene Sequencing. PLoS ONE **9**:e88982.

165. **Cruaud P**, **Vigneron A**, **Lucchetti-Miganeh C**, **Ciron PE**, **Godfroy A**, **Cambon-Bonavita M-A**. 2014. Influence of DNA extraction method, 16S rRNA targeted hypervariable regions, and sample origin on microbial diversity detected by 454 pyrosequencing in marine chemosynthetic ecosystems. Applied and Environmental Microbiology **80**:4626–4639.

166. **Neurath MF**, **Weigmann B**, **Finotto S**, **Glickman J**, **Nieuwenhuis E**, **Iijima H**, **Mizoguchi A**, **Mizoguchi E**, **Mudter J**, **Galle PR**, **Bhan A**, **Autschbach F**, **Sullivan BM**, **Szabo SJ**, **Glimcher LH**, **Blumberg RS**. 2002. The transcription factor T-bet regulates mucosal T cell activation in experimental colitis and Crohn's disease. J Exp Med **195**:1129–1143.

167. **Andersson AF**, **Lindberg M**, **Jakobsson H**, **Bäckhed F**, **Nyrén P**, **Engstrand L**. 2008. Comparative analysis of human gut microbiota by barcoded pyrosequencing. PLoS ONE **3**:e2836.

168. **Sarma-Rupavtarm RB**, **Ge Z**, **Schauer DB**, **Fox JG**, **Polz MF**. 2004. Spatial distribution and stability of the eight microbial species of the altered schaedler flora in the mouse gastrointestinal tract. Applied and Environmental Microbiology **70**:2791–2800.

169. **Highsmith AK**, **Jarvis WR**. 1985. Klebsiella pneumoniae: selected virulence factors that contribute to pathogenicity. Infect Control **6**:75–77.

170. **Kabha K**, **Nissimov L**, **Athamna A**, **Keisari Y**, **Parolis H**, **Parolis LA**, **Grue RM**, **Schlepper-Schafer J**, **Ezekowitz AR**, **Ohman DE**. 1995. Relationships among Capsular Structure, Phagocytosis, and Mouse Virulence in Klebsiella pneumoniae. Infection and Immunity **63**:847–852.

171. **Ofek I**, **Mesika A**, **Kalina M**, **Keisari Y**, **Podschun R**, **Sahly H**, **Chang D**, **McGregor D**, **Crouch E**. 2001. Surfactant protein D enhances phagocytosis and killing of unencapsulated phase variants of Klebsiella pneumoniae. Infection and Immunity **69**:24–33.

172. **Domenico P**, **Salo RJ**, **Cross AS**, **Cunha BA**. 1994. Polysaccharide capsule-mediated resistance to opsonophagocytosis in Klebsiella pneumoniae. Infection and Immunity **62**:4495–4499.

173. **Keisari Y**, **Wang H**, **Mesika A**, **Matatov R**, **Nissimov L**, **Crouch E**, **Ofek I**. 2001. Surfactant protein D-coated Klebsiella pneumoniae stimulates cytokine production in mononuclear phagocytes. J Leukoc Biol **70**:135–141.

174. **Montgomerie JZ**. 1979. Epidemiology of Klebsiella and hospital-associated infections. Rev Infect Dis **1**:736–753.

175. **Struve C**, **Krogfelt KA**. 2003. Role of capsule in Klebsiella pneumoniae virulence: lack of correlation between in vitro and in vivo studies. FEMS Microbiol Lett **218**:149–154.

176. **Campos MA**, **Vargas MA**, **Regueiro V**, **Llompart CM**, **Albertí S**, **Bengoechea JA**. 2004. Capsule polysaccharide mediates bacterial resistance to antimicrobial peptides. Infection and Immunity **72**:7107–7114.

177. **Llobet E**, **Tomás JM**, **Bengoechea JA**. 2008. Capsule polysaccharide is a bacterial decoy for antimicrobial peptides. Microbiology (Reading, Engl) **154**:3877–3886.

178. **Hapfelmeier S**, **Lawson MAE**, **Slack E**, **Kirundi JK**, **Stoel M**, **Heikenwalder M**, **Cahenzli J**, **Velykoredko Y**, **Balmer ML**, **Endt K**, **Geuking MB**, **Roy Curtiss 3**, **McCoy KD**, **Macpherson AJ**. 2010. Reversible Microbial Colonization of Germ-Free Mice Reveals the Dynamics of IgA Immune Responses. Science **328**:1705–1709.

179. **Pan Y-J**, **Lin T-L**, **Chen Y-H**, **Hsu C-R**, **Hsieh P-F**, **Wu M-C**, **Wang J-T**. 2013. Capsular types of Klebsiella pneumoniae revisited by wzc sequencing. PLoS ONE **8**:e80670.

180. **Darling AE**, **Mau B**, **Perna NT**. 2010. progressiveMauve: multiple genome alignment with gene gain, loss and rearrangement. PLoS ONE **5**:e11147.

181. **McConnell EL**, **Basit AW**, **Murdan S**. 2008. Measurements of rat and mouse gastrointestinal pH, fluid and lymphoid tissue, and implications for in-vivo experiments. J Pharm Pharmacol **60**:63–70.

182. **Hamner S**, **McInnerney K**, **Williamson K**, **Franklin MJ**, **Ford TE**. 2013. Bile Salts Affect Expression of Escherichia coli O157:H7 Genes for Virulence and Iron Acquisition, and Promote Growth under Iron Limiting Conditions. PLoS ONE **8**:e74647.

183. **Gunn JS**. 2000. Mechanisms of bacterial resistance and response to bile. Microbes Infect **2**:907–913.

184. **Eberhart LJ**, **Deringer JR**, **Brayton KA**, **Sawant AA**, **Besser TE**, **Call DR**. 2012. Characterization of a novel microcin that kills enterohemorrhagic Escherichia coli O157:H7 and O26. Applied and Environmental Microbiology **78**:6592–6599.

185. **Russell AB**, **Wexler AG**, **Harding BN**, **Whitney JC**, **Bohn AJ**, **Goo YA**, **Tran BQ**, **Barry NA**, **Zheng H**, **Peterson SB**, **Chou S**, **Gonen T**, **Goodlett DR**, **Goodman AL**, **Mougous JD**. 2014. A type VI secretion-related pathway in Bacteroidetes mediates interbacterial antagonism. Cell Host Microbe **16**:227–236.

186. **Zerbino DR**, **Birney E**. 2008. Velvet: algorithms for de novo short read assembly using de Bruijn graphs. Genome Res **18**:821–829.

187. **Seemann T**. 2014. Prokka: rapid prokaryotic genome annotation. Bioinformatics **30**:2068–2069.

188. **Boudeau J**, **Glasser AL**, **Masseret E**, **Joly B**, **Darfeuille-Michaud A**. 1999. Invasive ability of an Escherichia coli strain isolated from the ileal mucosa of a patient with Crohn's disease. Infection and Immunity **67**:4499–4509.

189. **Krause DO**, **Little AC**, **Dowd SE**, **Bernstein CN**. 2011. Complete genome sequence of adherent invasive Escherichia coli UM146 isolated from Ileal Crohn's disease biopsy tissue. Journal of Bacteriology **193**:583–583.

190. **Oshima K**, **Toh H**, **Ogura Y**, **Sasamoto H**, **Morita H**, **Park S-H**, **Ooka T**, **Iyoda S**, **Taylor TD**, **Hayashi T**, **Itoh K**, **Hattori M**. 2008. Complete genome sequence and comparative analysis of the wild-type commensal Escherichia coli strain SE11 isolated from a healthy adult. DNA Res **15**:375–386.

191. **Riley M**, **Abe T**, **Arnaud MB**, **Berlyn MKB**, **Blattner FR**, **Chaudhuri RR**, **Glasner JD**, **Horiuchi T**, **Keseler IM**, **Kosuge T**, **Mori H**, **Perna NT**, **Plunkett G**, **Rudd KE**, **Serres MH**, **Thomas GH**, **Thomson NR**, **Wishart D**, **Wanner BL**. 2006. Escherichia coli K-12: a cooperatively developed annotation snapshot--2005. Nucleic Acids Res **34**:1–9.

192. **Alikhan N-F**, **Petty NK**, **Ben Zakour NL**, **Beatson SA**. 2011. BLAST Ring Image Generator (BRIG): simple prokaryote genome comparisons. BMC Genomics **12**:402.

193. **Dhillon BK**, **Laird MR**, **Shay JA**, **Winsor GL**, **Lo R**, **Nizam F**, **Pereira SK**, **Waglechner N**, **McArthur AG**, **Langille MGI**, **Brinkman FSL**. 2015. IslandViewer 3: more flexible, interactive genomic island discovery, visualization and analysis. Nucleic Acids Res **43**:W104–8.

194. **Ma J**, **Bao Y**, **Sun M**, **Dong W**, **Pan Z**, **Zhang W**, **Lu C**, **Yao H**. 2014. Two functional type VI secretion systems in avian pathogenic Escherichia coli are involved in different pathogenic pathways. Infection and Immunity **82**:3867–3879.

195. **Sana TG**, **Baumann C**, **Merdes A**, **Soscia C**, **Rattei T**, **Hachani A**, **Jones C**, **Bennett KL**, **Filloux A**, **Superti-Furga G**, **Voulhoux R**, **Bleves S**. 2015. Internalization of Pseudomonas aeruginosa Strain PAO1 into Epithelial Cells Is Promoted by Interaction of a T6SS Effector with the Microtubule Network. MBio **6**:e00712.

196. **Clevers H**. 2013. The intestinal crypt, a prototype stem cell compartment. Cell **154**:274–284.

197. **Wilson SS**, **Tocchi A**, **Holly MK**, **Parks WC**, **Smith JG**. 2014. A small intestinal organoid model of non-invasive enteric pathogen-epithelial cell interactions. Mucosal

Immunol 1–10.

198. **Wilson CL**, **Ouellette AJ**, **Satchell DP**, **Ayabe T**, **López-Boado YS**, **Stratman JL**, **Hultgren SJ**, **Matrisian LM**, **Parks WC**. 1999. Regulation of intestinal alpha-defensin activation by the metalloproteinase matrilysin in innate host defense. Science **286**:113–117.

199. **Wu L**, **Estrada O**, **Zaborina O**, **Bains M**, **Shen L**, **Kohler JE**, **Patel N**, **Musch MW**, **Chang EB**, **Fu Y-X**, **Jacobs MA**, **Nishimura MI**, **Hancock REW**, **Turner JR**, **Alverdy JC**. 2005. Recognition of host immune activation by Pseudomonas aeruginosa. Science **309**:774–777.

200. **Llobet E**, **Campos MA**, **Giménez P**, **Moranta D**, **Bengoechea JA**. 2011. Analysis of the networks controlling the antimicrobial-peptide-dependent induction of Klebsiella pneumoniae virulence factors. Infection and Immunity **79**:3718–3732.

201. **Cullen TW**, **Schofield WB**, **Barry NA**, **Putnam EE**, **Rundell EA**, **Trent MS**, **Degnan PH**, **Booth CJ**, **Yu H**, **Goodman AL**. 2015. Gut microbiota. Antimicrobial peptide resistance mediates resilience of prominent gut commensals during inflammation. Science **347**:170–175.

202. **Salzman NH**, **Hung K**, **Haribhai D**, **Chu H**, **Karlsson-Sjöberg J**, **Amir E**, **Teggatz P**, **Barman M**, **Hayward M**, **Eastwood D**, **Stoel M**, **Zhou Y**, **Sodergren E**, **Weinstock GM**, **Bevins CL**, **Williams CB**, **Bos NA**. 2010. Enteric defensins are essential regulators of intestinal microbial ecology. Nat Immunol **11**:76–83.

203. **Mukherjee S**, **Hooper LV**. 2015. Antimicrobial defense of the intestine. Immunity **42**:28–39.

204. **Bry L**, **Falk P**, **Huttner K**, **Ouellette A**, **Midtvedt T**, **Gordon JI**. 1994. Paneth cell differentiation in the developing intestine of normal and transgenic mice. Proc Natl Acad Sci USA **91**:10335–10339.

205. **Dzul SP**, **Thornton MM**, **Hohne DN**, **Stewart EJ**, **Shah AA**, **Bortz DM**, **Solomon MJ**, **Younger JG**. 2011. Contribution of the Klebsiella pneumoniae capsule to bacterial aggregate and biofilm microstructures. Applied and Environmental Microbiology **77**:1777–1782.

206. **Macfarlane S**, **Macfarlane GT**. 2006. Composition and metabolic activities of bacterial biofilms colonizing food residues in the human gut. Applied and Environmental Microbiology **72**:6204–6211.

207. **Hancock RE**, **Chapple DS**. 1999. Peptide antibiotics. Antimicrob Agents Chemother **43**:1317–1323.

208. **Hibbing ME**, **Fuqua C**, **Parsek MR**, **Peterson SB**. 2010. Bacterial competition: surviving and thriving in the microbial jungle. Nat Rev Micro **8**:15–25.

209. **Garcia-Bustos JF**, **Pezzi N**, **Mendez E**. 1985. Structure and mode of action of microcin 7, an antibacterial peptide produced by Escherichia coli. Antimicrob Agents Chemother **27**:791–797.

210. **Pukatzki S**, **Ma AT**, **Sturtevant D**, **Krastins B**, **Sarracino D**, **Nelson WC**, **Heidelberg JF**, **Mekalanos JJ**. 2006. Identification of a conserved bacterial protein secretion system in Vibrio cholerae using the Dictyostelium host model system. Proc Natl Acad Sci USA **103**:1528–1533.

211. **Basler M**, **Ho BT**, **Mekalanos JJ**. 2013. Tit-for-tat: type VI secretion system counterattack during bacterial cell-cell interactions. Cell **152**:884–894.

212. **Russell AB**, **Hood RD**, **Bui NK**, **LeRoux M**, **Vollmer W**, **Mougous JD**. 2011. Type VI secretion delivers bacteriolytic effectors to target cells. Nature **475**:343–347.

213. **Aschtgen M-S**, **Bernard CS**, **De Bentzmann S**, **Lloubès R**, **Cascales E**. 2008. SciN is an outer membrane lipoprotein required for type VI secretion in enteroaggregative Escherichia coli. Journal of Bacteriology **190**:7523–7531.

214. **Wannemuehler MJ**, **Overstreet A-M**, **Ward DV**, **Phillips GJ**. 2014. Draft genome sequences of the altered schaedler flora, a defined bacterial community from gnotobiotic mice. Genome Announc **2**:e00287–14–e00287–14.

215. **Filisetti-Cozzi T**, **Carpita NC**. 1991. Measurement of Uranic Acids without Interference from Neutral Sugars. Analytical Biochemistry **197**:157–162.

216. **Blumenkrantz N**, **Asboe-Hansen G**. 1973. New method for quantitative determination of uronic acids. Analytical Biochemistry **54**:484–489.

217. **Domenico P**, **Landolphi DR**, **Cunha BA**. 1991. Reduction of capsular polysaccharide and potentiation of aminoglycoside inhibition in gram-negative bacteria by bismuth subsalicylate. J Antimicrob Chemother **28**:801–810.

218. **Bankevich A**, **Nurk S**, **Antipov D**, **Gurevich AA**, **Dvorkin M**, **Kulikov AS**, **Lesin VM**, **Nikolenko SI**, **Pham S**, **Prjibelski AD**, **Pyshkin AV**, **Sirotkin AV**, **Vyahhi N**, **Tesler G**, **Alekseyev MA**, **Pevzner PA**. 2012. SPAdes: a new genome assembly algorithm and its applications to single-cell sequencing. J Comput Biol **19**:455–477.

219. **Galardini M**, **Biondi EG**, **Bazzicalupo M**, **Mengoni A**. 2011. CONTIGuator: a bacterial genomes finishing tool for structural insights on draft genomes. Source Code Biol Med **6**:11.

220. **Langmead B**, **Salzberg SL**. 2012. Fast gapped-read alignment with Bowtie 2. Nat Methods **9**:357–359.

221. **Quinlan AR**. 2014. BEDTools: The Swiss-Army Tool for Genome Feature Analysis. Curr Protoc Bioinformatics **47**:11.12.1–11.12.34.

222. **Thorvaldsdóttir H**, **Robinson JT**, **Mesirov JP**. 2013. Integrative Genomics Viewer (IGV): high-performance genomics data visualization and exploration. Briefings in Bioinformatics **14**:178–192.

223. **Bolger AM**, **Lohse M**, **Usadel B**. 2014. Trimmomatic: a flexible trimmer for Illumina sequence data. Bioinformatics **30**:2114–2120.

224. **Kassim SY**, **Gharib SA**, **Mecham BH**, **Birkland TP**, **Parks WC**, **McGuire JK**. 2007. Individual matrix metalloproteinases control distinct transcriptional responses in airway epithelial cells infected with Pseudomonas aeruginosa. Infection and Immunity **75**:5640–5650.

225. **Martinon F**, **Chen X**, **Lee A-H**, **Glimcher LH**. 2010. TLR activation of the transcription factor XBP1 regulates innate immune responses in macrophages. Nat Immunol **11**:411–418.

226. **Fang G**, **Munera D**, **Friedman DI**, **Mandlik A**, **Chao MC**, **Banerjee O**, **Feng Z**, **Losic B**, **Mahajan MC**, **Jabado OJ**, **Deikus G**, **Clark TA**, **Luong K**, **Murray IA**, **Davis BM**, **Keren-Paz A**, **Chess A**, **Roberts RJ**, **Korlach J**, **Turner SW**, **Kumar V**, **Waldor MK**, **Schadt EE**. 2012. Genome-wide mapping of methylated adenine residues in pathogenic Escherichia coli using single-molecule real-time sequencing. Nat Biotechnol **30**:1232–1239.

227. **Murray IA**, **Clark TA**, **Morgan RD**, **Boitano M**, **Anton BP**, **Luong K**, **Fomenkov A**, **Turner SW**, **Korlach J**, **Roberts RJ**. 2012. The methylomes of six bacteria. Nucleic Acids Res **40**:11450–11462.

228. **Braaten BA**, **Nou X**, **Kaltenbach LS**, **Low DA**. 1994. Methylation patterns in pap regulatory DNA control pyelonephritis-associated pili phase variation in E. coli. Cell **76**:577–588.

229. **Kooistra O**, **Lüneberg E**, **Knirel YA**, **Frosch M**, **Zähringer U**. 2002. N-Methylation in polylegionaminic acid is associated with the phase-variable epitope of Legionella pneumophila serogroup 1 lipopolysaccharide. Identification of 5-(N,N-dimethylacetimidoyl)amino and 5-acetimidoyl(N-methyl)amino-7-acetamido-3,5,7,9-tetradeoxynon-2-ulosonic acid in the O-chain polysaccharide. Eur J Biochem **269**:560–572.

230. **Datsenko KA**, **Wanner BL**. 2000. One-step inactivation of chromosomal genes in Escherichia coli K-12 using PCR products. Proc Natl Acad Sci USA **97**:6640–6645.